UTILIZING MAIZE GENOMICS FOR PRE-BREEDING INSIGHTS

BY

CRYSTAL A. SORGINI

DISSERTATION

Submitted in partial fulfillment of the requirements
for the degree of Doctor of Philosophy in Crop Sciences
in the Graduate College of the
University of Illinois at Urbana-Champaign, 2018

Urbana, Illinois

Doctoral Committee:

Professor Stephen P. Moose, Chair
Associate Professor Elizabeth A. Ainsworth
Associate Professor Patrick J. Brown
Professor A. Lane Rayburn
Assistant Professor Martin M. Sachs

ABSTRACT

Tropospheric ozone (O_3) is estimated to cause billions of dollars in global crop losses, but few studies have investigated the effects of elevated O_3 on growth and development of C_4 crop plants. Free Air Concentration Enrichment (FACE) field experiments were used to evaluate the response of diverse maize inbred and hybrid lines under elevated O_3 concentrations ([O_3]). Lines were scored for flowering phenology and ear architecture traits. A multi-year analysis showed inconsistent effects of O_3 on development. Hybrid ear length and diameter and inbred ear length were all significantly reduced under elevated [O_3] compared to ambient conditions.

Knowledge about the identity and location of agriculturally important quantitative trait loci (QTL) provides the basis for marker assisted selection in breeding programs. B73 and Mo17 Nearly Isogenic Lines (NILs) were evaluated at the FACE facility for leaf damage and QTL were mapped. In Mo17 NILs, a significant leaf damage QTL was identified on chromosome 2 at ~161 Mb (AGPv3). Results show that B73 introgressions into Mo17 in this region made NILs more susceptible. Leaf damage scores from the field in 2016 and 2017 had a strongly significant correlation ($r = 0.93$). Field and growth chamber results best fit is non-linear. It appears chambers can identify damage versus no-damage, but not a continuous degree of damage as seen in the field. This indicates the potential for higher-throughput phenotyping and fine mapping of early season O_3 damage QTL in a controlled environment. Sensitive and tolerant NILs were identified. Co-dominant insertion/deletion markers flanking the QTL interval were designed and validated in parents and hybrids. This research supplies the resources for future experiments that combine growth chamber phenotyping and genetic fine-mapping to determine the gene(s) underlying this QTL for O_3 tolerance.

Current doubled haploid (DH) inducer markers are inefficient and have a higher probability of misclassification when used for classification of tropical germplasm. *Yg3-N1582*, a rare dominant mutant obtained from ethyl methanesulfonate (EMS) mutagenesis, has not been previously mapped. Phenotypically, *Yg3-N1582* has yellow color expression at coleoptile emergence that does not persist beyond the seedling stage, is homozygous-viable, and is non-lethal with no apparent deleterious effects. The *Yg3* mutation has potential as a haploid inducer marker in exotic germplasm and small breeding programs where the use of *R1-Navajo* and high oil inducers is not feasible. The *yg3* gene maps to 173-175Mb (AGPv3) on chromosome 5, which does not coincide with any previously characterized *yg* mutant. Transcriptome profiling

identified GRMZM2G165521 as a candidate gene that could underlie the mutant phenotype. GRMZM2G165521 is a predicted PPR protein involved in RNA editing and is orthologous to some mutants in rice that also condition '*yg'* phenotypes. Sequencing of GRMZM2G165521 in the *Yg3* background reveals a seven base pair insertion in the first intron relative to the wild-type reference line. This insertion results in an alternate transcription start site and open reading frame that eliminates the first exon of the PPR protein. The alignment of heterozygous *yg3* RNAseq reads confirm transcription at the site of the insertion.

ACKNOWLEDGEMENTS

I would like to acknowledge the guidance and support of my graduate committee; Dr. Stephen Moose (Chair), Dr. Lisa Ainsworth, Dr. Patrick Brown, Dr. Lane Rayburn, and Dr. Marty Sachs. I would like to express my sincere gratitude and appreciation to all the former Brown Lab members who assisted this research and the collaborative ideas presented in this dissertation; Ilse Barrios – Perez, Christopher Kaiser, Jingnu (Nunu) Xia, Derek Lewis, Pardeep Hirannaiah, Shilpa Manjunatha, Samuel Fernandes, Asher Tarun, Dr. Carrie Thurber, Race Higgins, Elizabeth Hawkins, and Dr. Payne Burks. Additionally, this research would not have been possible without the assistance of undergraduate workers; Chris Bauer, Paroma De, Emma Goodrich, Whitney Kratovil, Earl Mangulabnan, Hannah Reed, Laura Sanchez, Joe Sulzberger, Nicholas Sutton, Abby Vanderkloot, and Rachel Vaessen. I would like to express my sincere appreciation to the aMAIZEing FACE Project collaborators and technicians; Ainsworth Lab members, Leakey Lab members, Dr. Lauren McIntyre, Kannan Puthuval, Brad Dalsing, Christopher Montes, Chad Lantz, Christopher Moller, Ben Thompson, Jesse McGrath, and Aidan McMahon. Thank you to the Maize Genetics Cooperative Stock Center and Philip Stinard for all their insights about mutant maize. Thank you to Dr. Mark Settles for his feedback on marker design. I also would like to acknowledge Dr. Tony Studer for all of his academic support and mentoring. I would like to thank Melinda Laborg (IGB) and Dr. Jack Juvik for their administrative assistance. Additionally, words cannot express enough my sincere gratitude and appreciation for the administrative and academic support received from Dianne Carson of the Crop Sciences Department. This dissertation is dedicated to my family who have always supported me and encouraged me to do my best! Thank you, Mom, Dad, Jessica, Brianna, and Joshua.

This research would not have been possible without funding from my Monsanto Plant Breeding Fellowship and funding from the National Science Foundation (Grant number PGR-1238030).

TABLE OF CONTENTS

CHAPTER 1

EFFECTS OF OZONE ON FIELD-GROWN MAIZE DEVELOPMENT

ABSTRACT

Tropospheric ozone (O_3) is estimated to cause billions of dollars in global crop losses, but few studies have investigated the effects of elevated O_3 on growth and development of C_4 crop plants in a field setting. The goal of this study was to investigate how maize developmental traits and ear characteristics were affected by O_3-induced oxidative stress. To study the effect of O_3 on development and ear traits, diverse maize inbred and hybrid lines, as well as B73-Mo17 nearly isogenic lines (NILs), were grown under ambient (~40 ppb) and elevated (~100 ppb) [O_3] at the Free Air Concentration Enrichment (FACE) research facility in Savoy, IL from 2013-2017. Plants were measured for flowering time, plant and ear height, ear length, ear diameter, kernel row number, and kernels per row. A multi-year analysis showed inconsistent effects of O_3 on development. Hybrid ear length and diameter were significantly reduced under elevated O_3 compared to ambient conditions, with B73 x Mo17, B73 x NC350, B73 x Hp301, and B73 x CML333 hybrids most affected. Inbred ear length was also significantly reduced under elevated O_3. Ear row number and kernels per row were not significantly affected by O_3 in hybrids. Open pollinated inbred ears were more variable for ear row number and kernels per row traits and the effect was not significant. This suggests that elevated O_3 affects ears primarily by reducing kernel size during grain filling.

INTRODUCTION

Tropospheric O_3 is an air pollutant that causes billions of dollars in global crop losses (McGrath et al. 2015, Ainsworth 2017). However, there have been few studies that have investigated the effects of elevated O_3 on reproductive development in C_4 plants (Leisner & Ainsworth 2012). It has been shown that O_3 induced oxidative stress has negative effects on the reproductive growth and development of agricultural crops resulting in reduced yields (Black et al. 2000, Mauzerall &Wang 2001, Feng & Kobayashi 2009, Betzelberger et al. 2010, Wilkinson et al. 2012). Intraspecific variation within maize subspecies influence its response to abiotic stresses and results in lines that are relatively more tolerant or sensitive to environmental changes. Variation in maize lines in response to abiotic stress has been well documented. For example, variation within subspecies has been demonstrated to influence the response to heat stress (Bita et al. 2013), soil moisture (Suriyagoda et al. 2014) and nitrogen limitation (Lv et al.

2016). It is quite likely that this variation could be utilized to address other current stresses, such as O_3, and future unseen pressures. In fact, drought stress can induce oxidative stress similar to that observed with exposure to elevated O_3. This suggests that it is likely genotypic variation in O_3 induced stress exists and can be leveraged to not only find genotypes that are more resistant to oxidative stress, but also understand the underlying mechanism that results in increased sensitivity and resistance.

O_3 is a less stable allotrope of oxygen with high oxidizing potential. O_3 is a favorable gas of the stratosphere because it plays a vital role in absorbing harmful ultraviolet radiation from the sun, making Earth habitable (NOAA 2018). In the lower level of the atmosphere (the troposphere) O_3 is a pollutant that is formed from the effects of sunlight interacting with aerosol hydrocarbons and nitrogen oxides, the byproducts from vehicular and industrial emissions. O_3 pollution is transient in space and time and is thermosensitive. O_3 on the leaf surface does not induce substantial damage. Damage typically occurs inside the leaf where O_3 can interact with the hydrated cellular tissue to form reactive free oxides. Thus uptake is dependent upon stomatal conductance, which varies depending on stomatal aperture (Mauzerall & Wang 2001). The formation of reactive oxygen species (ROS) is thought to be associated with the breakdown of O_3 in the apoplast (Black et al. 2000). Plant response to oxidative stress involves the creation of ROS stress and its interaction with reaction hormones, Ca2+, and MAPK signal cascades. There appears to be significant overlap between O_3 response and pathogen response pathways in plants. O_3 mimics oxidative bursts generated by early signal pathways that regulate plant hypersensitive response (Rao & Davis 1999, Rao et al. 2000). Secondary ROS bursts activate the expression of defense genes and the ethylene, salicylic acid, and jasmonic acid signal pathways (Black et al. 2000). The cost associated with detoxification of O_3 is a reduction in photosynthesis (due to stomatal closure) and carbohydrate usage (to detoxify). The tradeoff between antioxidant metabolism and carbon gain results in a negative correlation between photosynthesis and seed yield (Betzelberger et al. 2010). It is proposed that sensitivity of seed crops to O_3 is greatest during the period between flowering and seed maturity (Lee et al. 1988, Pleijel et al. 1998).

Free Air Concentration Enrichment (FACE) research facilities allow for the investigation into predicted climate change scenarios. There are a lot of climate manipulation studies besides FACE. The power of FACE facilities is in the ability to study how changes in atmospheric gasses may alter growth in a field setting, with treatment application having only a minimal

effect on other abiotic and biotic factors. FACE treatment does not affect precipitation or wind like other atmospheric treatments do. FACE technologies have been adapted to enrich O_3 to study plant responses in real field settings (Morgan et al. 2004, Tang et al. 2011). A potential problem with FACE systems is being able to treat a large enough population to do modern genetic analysis. Previous work has shown that the SoyFACE research facility at the University of Illinois Urbana-Champaign can be successfully used to screen crops for O_3 tolerance and sensitivity (Ainsworth et al. 2014). Using modern screening SoyFACE studies have shown genetic variation in numerous traits for numerous species. The most recent research in crop species response to elevated O_3 has focused on identifying physiological variation and/or yield traits in soybean (Betzelberger et al. 2010), rice (Shi et al. 2009), and wheat (Zhu et al. 2011). Identifying intraspecific variation for oxidative stress tolerance is an important pre-breeding step (Ainsworth 2017). However, more efforts are needed for screening and mapping field grown crops, such as maize. This research intends to utilize the SoyFACE research facility and genetic variation to better understand and identify phenotypes and their genotype associations for oxidative stress response in maize.

In order to test the effect that O_3 pollution may have on reproductive success in maize, I grew numerous inbred and hybrid lines in ambient and elevated O_3. I tested the hypothesis that exposure to elevated O_3 would impact time to anthesis and silking, potentially skewing the anthesis to silking interval (ASI). I also tested the hypothesis that there would be significant variation in the response of height and ear height to O_3 pollution. Finally, I hypothesized that exposure to elevated O_3 would negatively affect ear characteristics and lines would show significant variation in the response.

MATERIALS AND METHODS

Genotypes Planted (2013- 2017)

In 2013, 203 diverse maize inbred lines (n=2) representing a wide range of the genetic variation in maize germplasm were grown under ambient (~40 ppb) and elevated [O_3] (~100 ppb) at the FACE research facility. Inbred lines were planted in a single-row 3.3m plots in eight elevated O_3 and eight ambient rings. B73 was planted as a check and replicated eight times within each ring for a total of 128 plots across the experiment. All other genotypes were grown in two ambient and two elevated O_3 rings for a total of four plots across the experiment.

In 2014 and 2015, maize inbred (n= 4) and hybrid (n= 4) lines were grown under ambient (~40 ppb) and elevated [O_3] (~100 ppb) at the FACE research facility. Each inbred line was planted in a single-row 3.3 m plot in four elevated O_3 and four ambient rings. Each hybrid line was planted in a two-row 3.3 m plots in four elevated O_3 and four ambient rings. In 2014, B73 was planted as check and replicated ten times within each inbred ring for a total of 80 plots across the experiment. All other inbred genotypes were replicated one time within each ring for a total of eight plots across the experiment. B73 x Mo17 was planted as a check and replicated ten times within each hybrid ring for a total of 80 plots across the experiment. All other hybrid genotypes were replicated one time within each ring for a total of eight plots across the experiment. In 2015, B73 was planted as check and replicated eight times within each inbred ring for a total of 64 plots across the experiment. Lines Mo17, C123, and Hp301 were replicated eight times within a ring for a total of 64 plots across the experiment. All other inbred genotypes were replicated five times within each ring for a total of 40 plots across the experiment. B73 x Mo17 was planted as a check and replicated nine times within each hybrid ring for a total of 64 plots across the experiment. Lines B73 x C123, B73 x Hp301 were replicated nine times within each hybrid ring for a total of 64 plots across the experiment. All other hybrid genotypes were replicated five times within each ring for a total of 40 plots across the experiment.

In 2016 and 2017, 50 B73 NILs (n= 4) and 50 Mo17 NILs (n= 4) developed by Eichten et al. (2011) were grown under ambient (~40 ppb) and elevated [O_3] (~100 ppb) at the FACE research facility. Each NIL line was planted in a single-row 1.65 m plot in four elevated O_3 and four ambient rings. B73 and Mo17 were grown as checks and replicated five times within each ring for a total of 40 plots across the experiment. Each NIL was replicated one time within each ring for a total of eight plots across the experiment.

Ozone Fumigation

Maize was exposed to elevated [O_3] (100 ppb) for eight hours each day from shortly after emergence until physiological maturity. Micro-pores in a segmented tube around the research ring circumference released O_3 according to wind direction and speed. Gas was monitored at the center of the ring and more or less gas was released to meet constant target concentrations. The fumigation system did not operate when leaves were wet or when wind speed dropped below 0.5 ms^{-1}. When the fumigation system was operating, O_3 concentrations were within 20% of the 100 ppb target concentration for 81% of the time.

Measurements and Analysis

Designated "development" plants were flagged and anthesis and silking were monitored daily. In 2013 there were six designated plants, in 2014-2017 there were eight plants. Anthesis was recorded when half of the designated plants in a row had at least one hanging anther. Silking was recorded when half of the designated plants had at least one silk emerged from the ear. Growing degree days (GDD) were determined using research site weather station data. ASI was derived from anthesis and silking observations. ASI was calculated from GDD by subtracting silking date from anthesis date. Significance thresholds were set at (***) $p < 0.001$, (**) $p < 0.01$, and (*) $p < 0.05$. Statistical analysis was performed on plot means using a model including ring pair, genotype (geno), and geno by O_3 treatment interaction (geno:treatment) as variables. Ring pair is defined as an ambient and elevated O_3 ring with the exact same genotype plot randomization design. Individual year T-test calculations were coded in R (R Core Team 2015). A multi-year analysis was completed using ASReml (Gilmour et al. 2009). Individual year statistical analysis was performed on plot means using a model with ring pair, geno, geno:treatment, and treatment by ring interaction (treatment:ring). The multiple year analysis was performed on plot means using a model with year, treatment, year by treatment interaction (year:treatment), geno, geno:treatment, year by genotype interaction (year:geno) and year by treatment by ring interaction (year:treatment:ring).

Height and ear height measurements for each population grown from 2013 to 2017 were collected. In each year height and ear height measurements were taken for all designated plants at 43 DAP and 90 DAP. Total height was defined as ground level to the flag leaf. Ear height was defined as ground level to the shank of the primary ear. Data was collected using barcode scanners and measuring tools. Significance thresholds were set at (***) $p < 0.001$, (**) $p < 0.01$, and (*) $p < 0.05$. Statistical analysis was performed on plot means using a model with ring pair, geno, and geno: treatment. Individual year T-test calculations were coded in R (R Core Team 2015). A multi-year analysis was completed using ASReml (Gilmour et al. 2009). Individual year statistical analysis was performed on plot means using a model with ring pair, geno, and geno:treatment and treatment:ring The multiple year analysis was performed on plot means using a model with year, treatment, year:treatment, geno, treatment:geno, year:geno and year:treatment:ring.

Ear measurements were collected for primary ears for maize inbred and hybrid lines in 2014 and 2015. In 2014, primary ears were harvested from each plant in a 3.3 m hybrid row and primary ears from eight contiguous plants were harvested from each inbred row. In 2015, primary ears from eight contiguous plants were harvested from each inbred and hybrid row. All primary ears were measured for length, diameter, row number, and kernels per row using barcode scanners and barcoded tools. Ears were placed in a caliper and measurements for length and diameter were scanned. Manual counts were completed for ear row number and kernels per row and counts were digitally recorded with a scanner. Total length was defined as total cob length. Diameter was measured at the widest point of the ear. Ear row number was defined as the number of rows around the ear circumference. Kernels per row was defined as the number of kernels in a single row on the ear. A total of 7,525 ears were processed in 2014 (4,797 hybrid ears and 2,728 inbred ears). A total of 5,118 ears were processed in 2015 (2,420 hybrid ears and 2,768 inbred ears). Statistical analysis was performed on plot means using a model with ring pair, geno, and geno: treatment. Individual year T-test calculations were coded in R (R Core Team 2015). Significance thresholds were set at (***) $p < 0.001$, (**) $p < 0.01$, and (*) $p < 0.05$.

RESULTS AND DISCUSSION

Flowering Time Traits

A multi-year analysis of the effects of O_3 on flowering traits from 2013-2015 showed a significant year by treatment effect. Elevated O_3 treatment significantly decreased days to anthesis, silking, and ASI in 2013 (Table 1.1). However, in 2014 and 2015, elevated O_3 treatment showed no significant effect on anthesis, silking, or ASI (Figures 1.1 & 1.2). Genotype independent T-tests on inbred lines (Table 1.2) show that in 2015, elevated O_3 treatment significantly decreased days to anthesis and silking in lines Hp301, Il14H, NC338, and Oh43 but did not affect ASI. Additionally, in line Ms71 days to anthesis were significnatly decreased under elevated O_3 treatement. Results differed between years due to the number of replicates per genotype. Genotype independent T-tests on hybrid lines (Table 1.3) shows that line B73 x Hp301 had a marginally significant decrease of days to anthesis and silking in ambient conditions in 2015. Overall, no consistent effect of elevated O_3 treatment was observed on hybrid flowering traits. B73-Mo17 NILs also showed no consistent trend on effect of flowering traits (Figure 1.3). In 2016, under elevated O_3 the time to anthesis and silking was longer by approximately a half day for line B73, but had no significant effect on ASI. This treatment effect was not repeated in

2017. This is likely due to environmental variation between the 2016 and 2017 growing seasons. The field season in 2016 was a wet year with above average rainfall while 2017 experienced drought conditions. Overall, there were no consistent trends observed in flowering time traits under oxidative stress.

Height and Ear Height

In 2013, exposure to elevated [O_3] significantly increased ($p < 0.001$) plant height by treatment effect in a set of 203 diverse inbred lines. In 2013, Mo17 ear height was significantly reduced ($p = 0.005$) under elevated [O_3]. In 2016, Mo17 height was also significantly reduced ($p= 0.004$) under elevated [O_3]. Overall, there were no consistent trends observed for height or ear height under elevated O_3 treatments (Table 1.4).

Ear Measurements

In B73 x Mo17 checks, ear length and diameter were significantly reduced under elevated O_3 compared to ambient O_3. Ear row number and kernels per row were not affected by O_3 (Figure 1.4). Hybrid ear length and diameter were significantly reduced under elevated O_3 compared to ambient conditions, with lines B73 x Mo17, B73 x NC350, B73 x Hp301, and B73 x CML333 most affected (Figure 1.5). Ear row number and the number of kernels per row were not significantly affected in hybrids (Figure 1.6). Inbred check B73 ear length was significantly reduced under elevated O_3 compared to ambient O_3 (Figure 1.7). The Mo17 check had less replication than the B73 check, but reduction in ear length appears more pronounced for Mo17 under elevated O_3. Inbred ear length was also significantly reduced under elevated O_3, with lines Hp301, Ki3, and C123 most affected (Figure 1.8). Ear row number and the number of kernels per row were significantly reduced under elevated O_3 in inbred lines Ki3 and C123 (Figure 1.9). Inbred lines Ki3 and C123 had non-uniform plot stands and reduced plant counts in each year of the experiment under ambient and elevated conditions. In short, these two inbred lines appeared to have inconsistent germination and growth patterns.

Understanding and breeding for yield is difficult because it is a complex quantitative trait, which makes the genetic basis remain unclear (Egli 2017). Therefore components are often used as a proxy to explain the genetic basis of yield QTLs (Yang et al. 2015). The "yield component method" is a pre-harvest estimation of grain yield via estimating the components that are thought to constitute overall yield. The components include ear row number, kernels per row, ear diameter, ear length, and kernel size (Lu et al. 2011). Ear row number and kernels per row are

strongly determined by genetics as opposed to environment and are predetermined early in development (Nielsen 2003). Ear length and diameter are based on genetics but can also be significantly affected by environment (Elmore & Abendroth 2016).

Ear size determination begins by the time a maize plant reaches V6 and finishes seven to ten days prior to silk emergence (Ritchie et al. 1993). Stress occurring during specific stages of maize plant development can affect yield components. It has been reported that stress during ear initiation and early formation (V6-V15) will reduce ear diameter and ear length. Additionally, ear elongation occurs at VT/R1 and if stress occurs in this time period the total length can be decreased. Yield losses have been estimated up to 13% per day of stress during this time period in hybrid maize lines (Shaw & Newman 1991, Abendroth et al. 2011). Inadequate nitrogen during this period can reduce ear diameter and ear length (Johnson 2013), and drought conditions during this time period can decrease ear length (Elmore & Abendroth 2016). Ears grown under elevated [O_3] showed significant reductions in length and diameter, while ear row number and kernels per row were not reduced. This implies that the ear diameter is being reduced during grain filling. It is not due to a decrease in number of kernels but rather a reduction in their size. These results suggest that the reduction in hybrid grain yield under elevated O_3 could be driven by reduced size/weight of individual kernels rather than by differences in kernel number. In contrast, the effects of elevated O_3 on open pollinated inbred ears were more variable and effect was not significant. Yendrek et al. (2017) investigated the effect of elevated [O_3] on gas exchange of the leaf subtending the ear. Measurements were taken on the leaf subtending the ear because previous research has established that most of the photosynthate used for grain filling in maize is provided by mid-canopy leaves after anthesis (Borras et al. 2004). Yendrek et al's. (2017) work suggests that a key trait for improvement of maize response to elevated [O_3] is maintenance of photosynthetic capacity during the grain filling period. Additionally, images of the harvested ears have been taken by Leakey et al. (*unpublished*) for high-throughput analysis of ear traits. Ear length and diameter manual measurements will be correlated with image analysis results when the dataset is available. Kernel size traits were digitally measured by Leakey et al. (*unpublished*) using the protocol described in Miller et al. (2017) and are currently be analyzed. Taken all together, this is suggestive that maize plants are experiencing stress under elevated [O_3] conditions that effect ear development during ear elongation and kernels are likely

most impacted during grain filling at the blister (R2), milk (R3), or dough (R4) stages of development.

CONCLUSIONS

A multi-year analysis of diverse maize inbred and hybrid lines showed no consistent effects on flowering and height traits when grown under elevated [O_3]. There are different trends observed in different genotypes in different years. This is most likely due to the number of replicates per genotype for a given year. Maize ears grown under elevated [O_3] have significantly reduced length and diameter, but ear row number and kernels per row are not affected. Results suggest that the reduction in hybrid grain yield under elevated O_3 could be driven by reduced size/weight of individual kernels rather than by differences in kernel number. Lines B73 x Mo17, B73 x NC350, B73 x Hp301, and B73 x CML333 were the most affected. In contrast, the effects of elevated O_3 on open pollinated inbred ears were more variable and effect was not significant. In B73 x Mo17 checks, ear length and diameter were significantly reduced under elevated O_3 compared to ambient O_3. While, the Mo17 check had less replication than the B73 check, it was observed that reduction in ear length appears more pronounced for Mo17 under elevated O_3. This research suggests that there is sufficient genotypic variation in maize ear characteristics response to O_3 induced stress that it can be utilized to not only find genotypes that are more resistant, but to also understand the underlying mechanism that results in increased sensitivity and resistance.

FIGURES AND TABLES

Table 1.1 Multi-Year (2013-2015) Analysis of the Effects of [O_3] on Flowering Traits. A multi-year analysis from 2013-2015 was completed using ASReml (Gilmour et al. 2009). Individual year statistical analysis was performed on plot means using a model with ring pair, geno, and geno:treatment and treatment:ring The multiple year analysis was performed on plot means using a model with year, treatment, year:treatment, geno, treatment:geno, year:geno and year:treatment:ring. Direction of effect is indicated by color coding; orange indicates significant decrease of trait values in elevated conditions and blue indicates significant decrease of trait values in ambient conditions. The analysis showed a significant year by treatment effect, but no consistent trends.

ASReml Model	Ozone Treatment Effect on Flowering Trait					
	Anthesis Days	Silking Days	ASI Days	Anthesis GDD	Silking GDD	ASI GDD
INBRED 2013	Trt p=0.004	Trt p=0.01	Trt:Geno p=0.03	Trt p=0.006 Trt:Geno p=0.016	Trt p=0.0114	Trt:Geno p=0.006
INBRED 2014	ns	ns	ns	ns	ns	ns
INBRED 2015	ns	ns	ns	ns	ns	ns
INBRED all years	Year:Trt p=0.01	ns	Trt:Geno p=0.01	Year:Trt p= 0.0125	Year:Trt p=0.008	Trt:Geno p= 0.06
HYBRID 2014	ns	ns	ns	ns	ns	ns
HYBRID 2015	ns	ns	ns	ns	ns	ns
HYBRID all years	ns	ns	ns	ns	ns	ns

Figure 1.1 Effect of Elevated [O_3] on Flowering Traits in Diverse Hybrid Lines. Maize hybrid lines were grown under four ambient rings (~40 ppb) and four elevated [O_3] rings (~100 ppb) at the FACE research facility. In 2014, B73 x Mo17 was planted as a check and replicated ten times within each hybrid ring for a total of 80 plots across the experiment. All other hybrid genotypes were replicated one time within each ring for a total of eight plots across the experiment. B73 x Mo17 was planted as a check and replicated nine times within each hybrid ring for a total of 64 plots across the experiment. Lines B73 x C123, B73 x Hp301 were replicated nine times within each hybrid ring for a total of 64 plots across the experiment. All other hybrid genotypes were replicated five times within each ring for a total of 40 plots across the experiment. GDD were determined using research site weather station data. ASI was calculated from GDD by subtracting silking date from anthesis date. Statistical analysis was performed on plot means. (A) Effect on hybrid lines in 2014. (B) Effect on hybrid lines in 2015. Treatment by genotype box-and-whisker plots show no significant effect of elevated O_3 treatment on maize hybrids flowering traits.

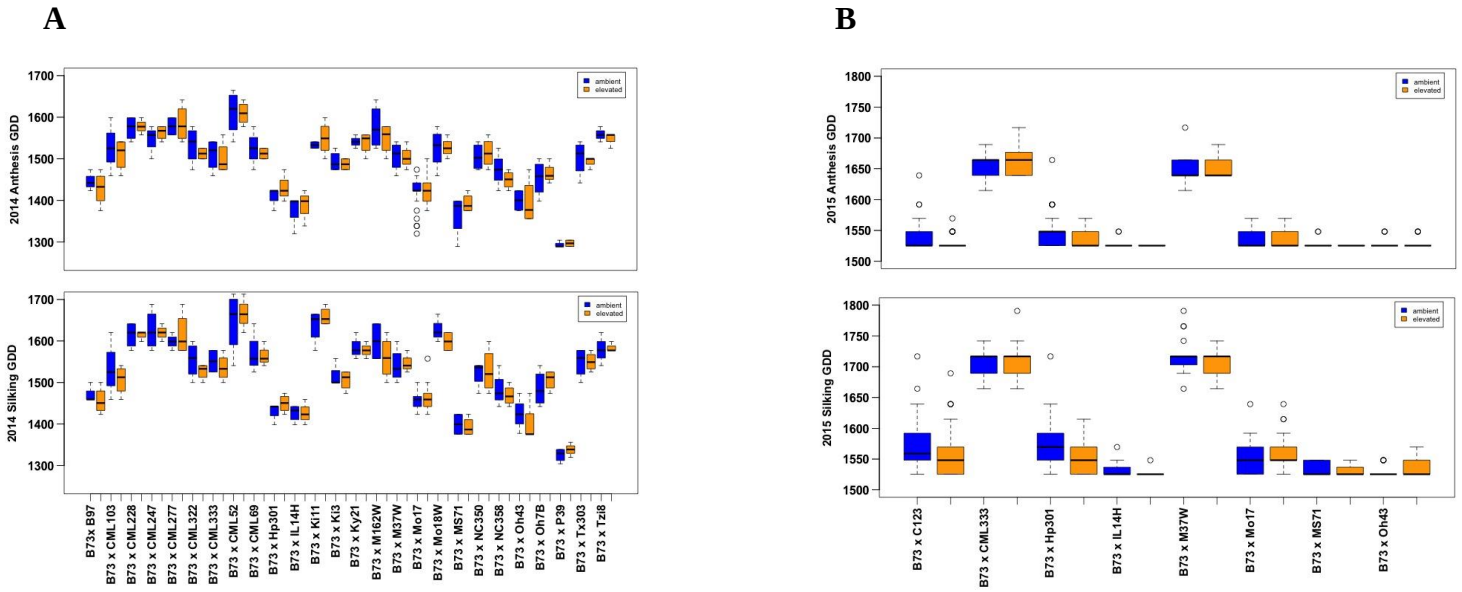

Figure 1.2 Effect of Elevated [O_3] on Flowering Traits in Diverse Inbred Lines. Maize inbred lines were grown under four ambient (~40 ppb) and four elevated [O_3] (~100 ppb) rings at the FACE research facility. In 2014, B73 was planted as check and replicated ten times within each inbred ring for a total of 80 plots across the experiment. All other inbred genotypes were replicated one time within each ring for a total of eight plots across the experiment. In 2015, B73 was planted as check and replicated eight times within each inbred ring for a total of 64 plots across the experiment. Lines Mo17, C123, and Hp301 were replicated eight times within a ring for a total of 64 plots across the experiment. All other inbred genotypes were replicated five times within each ring for a total of 40 plots across the experiment. GDD were determined using research site weather station data. ASI was calculated from GDD by subtracting anthesis date from silking data. Statistical analysis was performed on plot means. (A) Effect on inbred lines in 2014. (B) Effect on inbred lines in 2015. Treatment by genotype box-and-whisker plots show no significant effect of elevated O_3 treatment on maize inbred flowering traits.

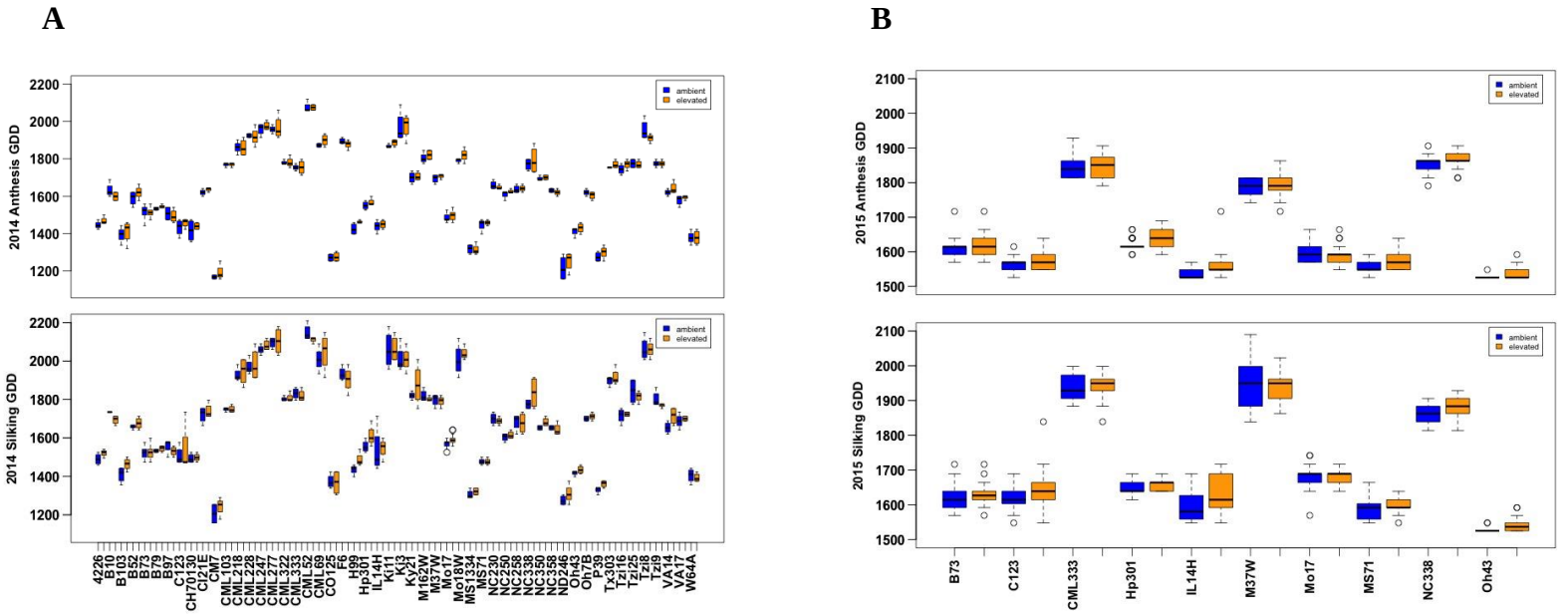

Table 1.2 Inbred Independent T-tests (2013-2015) for the Effects of [O_3] on Flowering Traits. In 2015, elevated O_3 significantly decreased Hp301, Il14H, NC338, and Oh43 anthesis and silking, but not ASI. Ms71 anthesis was also decreased in elevated [O_3]. Results differed between years due to the number of replicates per genotype. Orange indicates significant decrease of trait values in elevated conditions and blue indicates significant decrease of trait values in ambient conditions.

Year	Line	Replication	Ozone Treatment Effect on Flowering Trait					
			Anthesis GDD	Anthesis days	Silking GDD	Silking days	ASI GDD	ASI Days
2015	B73	n= 4	ns	ns	ns	ns	ns	ns
	C123	n= 4	ns	ns	ns	ns	ns	ns
	CML333	n= 4	ns	ns	ns	ns	ns	ns
	Hp301	n= 4	0.0048	0.0052	0.0031	0.003	ns	ns
	Il14H	n= 4	0.0371	0.0334	0.0552	0.0549	ns	ns
	M37W	n= 4	ns	ns	ns	ns	ns	ns
	Mo17	n= 4	ns	ns	ns	ns	ns	ns
	MS71	n= 4	0.0216	0.0216	ns	ns	ns	ns
	NC338	n= 4	0.0248	0.0213	0.0052	0.0051	ns	ns
	Oh43	n= 4	0.0069	0.0072	0.0066	0.0068	ns	ns
2014	Hp301	n= 4	ns	ns	ns	ns	ns	ns
	Il14H	n= 4	ns	ns	ns	ns	ns	ns
	MS71	n= 4	ns	ns	ns	ns	ns	ns
	NC338	n= 4	ns	ns	ns	ns	ns	ns
	Oh43	n= 4	ns	ns	ns	ns	ns	ns
2013	Hp301	n= 2	ns	ns	ns	ns	ns	ns
	Il14H	n= 2	ns	ns	ns	ns	ns	ns
	MS71	n= 2	ns	ns	ns	ns	ns	ns
	NC338	n= 2	ns	ns	ns	ns	ns	ns
	Oh43	n= 2	ns	ns	ns	ns	ns	ns

Table 1.3 Hybrid Independent T-tests (2013-2015) for the Effects of [O_3] on Flowering Traits. Line B73 x Hp301 had a marginally significant decrease of days to anthesis and silkings in ambient conditions in 2015. Overall, no significant effect of elevated O_3 treatment was observed on hybrid flowering traits. Statistical analysis was performed on plot means using a model with ring pair, geno, and geno:treatment. Direction of effect is indicated by color coding; orange indicates significant decrease of trait values in elevated conditions and blue indicates significant decrease of trait values in ambient conditions.

Year	Line	Replication	Ozone Treatment Effect on Flowering Trait					
			Anthesis GDD	Anthesis days	Silking GDD	Silking days	ASI GDD	ASI days
2015	B73 x C123	n= 4	ns	ns	ns	ns	ns	ns
	B73 x CML333	n= 4	ns	ns	ns	ns	ns	ns
	B73 x Hp301	n= 4	0.0267	0.0269	0.0149	0.0143	ns	ns
	B73 x Il14H	n= 4	ns	ns	ns	ns	ns	ns
	B73 x M37W	n= 4	ns	ns	ns	ns	ns	ns
	B73 x MO17	n= 4	ns	ns	ns	ns	ns	ns
	B73 x MS71	n= 4	ns	ns	ns	ns	ns	ns
	B73 x Oh43	n= 4	ns	ns	ns	ns	ns	ns
2014	B73 x Hp301	n= 4	ns	ns	ns	ns	ns	ns

Figure 1.3 Effect of Elevated [O_3] on Flowering Traits in B73 Checks 2016-2017. Maize B73 NILs and Mo17 NILs developed by Eichten et al. (2011) were grown under four ambient (~40 ppb) and four elevated [O_3] (~100 ppb) rings at the FACE research facility. The B73 check was replicated five times within each ring for a total of 40 plots across the experiment. In 2016, days to silking and anthesis were marginally longer under elevated [O_3] for B73. The effect was not observed in 2017. Flowering traits for B73 in 2016; (A) days to anthesis, (B) days to silking, (C) ASI. Flowering traits for B73 in 2017; (D) days to anthesis, (E) days to silking, (F) ASI. ***significant at $p < 0.001$, **significant at $p < 0.01$. This effect was not consistent and likely due to environmental variation between years. No significant effect when flowering time measured as GDD.

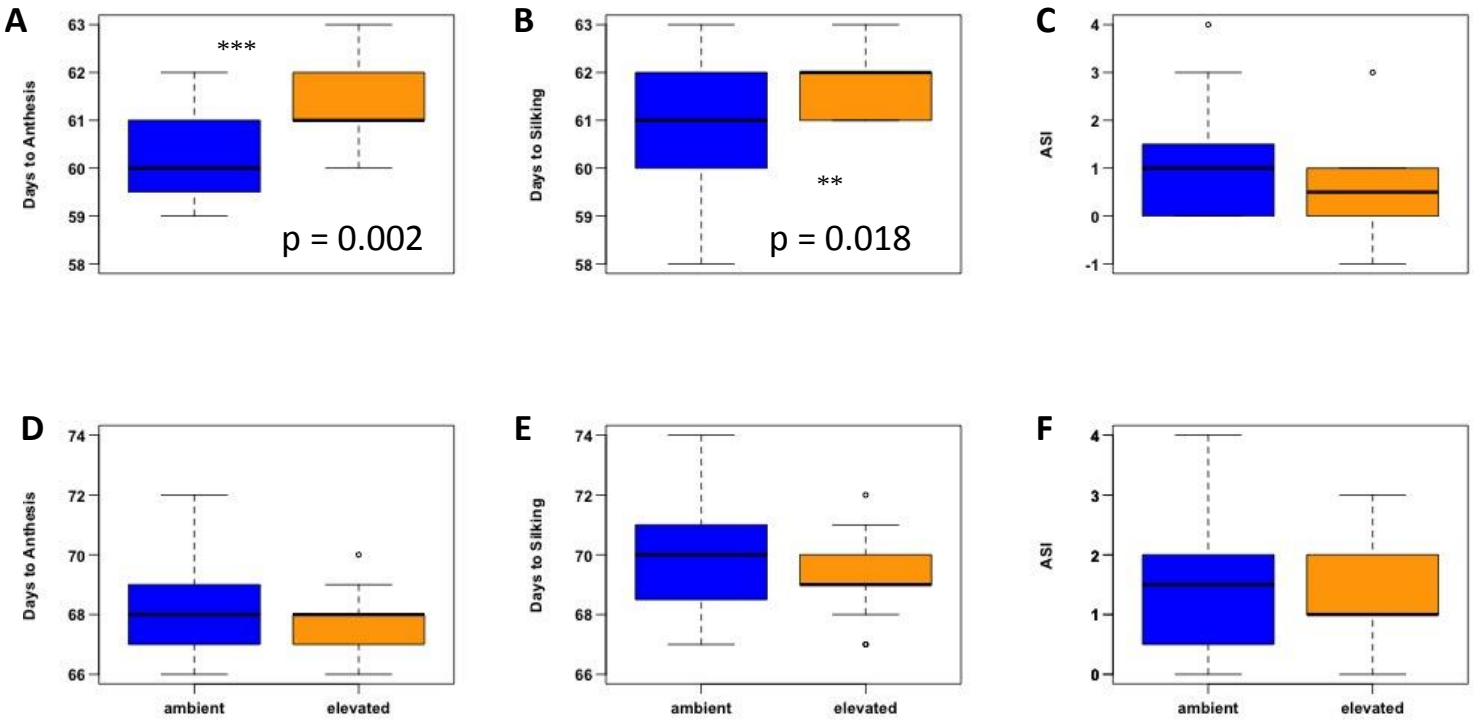

Table 1.4 Effect of [O_3] on Maize Height and Ear Height. Height and ear height measurements were taken for all designated plants at 43 DAP and 90 DAP. Total height was defined as ground level to the flag leaf. Ear height was defined as ground level to the shank of the primary ear. Each year observed different direction of genotype specific effects and no overall trend by treatment. There were no consistent trends observed for height or ear hight under elevated O_3 treatments. Direction of effect is indicated by color coding; orange indicates significant decrease of trait values in elevated conditions and blue indicates significant decrease of trait values in ambient conditions.

Population and Year	Number of Genotypes	Replicates by Treatment	Ozone Treatment Effect on Height Trait			
			Total Height 43 DAP	Total Height 90 DAP	Ear Height 43 DAP	Ear Height 90 DAP
Inbreds 2013	203	2	ns	By trt increased p < 0.001	ns	Mo17 decreased p = 0.005
Inbreds 2014	52	4	ns	ns	ns	ns
Inbreds 2015	10	4	ns	ns	ns	ns
Hybrids 2014	26	4	ns	ns	ns	ns
Hybrids 2015	8	4	ns	ns	ns	ns
B73 Checks 2016	1	4	ns	ns	ns	ns
Mo17Checks 2016	1	4	ns	Mo17 decreased p = 0.004	ns	ns
B73 Checks 2017	1	4	ns	ns	ns	ns
Mo17 Checks 2017	1	4	ns	ns	ns	ns

Figure 1.4 Effect of Elevated [O_3] on Ear Traits on the Hybrid Check. In 2014, B73 x Mo17 was planted as a check and replicated ten times within each hybrid ring for a total of 80 plots across the experiment. A total of 1,130 ears were measured. In 2015, B73 x Mo17 was planted as a check and replicated nine times within each hybrid ring for a total of 64 plots across the experiment. A total of 145 ears were measured. Ear length and diameter were significantly reduced under elevated O_3 compared to ambient O_3. Ear row number and kernels per row were not affected. ***significant at $p < 0.001$, *significant at $p < 0.05$. (A) Ear length (mm), (B) Ear diameter (mm), (C) Ear row number mean, and (D) Kernels per row mean.

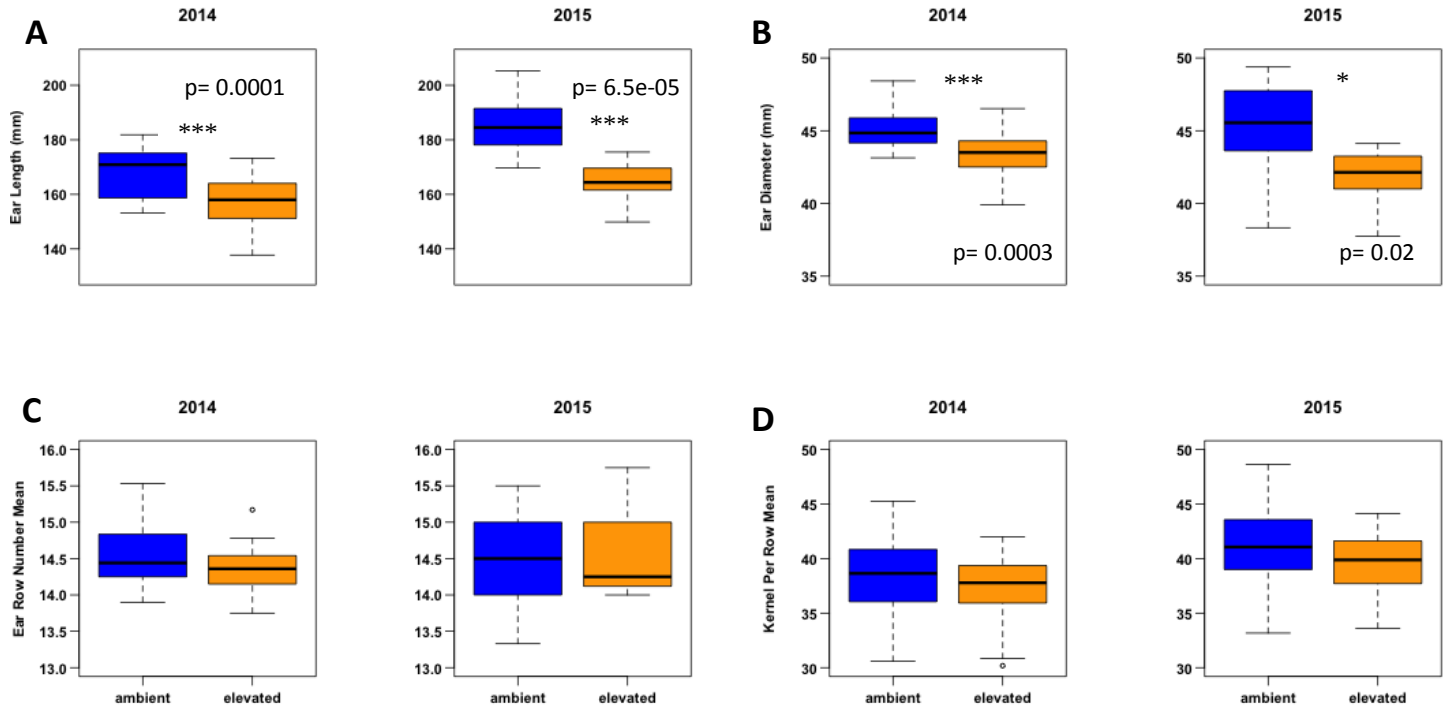

Figure 1.5 Effects of [O_3] on Ear Length and Diameter by Hybrid Genotype. Hybrids Ear length and diameter were significantly reduced under elevated O_3 compared to ambient conditions, with B73 x Mo17, B73 x NC350, B73 x Hp301, and B73 x CML333 most affected. ***significant at $p < 0.001$, **significant at $p < 0.01$, *significant at $p < 0.05$. (A) 2014 ear length and diameter genotype by treatment (B) 2015 ear length and diameter genotype by treatment.

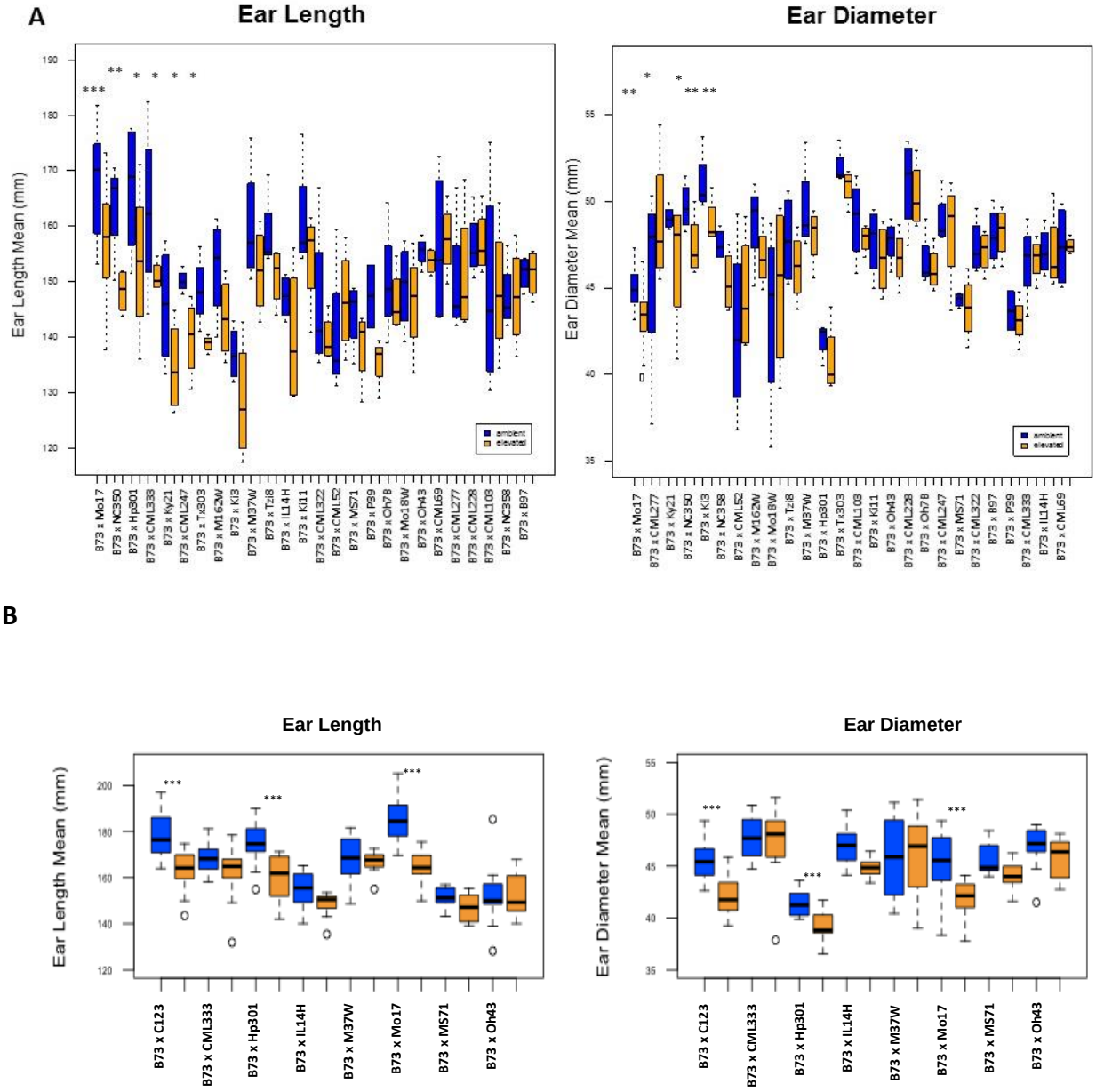

Figure 1.6 Effects of [O_3] on Ear Row Number and Kernels Per Row by Hybrid Genotype. No significant effects on hybrid ear row number or kernels per row were observed. (A) 2014 ear row number and kernels per row genotype by treatment (B) 2015 ear row number and kernels per row genotype by treatment.

A

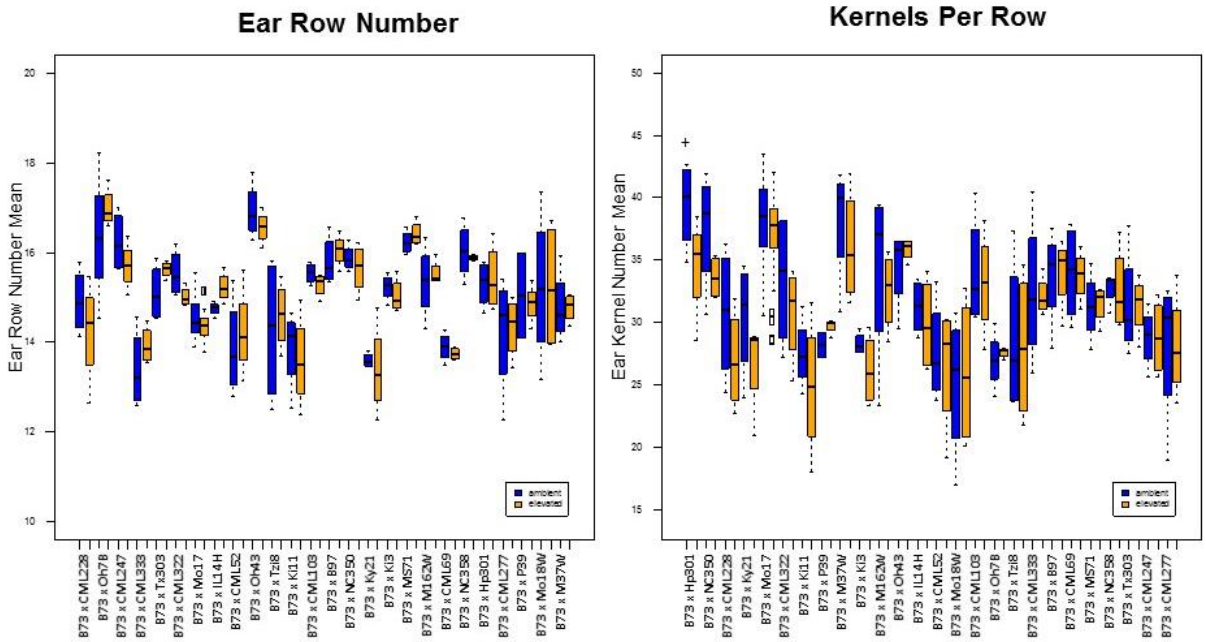

B

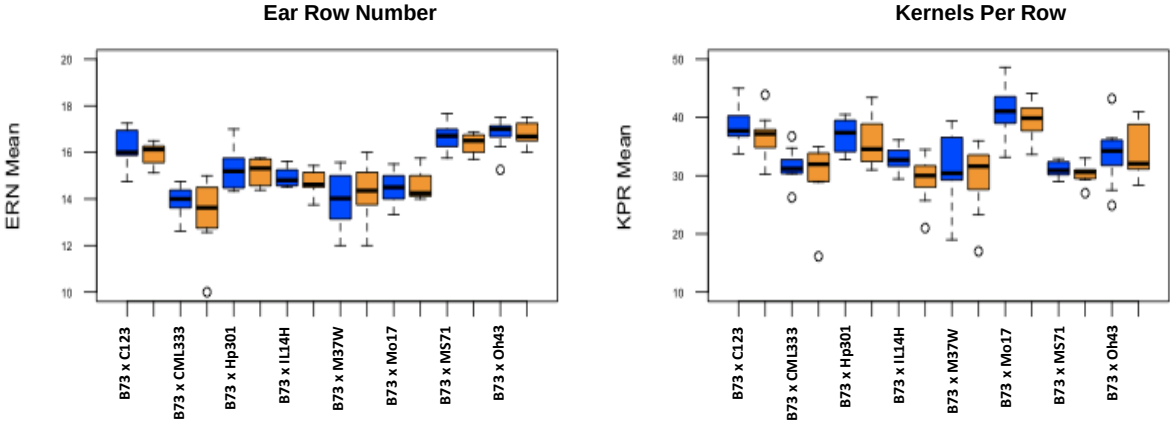

Figure 1.7 Effect of Elevated [O_3] on Ear Traits on Inbred Checks. B73 ear length was reduced under elevated O_3 compared to ambient O_3 in 2014. The Mo17 check had less replication than the B73 check, but reduction in ear length appears more pronounced under elevated O_3 for Mo17. In 2014, B73 was planted as check and replicated ten times within each inbred ring for a total of 80 plots across the experiment. Mo17 was replicated one time within each ring for a total of eight plots across the experiment. In 2015, B73 and Mo17 were planted eight times within each inbred ring for a total of 64 plots across the experiment. (A) 2014 results, (B) 2015 results.

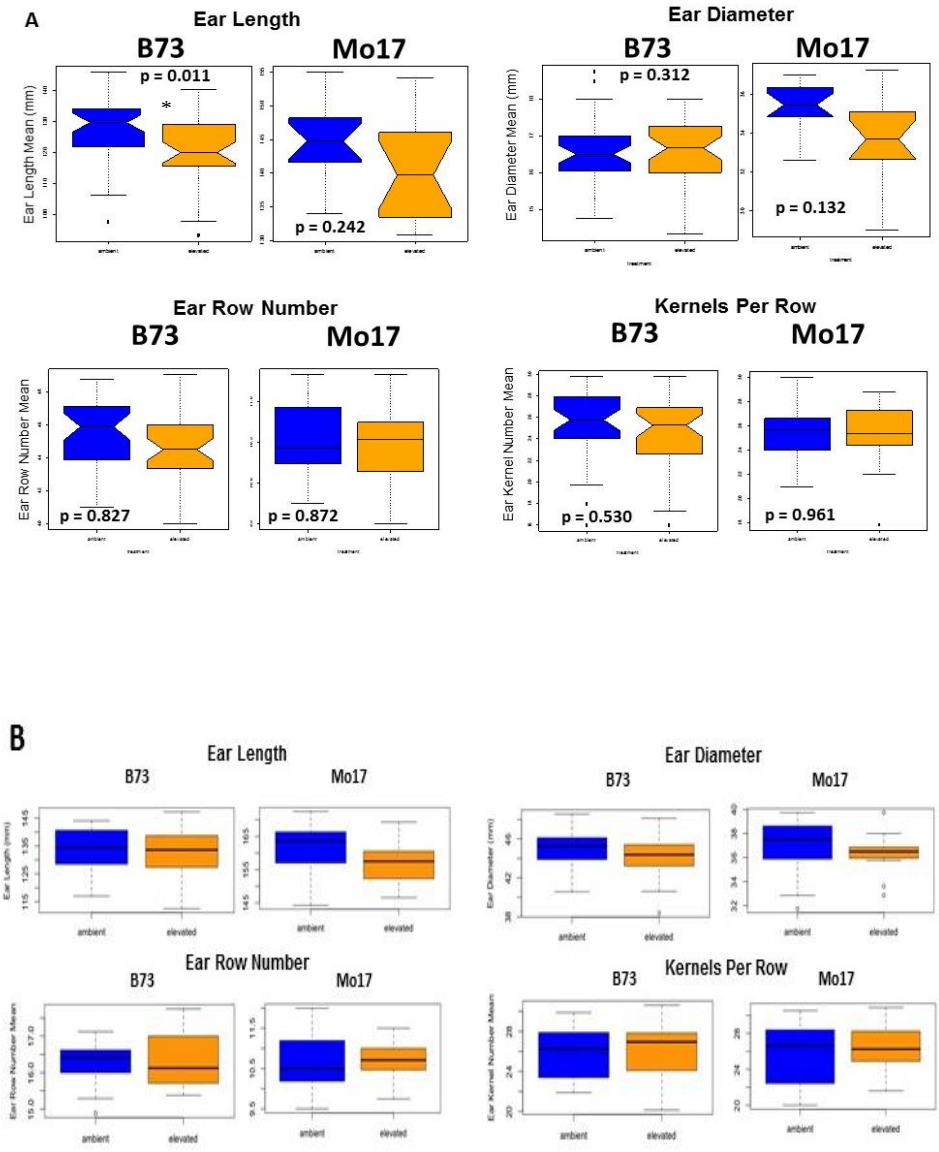

Figure 1.8 Effect of Elevated [O_3] on Inbred Ear Length and Diameter. Inbred ear length was significantly reduced under elevated O_3. ***significant at $p < 0.001$, **significant at $p < 0.01$, *significant at $p < 0.05$. (A) 2014 ear length and diameter genotype by treatment (B) 2015 ear length and diameter genotype by treatment.

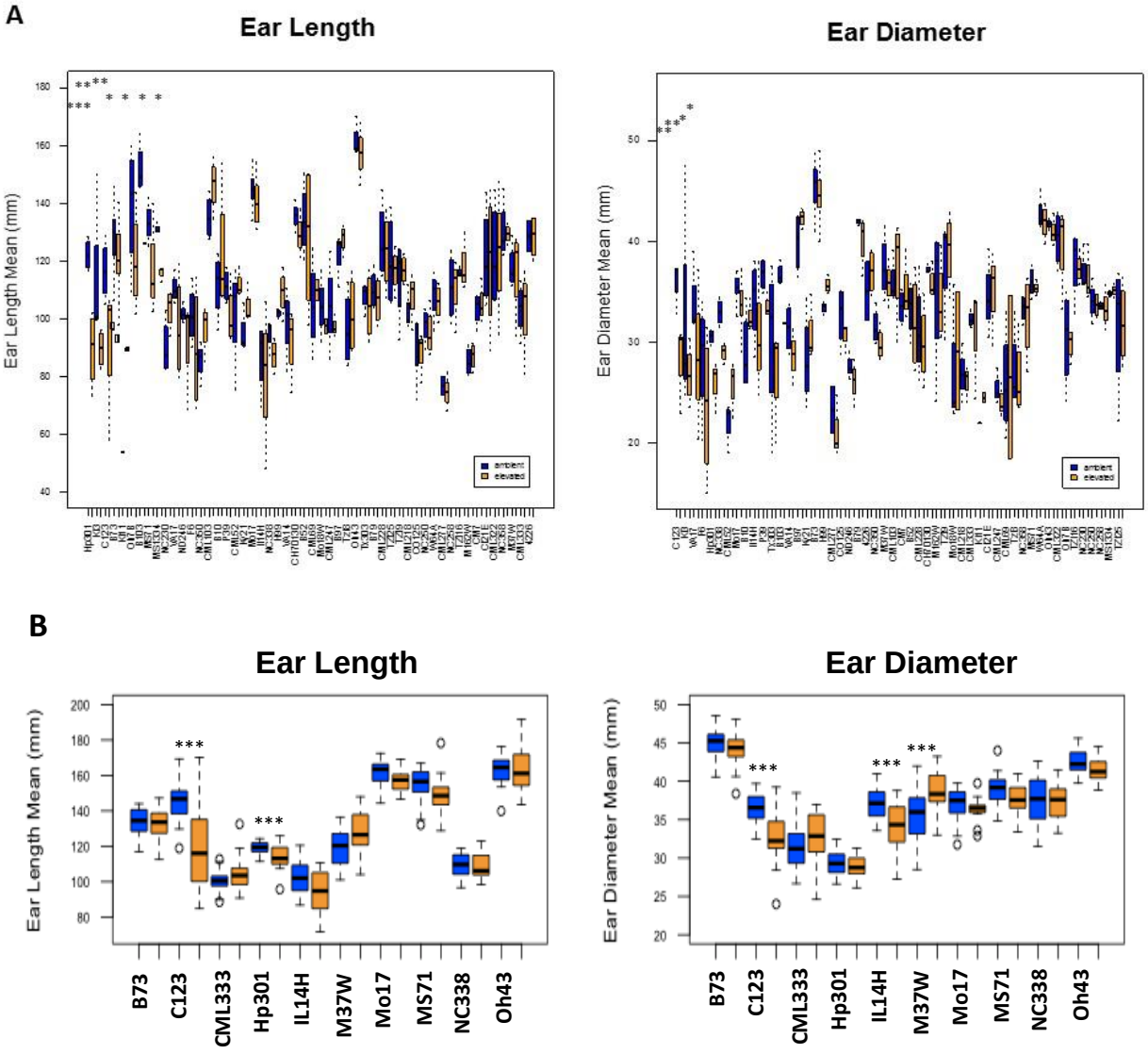

Figure 1.9 Effect of Elevated [O_3] on Inbred Ear Row Number and Kernels Per Row. Inbred lines Ki3 and C123 had non-uniform plot stands and reduced plant counts in each year of the experiment under ambient and elevated conditions. These two inbred lines appeared to have inconsistent germination and growth patterns. Open pollinated inbred ears were more variable for traits ear row number and kernels per row and effect was not significant. ***significant at $p < 0.001$, **significant at $p < 0.01$, *significant at $p < 0.05$. (A) 2014 ear row number and kernels per row genotype by treatment (B) 2015 ear row number and kernels per row genotype by treatment.

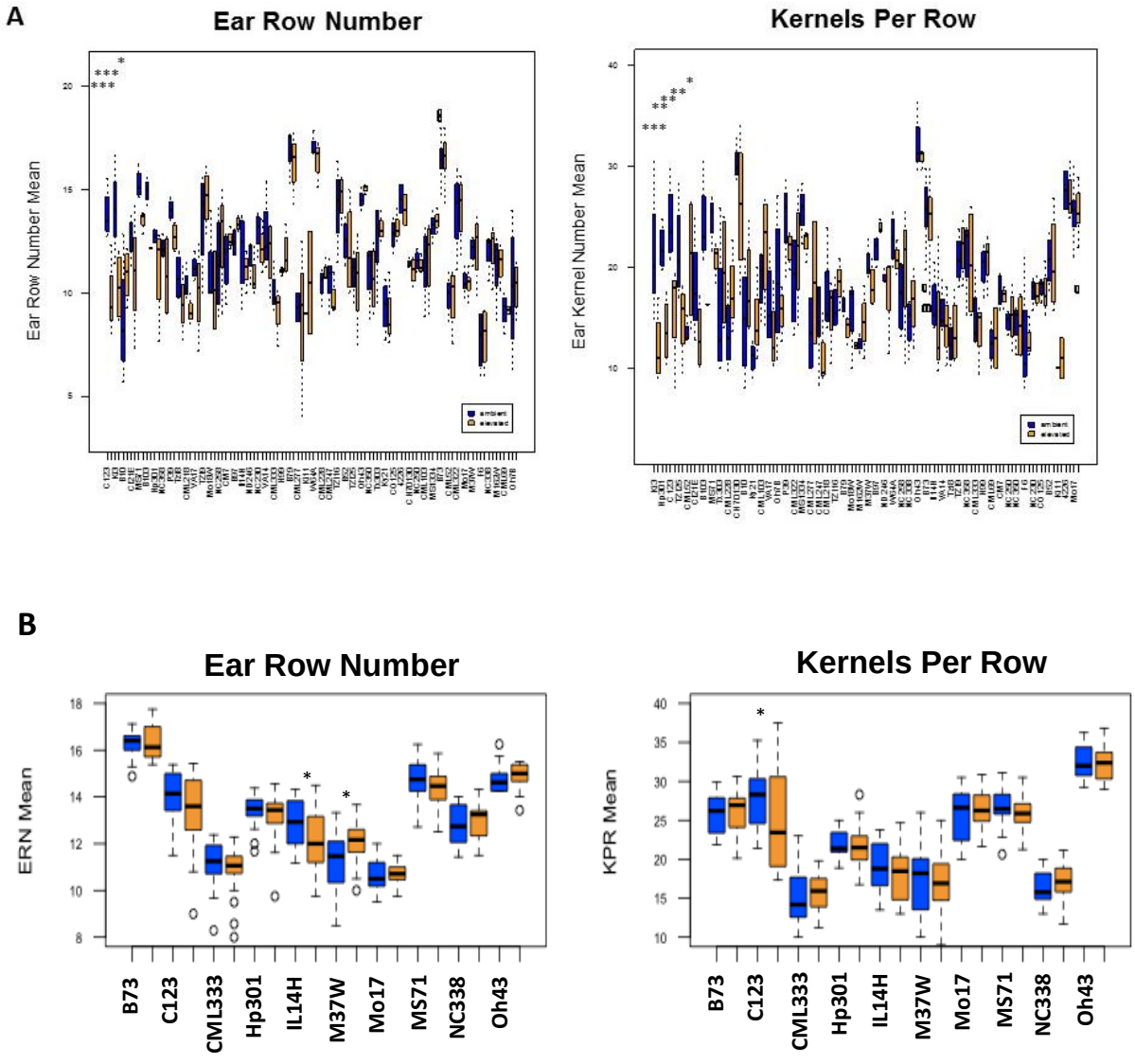

REFERENCES CITED

Abendroth, L. J., R.W. Elmore, M.J. Boyer, & Marlay, S.K. (2011). Corn growth and development. Iowa State University Extension Publication, #PMR–1009.

Ainsworth, E. A. (2017). Understanding and improving global crop response to ozone pollution. The Plant Journal, 90(5), 886-897.

Ainsworth, E. A., Serbin, S. P., Skoneczka, J. A., & Townsend, P. A. (2014). Using leaf optical properties to detect ozone effects on foliar biochemistry. Photosynthesis Research, 119(1-2), 65-76.

Betzelberger, A.M., Gillespie, K.M., McGrath, J.M., Koester, R.P., Nelson, R.L., & Ainsworth, E.A. (2010). Effects of chronic elevated ozone concentration on antioxidant capacity, photosynthesis and seed yield of 10 soybean cultivars. Plant Cell Environment, 33(9), 1569–1581.

Bita, C., & Gerats, T. (2013). Plant tolerance to high temperature in a changing environment: scientific fundamentals and production of heat stress-tolerant crops. Frontiers in Plant Science, 4(1), 273.

Black, V.J., Black, C.R., Roberts, J.A., & Stewart, C.A. (2000). Tansley review no. 115, Impact of ozone on the reproductive development of plants. The New Phytologist, 147(3), 421–447.

Borrás, L., Slafer, G. A., & Otegui, M. E. (2004). Seed dry weight response to source–sink manipulations in wheat, maize and soybean: a quantitative reappraisal. Field Crops Research, 86(2-3), 131-146.

Egli, D.B. (2017). Seed biology and yield of grain crops, 2nd Edition (CABI).

Eichten, S.R., Foerster, J.M., de Leon, N., Kai, Y., Yeh, C.T., Liu, S., Jeddeloh, J.A., Schnable, P.S., Kaeppler, S.M., & Springer, N.M., (2011). B73-Mo17 near-isogenic lines demonstrate dispersed structural variation in maize. Plant Physiology, 156(4), 1679-1690.

Elmore, R. & Abendroth, R. (2016). Number of rows and kernels set early in season. Iowa State University Extension, Integrated Crop Management Extension Newsletter, #IC-496.

Feng, Z., & Kobayashi, K. (2009). Assessing the impacts of current and future concentrations of surface ozone on crop yield with meta-analysis. Atmospheric Environment, 43(8), 1510–1519.

Gilmour, A.R., Gogel, B.J., Cullis, B.R., & Thompson, R. (2009). ASReml user guide release 3.0 VSN International Ltd., Hemel Hempstead, HP1 1ES, UK.

Johnson, G. (2013). Reduced ear size problems in sweet corn. University of Delaware State Extension, Weekly Crop Update #15.

Lee, E.H., Tingey, D.T., & Hogsett, W.E. (1988). Evaluation of ozone exposure indices in exposure-response modeling. Environmental Pollution, 53(1-4), 43–62.

Leisner, C.P., & Ainsworth, E.A. (2012). Quantifying the effects of ozone on plant reproductive growth and development. Global Change Biology, 18(2), 606–616.

Lu, M., Xie, C.X., Li, X.H., Hao, Z.F., Li, M.S., Weng, J.F., Zhang, D.G., Bai, L. & Zhang, S.H. (2011). Mapping of quantitative trait loci for kernel row number in maize across seven environments. Molecular Breeding, 28(2), 143-152.

Lv, Y., Liang, Z., Ge, M., Qi, W., Zhang, T., Lin, F., Peng, Z. & Zhao, H. (2016). Genome-wide identification and functional prediction of nitrogen-responsive intergenic and intronic long non-coding RNAs in maize (Zea mays L.). BMC Genomics, 17(1), 350-362.

Mauzerall, D. L., & Wang, X. (2001). Protecting agricultural crops from the effects of tropospheric ozone exposure: reconciling science and standard setting in the United States, Europe, and Asia. Annual Review of Energy and the Environment, 26(1), 237-268.

McGrath, J.M., Betzelberger, A.M., Wang, S., Shook, E., Zhu, X.-G., Long, S.P., & Ainsworth, E.A. (2015). An analysis of ozone damage to historical maize and soybean yields in the United States. PNAS, 112(46), 14390–14395.

Miller, N. D., Haase, N. J., Lee, J., Kaeppler, S. M., Leon, N., & Spalding, E. P. (2017). A robust, high-throughput method for computing maize ear, cob, and kernel attributes automatically from images. The Plant Journal, 89(1), 169-178.

Morgan, P.B., Bernacchi, C.J., Ort, D.R., & Long, S.P. (2004). An in vivo analysis of the effect of season-long open-air elevation of ozone to anticipated 2050 levels on photosynthesis in soybean. Plant Physiology, 135(4), 2348–2357.

Nielsen, R.L. (2003). Ear initiation and size determination in corn. News Network, Agronomy Deptment, Purdue University Extension, 20-33.

NOAA (2018). Stratospheric Ozone Page. http://www.ozonelayer.noaa.gov/index.htm

Pleijel, H., Danielsson, H., Gelang, J., Sild, E., & Selldén, G. (1998). Growth stage dependence of the grain yield response to ozone in spring wheat (Triticum aestivum L.). Agriculture, Ecosystems & Environment, 70(1), 61–68.

R Core Team. (2015). R: A language and environment for statistical computing. R Foundation for Statistical Computing, Vienna, Austria.

Rao, M.V., & Davis, K.R. (1999). Ozone-induced cell death occurs via two distinct mechanisms in Arabidopsis: the role of salicylic acid. The Plant Journal, 17(6), 603–614.

Rao, M. V., Lee, H. I., Creelman, R. A., Mullet, J. E., & Davis, K. R. (2000). Jasmonic acid signaling modulates ozone-induced hypersensitive cell death. The Plant Cell, 12(9), 1633-1646.

Ritchie, S.W., J.J. Hanway, & G.O. Benson. (1993). How a corn plant develops. Iowa State University, Special Report Number 48.

Shaw, R.H. & Newman, J.E. (1991). Weather stress in the corn crop. Purdue University Cooperative Extension Service, #NCH-18.

Shi, G., Yang, L., Wang, Y., Kobayashi, K., Zhu, J., Tang, H., Pan, S., Chen, T., Liu, G., & Wang, Y. (2009). Impact of elevated ozone concentration on yield of four Chinese rice cultivars under fully open-air field conditions. Agriculture, Ecosystems & Environment, 131(2-3), 178–184.

Suriyagoda, L. D., Ryan, M. H., Renton, M., & Lambers, H. (2014). Plant responses to limited moisture and phosphorus availability–a meta-analysis. Advances in Agronomy, 124(1), 133-200.

Tang, H., Liu, G., Han, Y., Zhu, J., & Kobayashi, K. (2011). A system for free-air ozone concentration elevation with rice and wheat: control performance and ozone exposure regime. Atmospheric Environment, 45(35), 6276–6282.

Wilkinson, S., Mills, G., Illidge, R., & Davies, W.J. (2012). How is ozone pollution reducing our food supply? Journal of Experimental Botany, 63(2), 527–536.

Yang, C., Liu, J., & Rong, T.Z. (2015). Detection of quantitative trait loci for ear row number in F2 populations of maize. Genetics and Molecular Research, 14(4), 14229–14238.

Yendrek, C.R., Erice, G., Montes, C.M., Tomaz, T., Sorgini, C.A., Brown, P.J., McIntyre, L.M., Leakey, A.D. and Ainsworth, E.A. (2017). Elevated ozone reduces photosynthetic carbon gain by accelerating leaf senescence of inbred and hybrid maize in a genotype-specific manner. Plant, Cell & Environment, 40(12), 3088-3100.

Zhu, X., Feng, Z., Sun, T., Liu, X., Tang, H., Zhu, J., Guo, W., & Kobayashi, K. (2011). Effects of elevated ozone concentration on yield of four Chinese cultivars of winter wheat under fully open-air field conditions. Global Change Biology, 17(8), 2697–2706.

CHAPTER 2

MAPPING LEAF DAMAGE QTL IN FIELD-GROWN NEARLY ISOGENIC LINES

ABSTRACT

Knowledge about the identity and location of agriculturally important QTL provides the basis for marker assisted selection in breeding programs. Few studies have mapped maize responses to elevated O_3. A two year study of leaf damage in field grown maize nearly isogenic lines was completed to identify maize QTL associated with variation in O_3-induced oxidative stress. Based on preliminary data showing that Mo17 was more susceptible to O_3 than B73, 100 B73-Mo17 NILs were screened in the field under ambient (~40 ppb) and elevated (~100 ppb) [O_3] at the FACE research facility in Savoy, IL. Leaf damage was scored on a 0-9 scale in two successive years at two time points: on the 5th true leaf at 43 DAP and on the 2nd leaf below the flag leaf at 90 DAP. Leaf damage was measured at two time points in 2016, and since the difference between parents was much greater at 43 DAP, this time point was used in 2017. Leaf damage was significantly higher in elevated O_3 rings in both B73 (90 DAP measurement only) and Mo17 (43 DAP & 90 DAP measurements). Mo17 was more sensitive than B73 in the early measurement, and some Mo17 NILs were much more sensitive than Mo17. In Mo17 NILs, a significant leaf damage QTL for the 43 DAP measurement was identified at ~161Mb on chromosome 2. Surprisingly, B73 introgressions into Mo17 in this region made NILs more susceptible. Leaf damage scores from the field in 2016 and 2017 had a strongly significant correlation ($r = 0.93$). Five sensitive Mo17 NILs (m007, m022, m030, m072, and m091) and one tolerant Mo17 NIL (m076) were identified. Two sensitive B73 NILs (b005 and b131) were also identified. Sensitive Mo17 NIL F_2 populations and co-dominant markers that flank the 2-LOD support interval were designed from the Mo17 SNP/Indel track. This research has identified a repeatable O_3 induced leaf damage QTL. This research has also developed populations and markers that can be used in future growth chamber fine mapping experiments.

INTRODUCTION

Variation in the response to O_3 suggests some genetic control. The substantial variation reported in CO_2 and O_3 FACE studies suggests that, at the minimum it is possible to breed for increased resistance. Using modern genetic approaches it is possible to isolate the genes that confer greater resistance. Intraspecific variation to elevated O_3 suggests genetic variation and the ability to detect markers (Betzelberger et al. 2010). Additionally, components of the O_3 sensing

and signaling pathways have been identified as good potential targets for biotechnology to improve crop productivity (Wilkinson et al. 2012). Understanding what leads to this genetic variation in response allows the generation of lines that are more resilient to abiotic stresses. Currently traditional breeding methods are being implemented, although modern genetic approach are highlighting the strength of marker assisted breeding. Linkage mapping in bi-parental crosses can have high power to detect quantitative trait loci (Yu & Buckler 2006, Zhu et al. 2008, Ersoz et al. 2009, Barabaschi et al. 2016). Identifying the associations between genetic markers and phenotypes is a useful tool that can accelerate plant breeding cycles and aid in discovering new molecular breeding approaches. Bi-parental crosses exploit recent recombination events that occurred in the establishment of the population (Lipka et al. 2015). QTL linkage mapping is a statistical correlation of molecular markers and the phenotype of interest. The advent of high throughput molecular technologies has led to breeding program marker-assisted selection (MAS) for desirable traits (He et al. 2014). Once a QTL is identified to be associated with a phenotype it is possible to backcross the QTL into another background or pyramid the QTL with other desirable traits. Additionally, it becomes possible to document the biological function of the QTL that regulates the trait of interest. This approach has been successfully used for many agronomically important traits and crops (Morrell et al. 2012).

Tropospheric O_3 is one of the most important environmental pollutants adversely affecting agriculture (Ainsworth et al. 2008 & 2017). A majority of tropospheric O_3 comes from anthropogenic emissions. Tropospheric O_3 is a direct driver of global warming and has indirect negative effects on plant production. O_3 has been shown to have negative effect on yield and quality traits of crop plants (Betzelberger et al. 2010, Frei et al. 2015). Climate change will have a significant impact on crop productivity and food security (Wheeler & Von Braun 2013) and is exacerbated by elevated [O_3] (Tai et al. 2014). Maize is one of the world's primary agricultural commodities for food, fodder, and fuel (FAO 2018). The global demand for maize crop production is increasing exponentially (Kay et al. 2013). It is estimated that by 2050 agricultural commodities need to sustain more than nine billion people (FAO 2018). Concurrently, it is projected that by 2050 tropospheric O_3 concentrations will increase substantially (Pachauri et al. 2014). Therefore, understanding how maize is affected by O_3-induced oxidative stress will contribute to improving maize crop productivity.

Plants affected by elevated [O_3] show physical symptoms. Elevated [O_3] can cause a range of effects including visible leaf injury. O_3-induced leaf damage traits have been reported for the past 35 years from countries all around the world (Krupa et al. 2001). Visible symptoms in foliar damage resulting from O_3 exposure can be considered as indicators of O_3 injury (Miller 1989). Both acute and chronic O_3 exposure induce oxidative stress due to the production of reactive oxygen species (ROS) in the apoplast (Frei et al. 2015), this production of ROS leads to cell death and necrotic symptoms (Rao & Davis 2001, Kangasjarvi et al. 2005). Chronic injury develops slowly over days to weeks. Chronic injury is characterized by chlorosis, stipple, necrosis, leaf edge yellowing, and premature senescence. Chronic injury is normally induced by long-term, low O_3 concentrations (Brace et al. 1999). A concern in diagnosing O_3-induced leaf damage is the ability to distinguish O_3 symptoms from a wide range of potential symptoms caused by other agents. Therefore, O_3-induced foliar symptoms are best identified through a systematic survey. Assessing leaf damage is important because it is often correlated with a decrease in carbon fixation and a decrease in water use efficiency (Rao & Davis 2001, Kangasjarvi et al. 2005). Leaf damage is much easier to score and thus is a good proxy for O_3 sensitivity/tolerance. Chronic exposure to O_3 can result in foliar damage that can reduce photosynthetic capacity. There is an associated phenotype of leaf bronzing that can be visually assessed and is associated with cell necrosis.

Few genetic mapping studies have been completed to identify QTL for O_3 tolerance (Frei et al. 2008, Brosche et al. 2010, Street et al. 2011, Tsukahara et al. 2013). Mapping is completed in general stages. First, the QTL(s) affecting the trait is broadly mapped. The QTL(s) will define a large genomic region(s) where one or more alleles affecting the trait segregate. The second stage involves fine mapping to focus in on the QTL(s) region to narrow down the genomic intervals containing the gene(s) affecting variation in the trait. In the final stage the causal gene(s) is pin pointed (MacKay et al. 2009). Mapping populations of Arabidopsis (Brosche et al. 2010), poplar (Street et al. 2011), rice (Kim et al. 2004, Frei et al. 2008, Tsukahara et al. 2013), and soybean (Burton et al. 2016) have been utilized and mapped leaf damage QTLs under elevated [O_3]. Most QTL mapping for O_3 tolerance has been completed in rice (Frei 2015). Rice mapping populations and a diversity panel have been screened for O_3 tolerance for both acute and chronic exposure experiments (Kim et al. 2004, Frei et al. 2008, Ueda et al. 2013, Tsukahara et al. 2013 & 2015).

The use of tolerant genotypes is a powerful strategy in adapting maize production to rising O_3 levels (Frei et al. 2015). The aim of this study was to i) assess variation in the tolerance and sensitivity of maize to elevated [O_3] using nearly isogenic lines, ii) identify leaf damage QTL(s) and, iii) develop populations and marker tools for fine mapping to confer O_3 tolerance and/or sensitive lines identified.

MATERIALS AND METHODS

FACE Facility Experimental Design

In 2016 and 2017, 50 B73 NILs (n= 4) and 50 Mo17 NILs (n= 4) developed by Eichten et al. (2011) were grown under ambient (~40 ppb) and elevated [O_3] (~100 ppb) at the FACE research facility. Each NIL line was planted in a single-row 1.65 m plot in four elevated O_3 and four ambient rings. B73 and Mo17 were grown as checks and replicated five times within each ring for a total of 40 plots across the experiment. Each NIL was replicated one time within each ring for a total of 8 plots across the experiment.

Maize was exposed to elevated [O_3] (100 ppb) for eight hours each day from shortly after emergence until physiological maturity. Micro-pores in a segmented tube around the research ring circumference released O_3 according to wind direction and speed. Gas was monitored at the center of the ring and more or less gas was released to meet constant target concentrations. The fumigation system did not operate when leaves were wet or when wind speed dropped below 0.5 ms^{-1}. When the fumigation system was operating, O_3 concentrations were within 20% of the 100 ppb target concentration for 81% of the time.

2016 Field Leaf Damage Scoring

Leaf damage was scored on a 0-9 scale (Figure 2.1) as a plot average at two time points. Foliar disease point scale was modified for leaf damage susceptibility in maize; zero (0-10%) and nine (90-100%) of the leaf area having damage. 43 DAP measurements were taken on the 5th true leaf and 90 DAP measurements were taken on the 2nd leaf below the flag leaf. Leaf scoring was reported in terms of damage. Damage scores were collected independently by two scientists and compared for reliability.

2017 Field Leaf Damage Scoring

Leaf damage was scored on a 0-9 scale at one time point. Foliar disease point scale was modified for leaf damage susceptibility in maize; zero (0-10%) and nine (90-100%) of the leaf

area having damage. 43 DAP measurements were taken on the 5th true leaf. Damage scores were collected independently by two scientists and compared for reliability.

Leaf Damage Statistical Analysis

Data values were calculated separately in elevated and ambient environments. Plot averages were taken for each NIL. Three models were tested and best fit chosen by AIC. The final model included random effects for ring, ring set, and genotype. Ring set is the cardinal direction location of the plot in each ring.

Linkage Mapping

QTL analysis was completed using stepwise regression coded in R (R Core Team 2015). First, a response QTL (Response = Elevated – Ambient) analysis was completed. The QTL analysis was also completed in separate environments. Three models were tested and AIC was used to choose the best fit. The final model included random effects for ring, ring set by ring interaction (ringset:ring), and genotype. Then the QTL analysis was then performed separately in B73 and Mo17 NILs. Additionally, the analysis was run analyzing B73 and Mo17 NILs together with recurrent parent ("RP") as a covariate in the model. Significance thresholds were determined by using 200 permutations and an alpha of 0.05.

Marker Design and Classification

Markers that flanked the identified QTL 2-LOD drop off were designed from the MaizeGDB Mo17 SNPs and indels track as described in Settles et al. (2014). Each marker was tested under common PCR conditions (0.5ul primers, 1.5ul DNA, 0.6 ul DMSO, 9.4ul H20, 12.5ul GO Taq master mix). Thermocycling conditions were as described in Martin et al. (2010); 94°C for 3 minutes, 94°C for 40 seconds, 57°C for 45 seconds, 72°C for 40 seconds, go to step2 for 34x, 72°C for 5 minutes, 10°C infinite hold. Amplified fragments were visualized by electrophoresis on 4%, 3%, and 2% agarose gels (0.5x TBE) stained with gel red at 90V for ~2 hours. Marker classes (dominant, co-dominant, PAV, and not polymorphic) were scored visually from gel images.

Fine Mapping Population Development

In 2015-2017 summer and winter nurseries, populations were developed to fine map in the B73-Mo17 NILs. Mo17 NILs were crossed with Mo17 resulting in an F_1. This F_1 was then selfed to create Mo17 NILs x Mo17 F_2s. Selected B73 NILs were crossed with B73 resulting in

an F_1. These F_1s were then selfed to create F_2s in the summer 2017 nursery. Additionally, in the 2017 summer nursery all B73 NILs were crossed with B73 to create the full F_1 population.

RESULTS AND DISCUSSION

Mo17 was more sensitive than B73 in the early measurement at 43 DAP, and some Mo17 NILs were much more sensitive than Mo17 (Figure 2.2). Leaf damage scores from the field in 2016 and 2017 had a strongly significant correlation (r = 0.93, Figure 2.3). Five sensitive Mo17 NILs (m007, m022, m030, m072, and m091) and one tolerant Mo17 NIL (m076) were identified. Two sensitive B73 NILs (b005 and b131) were identified (Figure 2.3). In Mo17 NILs, a repeatable significant leaf damage QTL was identified on chromosome 2 for the 43 DAP measurement at ~161Mb (Figure 2.4 & Table 2.1). B73 introgressions into Mo17 in this region made NILs more susceptible (Figure 2.4). Sensitive Mo17 NILs identified have on average five total introgression regions. All five sensitive NILs share a common introgression on chromosome 2 at ~ 161Mb. All the left hand boundaries of the LOD drop off support interval (Table 2.2) for this QTL cross the centromere (Figure 2.5 & Table 2.3), which can reduce the chances of recovering recombinants. Six out of eleven markers were classified as co-dominant (Figure 2.6 & Table 2.4). Co-dominant markers umc2125 at 64.9Mb (AGPv2) and IDP6768 at 178.2 Mb (AGPv2) can be used to screen for F_2 recombinants. The shortcoming of such a classical QTL study is that the resolution of mapping is limited by the number of genetic recombination events occurring in the mapping populations (Lipka et al. 2015). Populations have been created to fine map resistance in m076, sensitivity in b005 and b131, and sensitivity in Mo17 NILs (m007, m022, m030, m072, and m091). Sensitive B73 NILs (b005 and b131) have a two shared introgressions: one on chromosome 5 that is 1.86Mb and another on chromosome 6 that is 7.95 Mb. Resistant NIL m076 has six small homozygous introgressions on four chromosomes. A (m076 x Mo17) F_2 population has been generated to determine which region(s) is/are responsible. Interestingly, B73 introgressions into Mo17 in this region made NILs more susceptible (Figure 2.4). The direction of the QTL effect was unexpected since previous data had shown that B73 is more tolerant to elevated O_3 than Mo17. Although, just because B73 is more tolerant overall does not mean that it will have the tolerant allele for all QTL. However, it is still unexpected that only one major QTL was detected and the effect was in this direction. Other O_3 studies have reported multiple smaller QTL for leaf damage mapping.

B73 introgressions into Mo17 make it more susceptible. There are several possible explanations that could be investigated to resolve this result, i) genetic background matters, ii) there is cytoplasmic inheritance, or iii) the B73 alleles have been unmasked. At this time it is inconclusive, if the Mo17 introgression into B73 in this region has no effect. All NILs were derived from a B73 x Mo17 hybrid with B73 cytoplasm. An experiment using F_2 populations to determine whether the cytoplasm (B73 versus Mo17) has an effect on the detection of the QTL effect could be completed. F_2 populations can determine whether the QTL effect is only present in certain cytoplasms. To test for genetic background effects B73 NILs with a Mo17 introgression in this location could be leveraged. When particular natural variants are placed into different backgrounds the phenotypic consequences of that allele may be profoundly different than in their own background (Chandler et al. 2013). Genetic background effects have been observed in most genetically tractable organisms where isogenic lines are used, including mice (Strunk et al. 2004), nematodes (Remold & Lenski 2004), fruit flies (Gibson & van Helden1997), yeast (Dowell et al. 2010), rice (Cao et al. 2007), Arabidopsis (Huang et al. 2010) and bacteria (Wang et al 2014).

CONCLUSIONS

This research has identified a repeatable O_3 induced leaf damage QTL on chromosome 2 ~161Mb. This research has also developed populations and markers that can be used in future growth chamber fine mapping experiments.

FIGURES AND TABLES

Figure 2.1 Leaf Damage Scale. Leaf damage was scored on a 0-9 scale. Visual rating scales were adapted from foliar disease scoring methods. Not shown: '0' mark for no damage,'1' and '2' marks, and the '9' mark for a dead leaf. (A) Cartoon interpretation of percentage leaf damage coverage. (B) Field pictures of leaf damage.

A

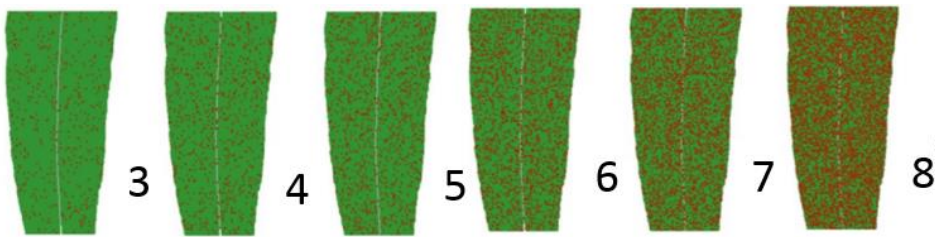

B

Figure 2.2 Leaf Damage Response. 43 DAP and 90 DAP measurements shown. Solid vertical line indicates overall mean. Dashed vertical lines indicate means of parental (B73 and Mo17) checks. (Top) 2016 measurements, (Bottom) 2017 measurements. No 90 DAP measurement was taken in 2017. B73-Mo17 NIL screens showed that Mo17 was more susceptible to O_3 than B73 in the early measurement. And, some Mo17 NILs were much more sensitive than Mo17.

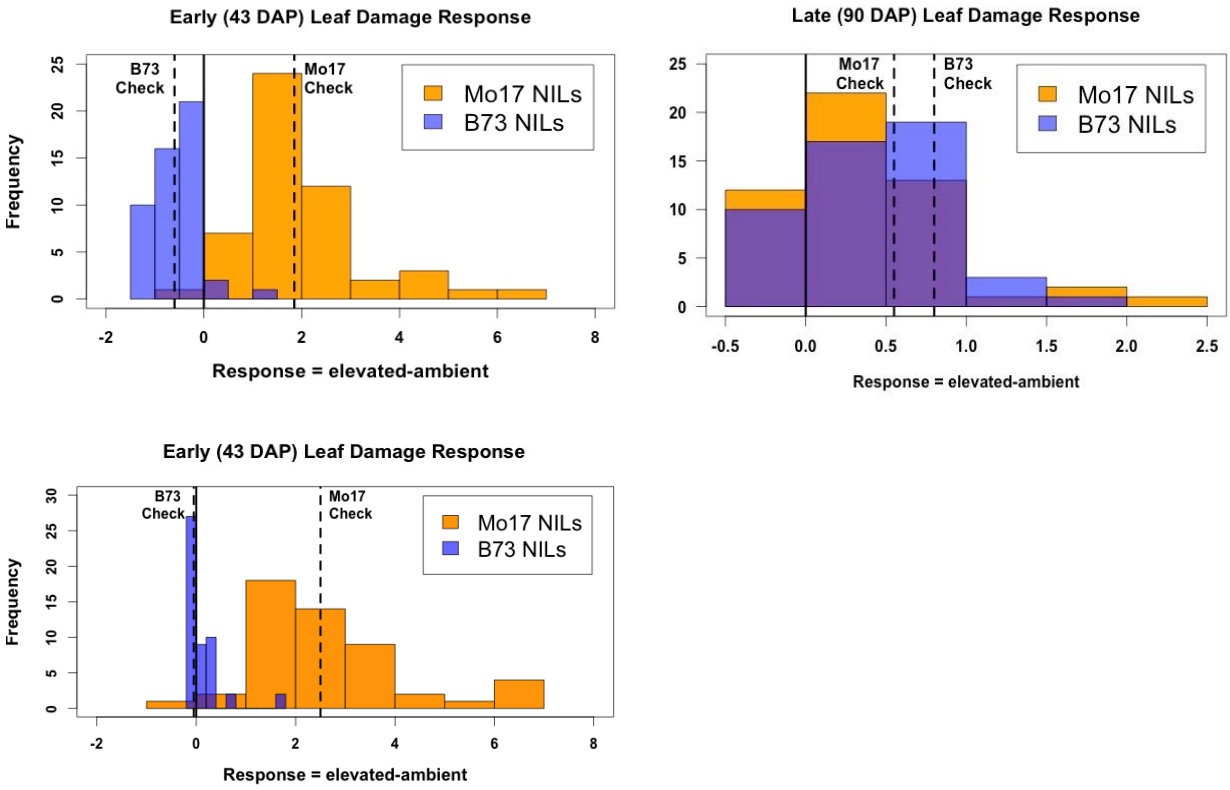

Figure 2.3 Field Leaf Damage Correlation. 2017 leaf damage scores were plotted against 2016 leaf damage scores and the correlation calculated (r = 0.94). Sensitive (m007, m022, m030, m072, m091, b005, and b131) and tolerant (m076) identified NILs are labeled.

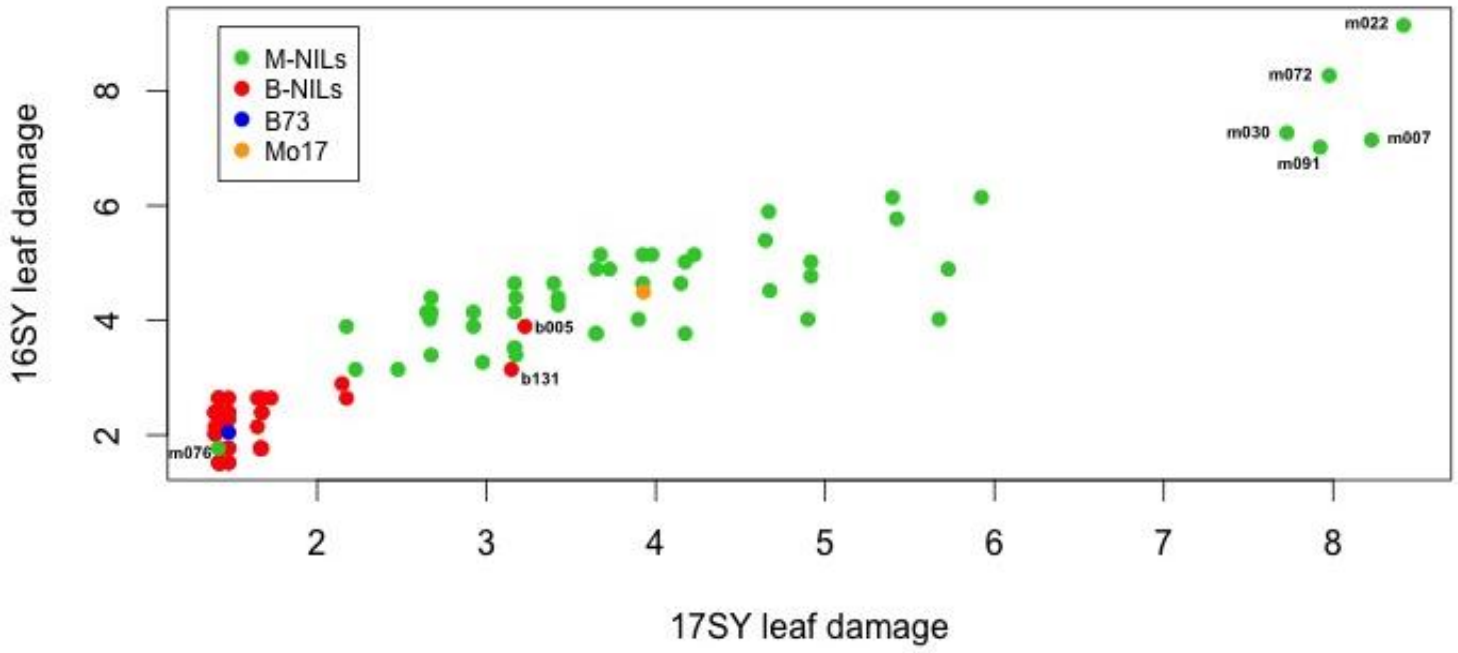

Figure 2.4 Leaf Damage Response QTL. 2016 measurements identified a suspected leaf damage QTL on Chr 2 ~161Mb. In, 2017 complete replication in the field validates the same QTL on Chr 2 ~161Mb. Combined Years analysis reveals the same QTL on Chr 2 ~161Mb. Threshold significance was determined by using 200 permutations, alpha of 0.05. Surprisingly, one large QTL was detected and B73 alleles into the Mo17 background in this region made NILs more susceptible. (Top) 2016 results, (Middle) 2017 results, (Bottom) 2016 and 2017 combined data results. (Left) QTL mapping results, (Right) QTL effects.

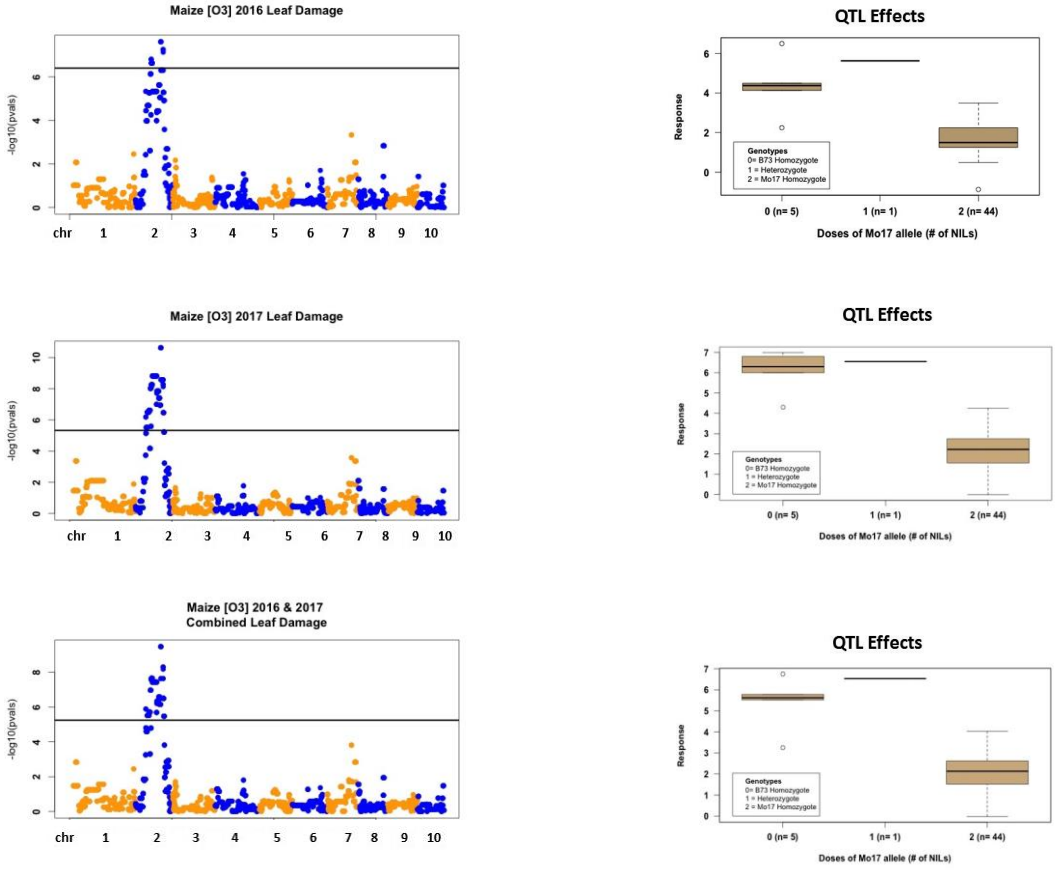

Table 2.1 Stepwise Regression QTL Linkage Mapping Results. Mo17 NILs were analyzed separate from B73 NILs. "RP" = B73 and Mo17 NILs analyzed together with recurrent parent as a covariate. Geno effect indicates if the model was run as a response QTL or separately in the elevated ("ele") environment. Geno[1782,] = Chr.2 160938561.9bp 135.22cM (AGPv2). In stepwise regression the SNP previously identified is added to the model and rerun. Threshold significance was determined by using 200 permutations, alpha of 0.05.

Data Values	Time Point	Geno Effect	Collection Year	Step1 [geno,]	Step2 [geno,]	Step3 [geno,]
Mo17 NIL	43DAP	response	16SY	1782***	4982^{NS}	1896^{NS}
Mo17 NIL	43DAP	response	17SY	1782***	5519^{NS}	2425^{NS}
Mo17 NIL	43DAP	response	16SY+17SY	1782***	5519^{NS}	393^{NS}
Mo17 NIL	43DAP	ele	16SY	1782***	2081^{NS}	3109^{NS}
Mo17 NIL	43DAP	ele	17SY	1782***	2425^{NS}	5519^{NS}
Mo17 NIL	43DAP	ele	16SY+17SY	1782***	4985^{NS}	2500^{NS}
RP	43DAP	response	16SY	1782***	1506^{NS}	1491^{NS}
RP	43DAP	response	17SY	1782***	6801^{NS}	5519^{NS}
RP	43DAP	response	16SY+17SY	1782***	5519^{NS}	876^{NS}
RP	43DAP	ele	16SY	1782***	1506^{NS}	1491^{NS}
RP	43DAP	ele	17SY	1782***	6801^{NS}	5519^{NS}
RP	43DAP	ele	16SY+17SY	1782***	5519^{NS}	876^{NS}

Table 2.2 Leaf Damage QTL LOD Support Intervals. Boundaries of the 1-LOD, 1.5-LOD, and 2-LOD drop off support intervals for the identified QTL were calculated.

Data Collection Year	LOD Drop Off Support	Left Interval Position (bp) AGPv2	Left Interval Position (cM) AGPv2	Right Interval Position (bp) AGPv2	Right Interval Position (cM) AGPv2	Support Interval Size (Mb)
2016	2-LOD	58,587,858.75	119.55	~184,137,304.8	140.01	125.5
	1.5-LOD	58,587,858.75	119.55	~184,137,304.8	140.01	125.5
	1-LOD	~62,736,623.57	122.55	~184,137,304.8	140.01	121.4
2017	2-LOD	78,020,679.50	128.96	163,562,440.5	136.61	85.5
	2+ LOD	78,020,679.50	128.96	177,871,738.0	139.58	99.8
	1.5-LOD	160,938,561.90	135.22	163,562,440.5	136.61	2.6
	1-LOD	160,938,561.90	135.22	163,562,440.5	136.61	2.6
2016 and 2017 Combined	2-LOD	~62,736,623.57	122.55	~178,293,533.5	140.01	115.5
	1.5-LOD	160,938,561.90	135.22	~178,293,533.5	140.01	17.3
	1-LOD	160,938,561.90	135.22	163,562,440.5	136.61	2.6

Figure 2.5 Leaf Damage QTL on Chromosome 2 and LOD Support Intervals. Mapping results for (Top) 2016 results, (Middle) 2017 results, (Bottom) 2016 and 2017 combined data results. (Left) Identified leaf damage QTL peak on chromosome with 2-LOD support interval boundary. (Right) Close up view of QTL peak on chromosome 2 with 1-LOD, 1.5-LOD, and 2-LOD drop off support interval boundaries (AGPv2).

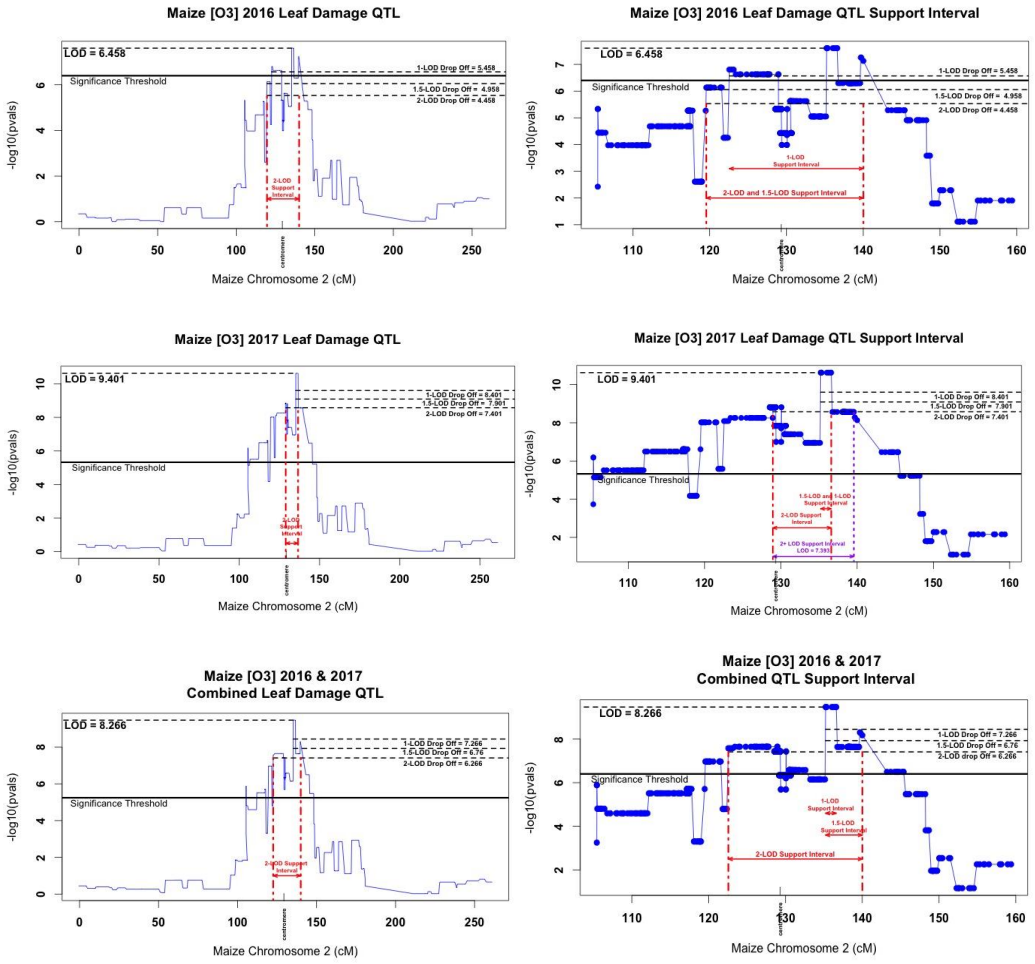

Table 2.3 Chromosomal Features Near the Identified QTL. The location of the LOD drop off support interval for the identified QTL cross the centromere, which can reduce the probability of recovering recombinants. B73-Mo17 NILs were designed in the genome draft AGPv2 and converted to AGPv3 because the Mo17 SNP/INDEL track is in AGPv3. The current genome build release for the B73 reference genome is AGPv4, which is shown for comparison.

Feature	Chromosome	Position (bp) AGPv2	Position(cM) AGPv2	Position (bp) AGPv3	Position (bp) AGPv4
QTL Peak	2	160,938,561.90	135.22	161,572,157	165,495,915
Centromere	2	93,935,718.50	129.31	94,566,099	96,718,457

Table 2.4 Mo17 SNP/Indel Track Marker Classifications. Markers from (Settles et al. 2014) are designed to amplify annotated insertion-deletion polymorphisms of seven base pairs or greater between B73 and Mo17. Results of marker classification are shown in the last column.

Locus Name	B73v2 Chr	B73 Product Start	B73 Product Stop	W22 Product	B73 Product	Size Difference	% Difference	B73/W22 Indel Marker	B73/Mo17 Marker Class
IDP7860	2	57,743,599	57,744,366	542	768	226	29%	PCR InDel	co-dominant
umc2125	2	64,930,287	64,930,445	171	159	12	7%	PCR InDel	co-dominant
TIDP7149	2	83,334,820	83,335,380	585	561	24	4%	PCR InDel	Not polymorphic
IDP6805	2	164,859,410	164,859,784	354	375	21	6%	PCR InDel	B73 dominant
IDP9040	2	170,635,010	170,635,682	599	673	74	11%	PCR InDel	PAV
IDP3909	2	173,944,658	173,945,064	378	407	29	7%	PCR InDel	B73 dominant
IDP4142	2	175,092,085	175,092,503	452	419	33	7%	PCR InDel	co-dominant
IDP7292	2	187,881,371	187,881,955	464	585	121	21%	PCR InDel	co-dominant
IDP7761	2	169,494,453	169,494,832	985	380	605	61%	PCR InDel	PAV
umc1755	2	174,609,765	174,609,861	103	97	6	6%	PCR InDel	co-dominant
IDP6768	2	178,224,010	178,224,308	602	299	303	50%	PCR InDel	co-dominant

Figure 2.6 Marker Classification Using Gel Images. Gels were run on 4% 0.5 TBE gel at 90V for two hours. (A) Markers IDP7860, umc2125, and IDP6805. (B) Markers IDP9040, IDP3909, IDP4142, and IDP7191. (C) Markers IDP7761, umc1755, and IDP6768. (D) Close up view of co-dominant marker IDP6768. PCR amplification was completed with B73, Mo17, and 1:1 Inbred DNAs. Co-dominant markers identified can be utilized to screen F_2s for recombinants. Recovered recombinants can be advanced to the F_3 for fine mapping. Three bands represent a co-dominant marker that can be utlized to screen for recombinants in the F_2 population.

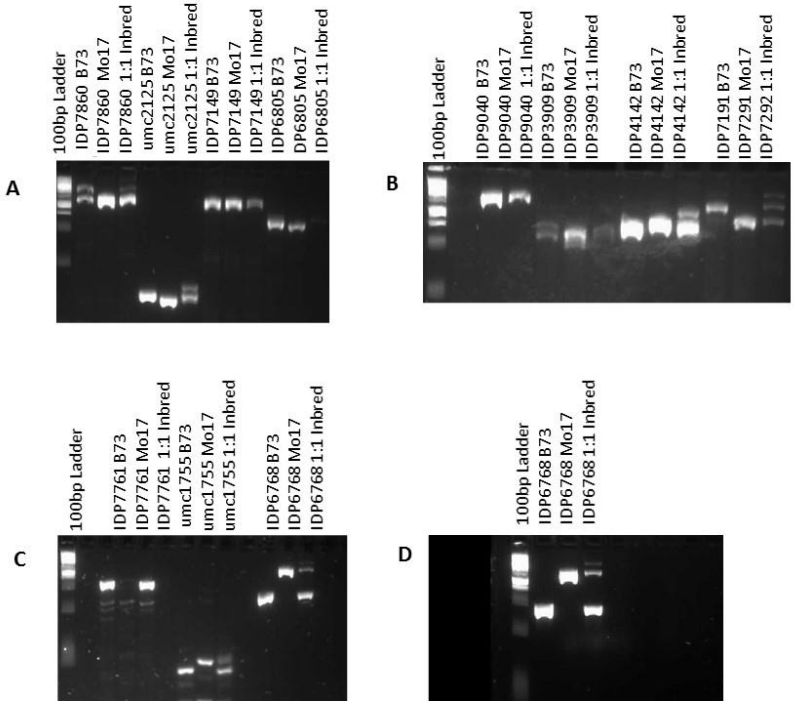

REFERENCES CITED

Ainsworth, E. A. (2017). Understanding and improving global crop response to ozone pollution. The Plant Journal, 90(5), 886-897.

Ainsworth, E. A., Rogers, A., & Leakey, A. D. (2008). Targets for crop biotechnology in a future high-CO_2 and high-O_3 world. Plant Physiology, 147(1), 13-19.

Barabaschi, D., Tondelli, A., Desiderio, F., Volante, A., Vaccino, P., Valè, G., & Cattivelli, L. (2016). Next generation breeding. Plant Science, 242(1), 3–13.

Betzelberger, A.M., Gillespie, K.M., McGrath, J.M., Koester, R.P., Nelson, R.L., & Ainsworth, E.A. (2010). Effects of chronic elevated ozone concentration on antioxidant capacity, photosynthesis and seed yield of 10 soybean cultivars. Plant, Cell, & Environment, 33(9), 1569–1581.

Brace, S., Peterson, D. L., & Bowers, D. (1999). A guide to ozone injury in vascular plants of the Pacific Northwest. US Department of Agriculture, Forest Service, Pacific Northwest Research Station.

Brosché, M., Merilo, E., Mayer, F., Pechter, P., Puzõrjova, I., Brader, G., Kangasjärvi, J., & Kollist, H. (2010). Natural variation in ozone sensitivity among Arabidopsis thaliana accessions and its relation to stomatal conductance. Plant, Cell, & Environment, 33(6), 914–925.

Burton, A.L., Burkey, K.O., Carter, T.E., Orf, J., & Cregan, P.B. (2016). Phenotypic variation and identification of quantitative trait loci for ozone tolerance in a Fiskeby III × Mandarin (Ottawa) soybean population. Theoretical and Applied Genetics, 129(6), 1113–1125.

Cao, Y., Ding, X., Cai, M., Zhao, J., Lin, Y., Li, X., Xu, C. & Wang, S. (2007). The expression pattern of a rice disease resistance gene Xa3/Xa26 is differentially regulated by the genetic backgrounds and developmental stages that influence its function. Genetics, 177(1), 523-533.

Chandler, C.H., Chari, S. & Dworkin, I. (2013). Does your gene need a background check? How genetic background impacts the analysis of mutations, genes, and evolution. Trends in Genetics, 29(6), 358-366.

Dowell, R.D., Ryan, O., Jansen, A., Cheung, D., Agarwala, S., Danford, T., Bernstein, D.A., Rolfe, P.A., Heisler, L.E., Chin, B. & Nislow, C. (2010). Genotype to phenotype: a complex problem. Science, 328(5977), 469-469.

Eichten, S.R., Foerster, J.M., Leon, N. de, Kai, Y., Yeh, C.-T., Liu, S., Jeddeloh, J.A., Schnable, P.S., Kaeppler, S.M., & Springer, N.M. (2011). B73-Mo17 near-isogenic lines demonstrate dispersed structural variation in maize. Plant Physiology, 156(4), 1679–1690.

Ersoz, E.S., Yu, J., & Buckler, E.S. (2009). Applications of linkage disequilibrium and association mapping in maize. In Molecular Genetic Approaches to Maize Improvement, P.D.A.L. Kriz, and P.D.B.A. Larkins, eds., Springer, Berlin, Heidelberg, 173–195.

FAO. (2018). FAOSTAT, http://www.fao.org/faostat/en/#home

Frei, M. (2015). Breeding of ozone resistant rice: Relevance, approaches and challenges. Environmental Pollution, 197(1), 144–155.

Frei, M., Tanaka, J.P., & Wissuwa, M. (2008). Genotypic variation in tolerance to elevated ozone in rice: dissection of distinct genetic factors linked to tolerance mechanisms. Journal of Experimental Botany, 59(13), 3741–3752.

Gibson, G. & van Helden, S. (1997). Is function of the Drosophila homeotic gene Ultrabithorax canalized? Genetics, 147(3), 1155-1168.

He, J., Zhao, X., Laroche, A., Lu, Z.-X., Liu, H., & Li, Z. (2014). Genotyping-by-sequencing (GBS), an ultimate marker-assisted selection (MAS) tool to accelerate plant breeding. Frontiers in Plant Science, 5(1), 484-512.

Huang, X., Effgen, S., Meyer, R.C., Theres, K. & Koornneef, M. (2012). Epistatic natural allelic variation reveals a function of AGAMOUS-LIKE6 in axillary bud formation in Arabidopsis. The Plant Cell, 24(6), 2364-2379.

Kangasjarvi, J., Jaspers, P., & Kollist, H. (2005). Signaling and cell death in ozone-exposed plants. Plant, Cell & Environment, 28(8), 1021-1036.

Kay, D.K., Mueller, N.D., West, P.C., & Foley, J.A. (2013). Yield trends are insufficient to double global crop production by 2050. PLOS One, 8(6), 66428-66453.

Kim, K. M., Kwon, Y. S., Lee, J. J., Eun, M. Y., & Sohn, J. K. (2004). QTL mapping and molecular marker analysis for the resistance of rice to ozone. Molecules & Cells, 17(1), 188-207.

Krupa, S., McGrath, M.T., Andersen, C.P., Booker, F.L., Burkey, K.O., Chappelka, A.H., Chevone, B.I., Pell, E.J. & Zilinskas, B.A. (2001). Ambient ozone and plant health. Plant Disease, 85(1), 4-12.

Lipka, A.E., Kandianis, C.B., Hudson, M.E., Yu, J., Drnevich, J., Bradbury, P.J., & Gore, M.A. (2015). From association to prediction: statistical methods for the dissection and selection of complex traits in plants. Current Opinion in Plant Biology, 24(1), 110–118.

Mackay, T. F., Stone, E. A., & Ayroles, J. F. (2009). The genetics of quantitative traits: challenges and prospects. Nature Reviews Genetics, 10(8), 565-572.

Miller J.E., Heagle A.S., Vozzo S.F., Philbeck R.B. & Heck W.W. (1989) Effects of ozone and water-stress, separately and in combination, on soybean yield. Journal of Environmental Quality, 18(3), 330–336.

Morrell, P.L., Buckler, E.S., & Ross-Ibarra, J. (2012). Crop genomics: advances and applications. Nature Reviews Genetics, 13(2), 85–96.

Pachauri, R.K., Allen, M.R., Barros, V.R., Broome, J., Cramer, W., Christ, R., Church, J.A., Clarke, L., Dahe, Q., Dasgupta, P. & Dubash, N.K.. (2014). Climate change 2014: synthesis report. Contribution of Working Groups I, II and III to the fifth assessment report of the Intergovernmental Panel on Climate Change (IPCC), 151.

R Core Team. (2015). R: A language and environment for statistical computing. R Foundation for Statistical Computing, Vienna, Austria.

Rao, M.V., & Davis, K.R. (1999). Ozone-induced cell death occurs via two distinct mechanisms in Arabidopsis: the role of salicylic acid. The Plant Journal, 17(6), 603–614.

Remold, S.K. & Lenski, R.E. (2004). Pervasive joint influence of epistasis and plasticity on mutational effects in Escherichia coli. Nature Genetics, 36(4), 423-437.

Settles, A.M., Bagadion, A.M., Bai, F., Zhang, J., Barron, B., Leach, K., Mudunkothge, J.S., Hoffner, C., Bihmidine, S., Finefield, E. & Hibbard, J. (2014). Efficient molecular marker design using the MaizeGDB Mo17 SNPs and Indels track. G3: Genes, Genomes, Genetics, 4(6), 1143-1145.

Street, N.R., James, T.M., James, T., Mikael, B., Jaakko, K., Mark, B., & Taylor, G. (2011). The physiological, transcriptional and genetic responses of an ozone- sensitive and an ozone tolerant poplar and selected extremes of their F2 progeny. Environmental Pollution, 159(1), 45–54.

Strunk, K.E., Amann, V. & Threadgill, D.W. (2004). Phenotypic variation resulting from a deficiency of epidermal growth factor receptor in mice is caused by extensive genetic heterogeneity that can be genetically and molecularly partitioned. Genetics, 167(4), 1821-1832.

Tai, A. P., Martin, M. V., & Heald, C. L. (2014). Threat to future global food security from climate change and ozone air pollution. Nature Climate Change, 4(9), 817.

Tsukahara, K., Sawada, H., Kohno, Y., Matsuura, T., Mori, I.C., Terao, T., Ioki, M. & Tamaoki, M. (2015). Ozone-induced rice grain yield loss is triggered via a change in panicle morphology that is controlled by ABERRANT PANICLE ORGANIZATION 1 gene. PLOS One, 10(4), 123308-123317.

Tsukahara, K., Sawada, H., Matsumura, H., Kohno, Y., & Tamaoki, M. (2013). Quantitative trait locus analyses of ozone-induced grain yield reduction in rice. Environmental and Experimental Botany, 88(1), 100–106.

Ueda, Y., Uehara, N., Sasaki, H., Kobayashi, K., & Yamakawa, T. (2013). Impacts of acute ozone stress on superoxide dismutase (SOD) expression and reactive oxygen species (ROS) formation in rice leaves. Plant Physiology and Biochemistry, 70(1), 396-402.

Wang, Y., Arenas, C.D., Stoebel, D.M. & Cooper, T.F. (2013). Genetic background affects epistatic interactions between two beneficial mutations. Biology Letters, 9(1), 20120328.

Wheeler, T., & Von Braun, J. (2013). Climate change impacts on global food security. Science 341(6145), 508–513.

Wilkinson, S., Mills, G., Illidge, R., & Davies, W.J. (2012). How is ozone pollution reducing our food supply? Journal of Experimental Botany, 63(2), 527–536.

Yu, J., & Buckler, E.S. (2006). Genetic association mapping and genome organization of maize. Current Opinion in Biotechnology, 17(2), 155–160.

Zhu, C., Gore, M., Buckler, E.S., & Yu, J. (2008). Status and prospects of association mapping in plants. The Plant Genome, 1(1), 5–20.

CHAPTER 3

EFFECTS OF OZONE ON CHAMBER-GROWN MAIZE LEAVES

ABSTRACT

Development of pipelines to analyze crop plants under elevated [O_3] is important for pre-breeding identification of tolerant lines. A subset of the NAM founders were screened for leaf damage in a growth chamber experiment under ambient and elevated O_3 conditions. Each chamber included a panel consisting of lines: B73, CML322, CML333, Ki3, M37W, Mo18W, MS71, NC358, and P39. Each fully-emerged leaf was classified as green, lesioned, or dead at 21 DAP and 32 DAP. Height to whorl and tiller number were measured at 32 DAP. Results showed that B73 grown under this level of O_3 for three to four weeks could be clearly differentiated from ambient-grown B73 based on leaf lesion phenotypes. In general, O_3 treatment decreased the number of green leaves while increasing the number of lesioned and dead leaves. Individual lines show varying effect size of O_3 treatment; most lines show the same general trends. B73 and MS71 were significantly affected by O_3 treatment in all traits analyzed (green leaf number, lesioned leaf number, and height). NAM founder lines CML322, M37W, Mo18W, Ms71, NC358 were significantly affected by O_3 treatment for traits green and lesioned leaf number but not height. Based on this preliminary data, selected tolerant and sensitive B73 x Mo17 NILs and hybrids (n= 20) were grown under elevated O_3 (~150 ppb) in growth chambers (n=7). The chambers can identify damage verses no-damage, but not a continuous degree of damage like that seen in the field. In a Mo17 background, the B73 QTL allele on chromosome 2 appeared to confer O_3 sensitivity in a dominant fashion, whereas the B73 allele(s) conferring resistance in m076 appear to act additively. Two sensitive B73 NILs (b005 and b131) appear to confer O_3 sensitivity in a dominant fashion. These results indicate it is feasible to complete higher-throughput phenotyping and fine-mapping of early season O_3 damage QTL in a controlled environment.

INTRODUCTION

Conventional breeding integrates phenotypic data from thousands of lines across many environments and across many years. This approach is very difficult to adopt for breeding O_3 resistance in crops. Tropospheric O_3 concentrations are usually very inconsistent across this scale of lines and environments (Ainsworth et al. 2008). The spatial and temporal heterogeneity of O_3 levels make it unlikely that natural selection pressure will inadvertently breed in O_3 resistance

concurrent with ongoing breeding efforts (Ainsworth et al. 2008, Frei et al. 2015). The dynamic nature of O_3 leaves little potential for crop adaptation through altered management practices (Teixeira et al. 2011). Therefore, efforts are focused on breeding and biotechnological improvement of crops for O_3 tolerance (Ainsworth et al. 2008, Frei 2015). Marker assisted selection (MAS) harnesses the naturally occurring genetic diversity within a species. This approach requires the identification of genetic markers that are associated with O_3 tolerance. Two viable mapping strategies are bi-parental linkage mapping and genome wide association studies. The literature suggests that conducting mapping experiments in smaller scale chamber experiments followed by verification in different environmental conditions with controlled O_3 levels is a feasible approach (Frei et al 2015).

The genetic gain equation ($\Delta G=h^2 \sigma p\ i/L$) effectively relates the basic steps of plant breeding through the principles of quantitative genetics. It is used to model the efficient allocation of resources in a breeding program. σp is the phenotypic variation in a population. Genomics can help expand and more efficiently assemble desirable phenotypic variation by characterizing the genetic diversity of a population and how it is structured. And, understanding the functions of genes and their regulation can lead to the discovery of desirable variants. Heritability, h^2, can also be increased by genomics. Molecular markers can characterize architecture and estimate additive variation and increase favorable gene action.

The aim of this study was to assess the feasibility of higher-throughput phenotyping and fine-mapping of early season ozone damage QTL in a controlled environment. Two hypotheses were tested; i) maize exposure to elevated [O_3] (~150ppb) in a growth chamber will result in an abiotic stress response, which will accelerate senescence, measurable by altered leaf conditions (green, lesioned, dead leaves), and increase height. And, ii) correlations between field and growth-chamber data can determine if fine-mapping of early season ozone damage QTL in a controlled environment is feasible.

MATERIALS AND METHODS

EXPERIMENT ONE

NAM Subset Growth Chamber Experimental Design

A subset of NAM founders were grown under elevated [O_3] (~150 ppb) in growth chambers (n=4) and ambient chambers (n=4) at the Carl R. Woese Institute for Genomic Biology. An incomplete block design was implemented. Each chamber was setup in a 10 x 5

(n=50 plants per chamber) layout. Each chamber contained five blocks with ten plants per block. Each block had a B73 check. B73 was replicated ten times a chamber for a total of 80 pots across the experiment. Selected NAM lines were replicated five times within a chamber for a total of 40 pots across the experiment. In each chamber pair plant location was randomized (Figure 3.1). Each EGC growth chamber included:

(1) B73 parental checks (n=4)

(2) NAM founders CML322, CML333, Ki3, M37W, Mo18W, MS71, NC358, and P39 (n =9)

The chamber conditions were: Lights: ON 1PM, OFF 4AM (15h), Temp: 25°C day, 21°C night, Relative humidity: 60%, Light level: 700 par, Ozone: 150ppb from 4PM-1AM (9 h).

Data Collection

Total leaf count, green leaf count, lesioned leaf count, dead leaf count, height of main stalk to whorl, total height including tillers, and tiller measurements were collected. Two rounds of measurements were completed. The 1st round of phenotypic measurements for leaf counts was completed 21 DAP for all eight chambers. The 2nd round of phenotypic measurements for leaf counts and height was completed 31 DAP for chambers one through four and 32 DAP for chambers five through eight.

Data Analysis

Statistical analysis was performed on chamber means. Independent T-tests were performed on genotype by trait:treatment. Significance adjusted for multiple testing using Bonferroni. Linear mixed effect modeling was completed using Lme4 (Bates et al. 2015) using a model with: treatment as a fixed effect, chamber within treatment as a random effect, block within chamber within treatment as random effect, geno as a fixed effect, and geno*trt as a fixed effect. The mixed model p-values were calculated using Satterthwaite approximation, Kenward-Roger approximation, and the normal distribution approximation. Approximation methods estimate degrees of freedom differently; Satterthwaite pools degrees of freedom, Kenward-Roger assumes the t distribution, and the normal distribution assumes infinite degrees of freedom. Significance threshold was set at (**) $p<0.01$ for all p-value methods. Then the significance threshold was relaxed with the p-value set to (*) $p < 0.05$.

EXPERIMENT TWO

Leaf Damage NIL Growth Chamber Experimental Design

Selected tolerant and sensitive NILs plus their hybrid were grown under elevated O_3 (~150 ppb) in growth chambers (n=7) at the Carl R. Woese Institute for Genomic Biology. An incomplete block growth chamber design was implemented using elevated chambers. Ambient chambers were not utilized in this experiment because in 2016 field phenotyping of leaf damage in ambient rings average scores were zero (=100% green/ no damage observed). Each chamber was setup in a 4 x 8 (n=32 plants per chamber) layout to allow plants to grow without overcrowding through the 6th leaf stage. Each chamber contained four blocks with eight plants per block. Each block had B73, Mo17, and B73 x Mo17 checks. Each check was replicated four times within a chamber for a total of 28 pots across the experiment. Selected NIL lines and hybrids were replicated one time within a chamber for a total of seven pots across the experiment. In each chamber plant location was randomized (Figure 3.2). Each EGC growth chamber included:

(1) B73 parental checks (n=4)

(2) Mo17 parental checks (n=4)

(3) B73 x Mo17 hybrid checks (n= 4)

(4) Seven sensitive Mo17 NILs (m002, m072, m007, m030, m091, m016, and m038) and their hybrids with Mo17

(5) One tolerant Mo17 NIL (m076) and its hybrid with Mo17

(6) Two sensitive B73 NILs (b131 and b005) and its hybrids with Mo17

The chamber conditions were: Lights: ON 1PM, OFF 4AM (15 h), Temp: 25°C day, 21°C night, Relative humidity: 60%, Light level: 700 par, Ozone: 150ppb from 4PM-1AM (9 h).

Growth Chamber Leaf Damage Scoring and Imaging

Leaf damage was scored on a 0-9 scale at one time point on the 5th and 6th true leaf at 32 DAP. Foliar disease point scale was modified for leaf damage susceptibility in maize; zero (0-10%) and nine (90-100%) of the leaf area having damage. Chamber averages were taken for each NIL, hybrid, and check. Leaf damage scores were collected independently by two scientists and compared for reliability. Additionally, each leaf of each plant was imaged.

Field and Growth Chamber Statistical Analysis

Growth chamber values were calculated in elevated environment. The data was assessed by Shapiro Wilk normality tests and QQ plot analysis using chamber 5^{th} leaf damage scores, chamber 6^{th} leaf damage scores, chamber 5^{th} & 6^{th} leaf combined ("leaf_variable") damage scores, and the field leaf damage scores of the 5^{th} leaf elevated only. To determine best fits for the data distributions three models were tested and best was chosen by Akaike information criterion (AIC). The final models included random effects for leaf_variable, chamber, block:chamber, and genotype. Linear, quadratic, and cubic fitted regression lines were evaluated. All calculations and analysis were coded using R (R Core Team 2015).

RESULTS AND DISCUSSION

In general, chamber O_3 treatment decreased the number of green leaves while increasing the number of lesioned and dead leaves. Individual lines show varying effect size of O_3 treatment. Most lines show the same general trends (Figure 3.3). Maize plant exposure to elevated [O_3] in a growth chamber setting resulted in an abiotic stress response that was distinguishable by leaf trait phenotyping (Table 3.1). The growth chamber experiment showed that B73 grown under ~150 ppb O_3 for three to four weeks could clearly be differentiated from ambient-grown B73 based on leaf lesion types (Figure 3.4). Lme4 estimated p-values show that NAM Founder lines B73 and MS71 were significantly affected by O_3 treatment in all three traits analyzed (green leaf number, lesioned leaf number, and height) using less stringent p-value approximations Kenward-Roger and the normal distribution ($p < 0.05$). NAM founder lines CML322, M37W, Mo18W, Ms71, NC358 were significantly affected by O_3 treatment for traits green leaf number and lesioned leaf number but not height (Table 3.2, $p < 0.01$).

The chambers can identify damage verses no-damage, but not a continuous degree of damage like that seen in the field (Figure 3.5). The best fit is non-linear (Figure 3.5 D-F). The best fit is non-linear because the chamber damage scores did not have a normal distribution. In a Mo17 background, the B73 QTL allele on chromosome 2 appears to confer O_3 sensitivity in a dominant fashion, whereas the B73 allele(s) conferring resistance in m076 appear to act additively (Figure 3.6). Sensitive B73 NILs, b005 and b131, appear to confer O_3 sensitivity in a dominant fashion (Figure 3.6). Compared to the field studies, growth was more rapid in the chamber experiment, which also had higher O_3 levels, future experiments should either i) collect data at 21 DAP or ii) reduce the [O_3].

Identifying intraspecific variation in cultivar responses to elevated [O_3] is the first step towards breeding for O_3 tolerance (Ainsworth 2017). Among plants there are two types of variation, environmental and heritable. Heritable variation is essential to plant breeding because it allows for genetic improvements. A mixed population of plants will exhibit many heritable variations. From this pool of variation, plants with the traits most important for the development of an improved cultivar are selected. Heritable variation is identified when different plants of the same species are growing in a uniform environment exhibit contrasting forms of the traits being measured. These variations are expressed again in the progenies, although the degree with which they are expressed vary with the environment.

Traits in a plant develop as a result of the action of genes in the chromosomes and the interactions of the plant with the environment. The influence of each gene may be exerted individually or in combination with other genes. Within the same species heritable variation involves contrasting forms of specific plant alleles. The breeding behavior of a plant is determined by the particular combination of alleles for the different genes it possesses. Insight into the nature of gene action involved in the expression of the quantitative trait being bred for is essential for starting a breeding program. Four general types of genes action are recognized: additive, dominance, epistasis, and overdominance. Success of any crop improvement program is mainly dependent upon information regarding nature and magnitude of gene effects controlling economic quantitative traits (Shalaby 2013). Understanding gene action is of paramount importance to plant breeders (Fasoula & Fasoula 2010). In plant breeding, knowledge of gene action helps in the selection of parents for use in the hybridization and also in the choice of appropriate procedures for the genetic improvement of various quantitative traits.

Studying the impact of changing atmospheric gases is difficult. The FACE technology, developed to study CO_2 is readily adaptable to study O_3. In fact, this has been used to study the impact of O_3 on various crops. Given the constraints of breeding for O_3 resistant traits, conducting mapping experiments in smaller scale chamber experiments followed by verification in different environmental conditions with controlled O_3 levels appears to be a feasible approach (Frei et al. 2015). These results shows that there is adequate genetic variation in maize populations, and provides the suitable tools, to fine map maize response to O_3 stress. These developed resources provide the opportunity to isolate QTL and causative genes that will aid in the development of resistant lines. Our results show that the chambers can identify damage

verses no-damage, but not a continuous degree of damage like that seen in the field. The best fit is non-linear. F_2 and F_3 populations have been developed and markers identified. These resources can be utilized to further fine map the leaf damage QTL identified on chromosome 2 at ~161 Mb. Additionally, they can be used to map sensitive B73 NILs, b007 and b003, and tolerant Mo17 NIL m076 down to a single introgression.

CONCLUSIONS

To make progress in plant improvement requires genetic variability, reliable selection methods, time, and resources. Chamber experiments show the ability to differentiate leaf damage variation among diverse lines and the ability to make inferences about gene action. Our results show that the chambers can identify damage verses no-damage, but not a continuous degree of damage like that seen in the field. This research indicates the potential for high-throughput phenotyping and fine-mapping of early season O_3 damage QTL in a controlled environment.

Figure 3.1 NAM Subset Chamber Experimental Design. An incomplete block design was implemented. Each chamber was setup in a 10 x 5 (n=50 plants per chamber) layout. Each chamber contained 5 blocks with 10 plants per block. Each block had a B73 check. B73 was replicated 10 times a chamber for a total of 80 pots across the experiment. Selected NAM lines were replicated 5 times within a chamber for a total of 40 pots across the experiment. In each chamber pair plant location was randomized. Ambient chambers n=4, Elevated [O_3] (~150ppb, 700 par) chambers n=4. Each chamber included NAM founders CML322, CML333, Ki3, M37W, Mo18W, MS71, NC358, and P39.

	1	2	3	4	5	6	7	8	9	10
1	B73	Mo18W	Mo18W	NC358	B73	Mo18W	CML333	MS71	CML322	NC358
2	CML333	CML322	B73	MS71	Ki3	CML333	Mo18W	CML322	B73	Ki3
3	MS71	NC358	CML333	B73	P39	M37W	B73	NC358	M37W	Mo18W
4	M37W	B73	M37W	CML322	MS71	CML322	Ki3	B73	MS71	P39
5	P39	Ki3	P39	KI3	NC358	B73	M37W	P39	CML333	B73

Figure 3.2 B73-Mo17 NIL Chamber Experimental Design. An incomplete block design was implemented. Each chamber was setup in a 4 x 8 (n=32 plants per chamber) layout to allow plants to grow without overcrowding through the 6th leaf stage. Each chamber contained four blocks with eight plants per block. Each block had B73, Mo17, and B73 x Mo17 checks. Each check was replicated four times within a chamber for a total of 28 pots across the experiment. Selected NIL lines and hybrids were replicated one time within a chamber for a total of 7 pots across the experiment. In each chamber plant location was randomized. Elevated [O_3] (~150 ppb, 700 par) chambers n=7, no ambient chambers were utilized. S_BHYB = sensitive B72 NIL hybrid, S_mHYB = sensitive Mo17 NIL hybrid, S_mNIL = sensitive Mo17 NIL, T_mHYB = tolerant Mo17 NIL hybrid, B73 = check, Mo17 = check, BxM = B73 x Mo17 = check.

	1	2	3	4	5	6	7	8
1	S_bHYB	BxM	B73	T_mHYB	S_mNIL	S_mNIL	S_mHYB	B73
2	S_mHYB	S_mHYB	S_mNIL	BxM	S_mHYB	MO17	MO17	S_bNIL
3	S_mNIL	S_mHYB	S_bHYB	S_mHYB	B73	S_bNIL	S_mNIL	BxM
4	B73	MO17	S_mNIL	MO17	S_mNIL	BxM	T_mNIL	S_mHYB

Figure 3.3 NAM Founders Subset Elevated [O_3] Screen Trait by Genotype. Individual lines show varying effect size of O_3 treatment. Most lines show the same general trends. (A) Total number of leaves, (B) Number of green leaves, (C) Number of lesioned leaves, (D) Number of dead leaves, (E) Height, (F) Total Height, (G) Number of tillers. Blue indicates ambient chambers, orange indicates elevated [O_3] chambers.

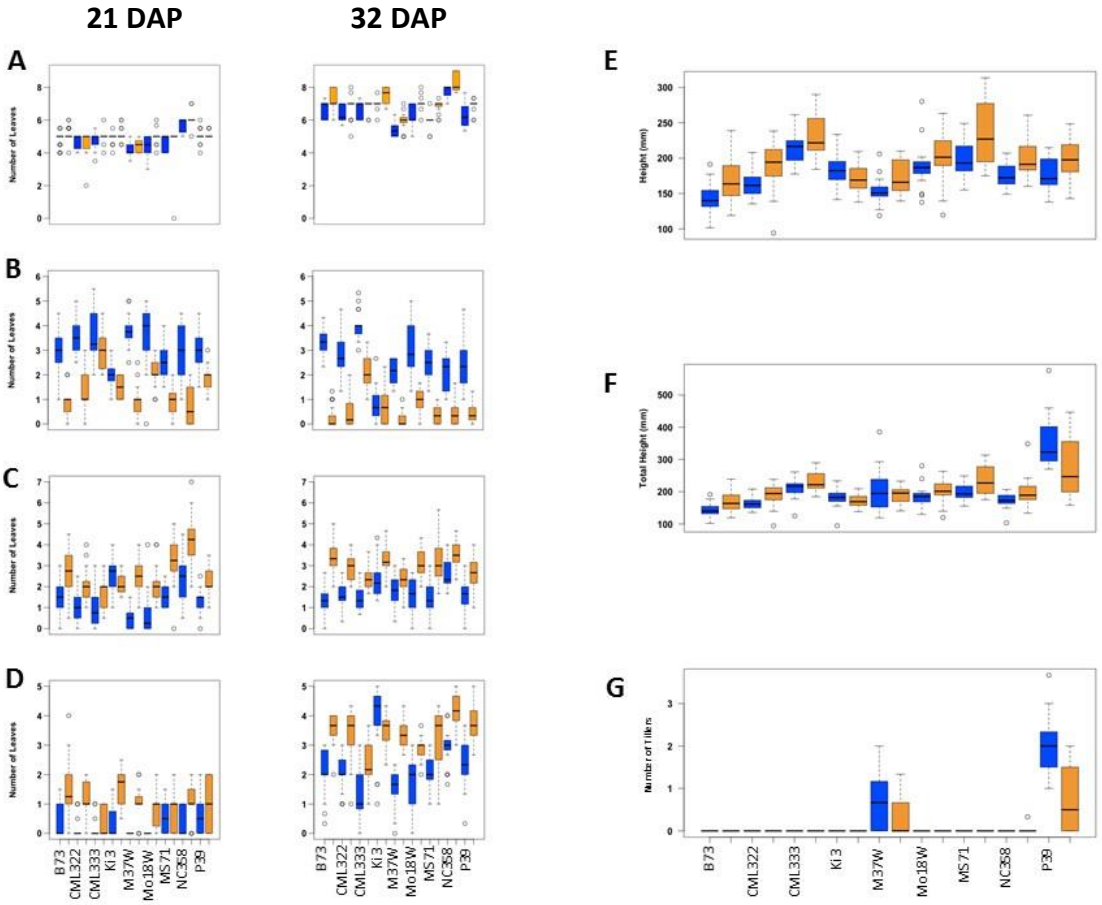

Table 3.1 NAM Founders Subset Elevated [O_3] Screen Independent T-tests Trait by Genotype. Maize plant exposure to elevated O_3 in a growth chamber setting resulted in an abiotic stress response that was distinguishable by leaf trait phenotyping. Direction of effect is indicated by color coding; blue indicates significant increase of trait values in ambient conditions. Orange indicates significant increase of trait values in elevated conditions. Significance adjusted for multiple testing using Bonferroni.

	Total 21 DAP	Total 32 DAP	Green 21 DAP	Green 32 DAP	Lesion 21 DAP	Lesion 32 DAP	Dead 21 DAP	Dead 32 DAP	Height 32 DAP	Tiller Number	Total Height
B73	4.41E-02	6.12E-06	1.98E-15	1.76E-15	9.34E-09	1.98E-15	8.83E-10	1.76E-15	1.27E-04	NA	1.27E-04
CML322	ns	ns	4.62E-10	2.50E-10	6.11E-04	1.51E-07	2.48E-06	7.39E-06	3.27E-02	NA	3.27E-02
CML333	ns	ns	ns	1.15E-10	7.55E-02	1.10E-05	ns	4.20E-05	ns	NA	ns
Ki3	ns	3.77E-04	1.68E-02	ns	ns	7.75E-04	2.50E-07	ns	ns	NA	ns
M37W	ns	1.52E-02	1.98E-15	3.37E-14	2.63E-10	5.26E-02	1.68E-06	1.58E-10	ns	1.70E-02	ns
Mo18W	5.97E-03	6.10E-04	1.16E-03	5.77E-07	1.14E-03	2.74E-06	1.93E-05	2.24E-06	ns	NA	ns
MS71	ns	7.42E-08	6.99E-08	4.50E-12	2.48E-06	6.52E-06	ns	4.00E-03	2.82E-02	NA	2.82E-02
NC358	2.42E-02	1.80E-02	1.81E-06	2.40E-08	1.07E-04	1.08E-03	3.22E-03	1.99E-06	2.89E-02	NA	2.89E-02
P39	ns	1.18E-02	4.92E-06	3.05E-07	5.42E-04	4.94E-04	ns	1.37E-07	ns	3.34E-07	2.40E-02

Figure 3.4 Effects of O_3 on Chamber-Grown B73. Results showed that B73 grown under this level of O_3 for 3-4 weeks could be clearly differentiated from ambient-grown B73 based on leaf lesion phenotypes. 100% stacked bar plots show green leaf, lesioned leaf, and dead leaf counts. (A) 21 DAP, (B) 32 DAP.

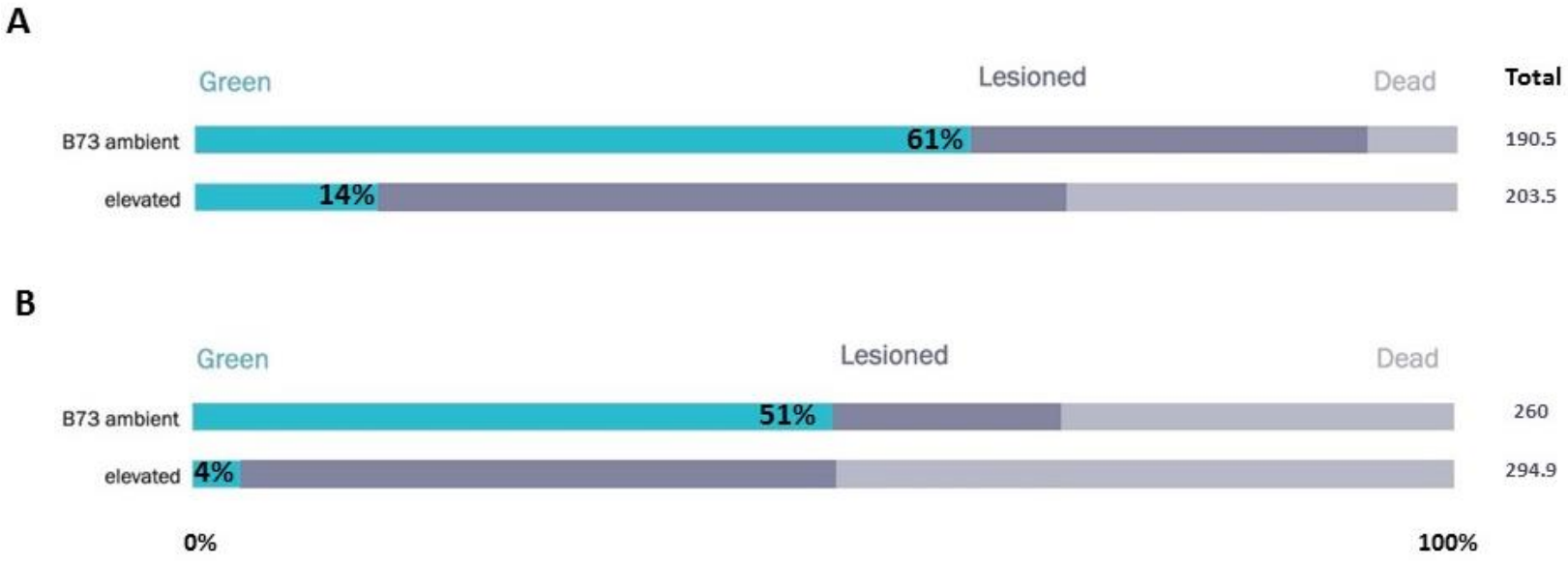

Table 3.2 NAM Founders Subset P-Values from Lme4 Modeling. Lme4 estimated p-values show that NAM Founder lines B73 and MS71 were significantly affected by O_3 treatment in all three traits analyzed using less stringent p-value ($p < 0.05$) approximations Kenward-Roger and the normal distribution. NAM founder lines CML322, M37W, Mo18W, Ms71, NC358 were significantly affected ($p < 0.01$) by O_3 treatment for traits green leaf number and lesioned leaf number but not height for stringent p-value approximation method Satterthwaite. Direction of effect indicated by color coding; Orange indicates significant increase of trait values in elevated conditions. Blue indicates significant increase of trait values in ambient conditions. p.Satt = Satterthwaite approximation, p.KR = Kenward-Roger approximation, p.z = Normal distribution approximation. Approximation methods estimate degrees of freedom differently; p.Satt pools degrees of freedom, p.KR assumes the t distribution, and p.z assumes infinite degrees of freedom using the normal distribution.

	Green 21 DAP			**Lesioned 21 DAP**			**Height 32DAP**		
	lmer.test	pbkr.test	norm.dist	**lmer.test**	pbkr.test	norm.dist	**lmer.test**	pbkr.test	norm.dist
	p.Satt	p.KR	p.z	**p.Satt**	p.KR	p.z	**p.Satt**	p.KR	p.z
B73	**1.180E-12**	0.000E+00	0.000E+00	**9.309E-04**	2.530E-05	2.520E-05	**7.853E-02**	4.725E-02	4.676E-02
CML322	**2.850E-12**	0.000E+00	2.220E-16	**4.322E-03**	1.478E-03	1.477E-03	ns	ns	ns
CML333	**2.216E-02**	1.959E-02	1.959E-02	**4.552E-02**	3.406E-02	3.405E-02	ns	ns	ns
Ki3	**5.536E-02**	5.176E-02	5.176E-02	ns	ns	ns	ns	ns	ns
M37W	**0.000E+00**	0.000E+00	0.000E+00	**3.171E-06**	8.780E-10	8.690E-10	ns	ns	ns
Mo18W	**6.450E-07**	7.245E-08	7.220E-08	**7.719E-04**	1.106E-04	1.103E-04	ns	ns	ns
MS71	**2.250E-08**	4.862E-10	4.830E-10	**5.253E-05**	5.890E-07	5.860E-07	**4.356E-02**	2.129E-02	2.093E-02
NC358	**3.540E-12**	4.441E-16	2.220E-16	**1.233E-05**	2.660E-08	2.640E-08	ns	ns	ns
P39	**8.560E-06**	1.887E-06	1.880E-06	**1.039E-02**	5.102E-03	5.099E-03	ns	ns	ns

Figure 3.5 Field and Chamber Leaf Damage Scores. It appears that in the chambers you can identify damage and no-damage, but not a continuous degree of damage like seen in the field. Field 5th leaf elevated damage scores were plotted against (A & D) chamber 5th and 6th leaf combined damage scores, (B & E) chamber 5th leaf damage scores, and (C & F) chamber 6th leaf damage scores. The best fit is non-linear (D-F). Indicating a potential for higher-throughput phenotyping and fine-mapping of early season O_3 damage QTL in a controlled environment.

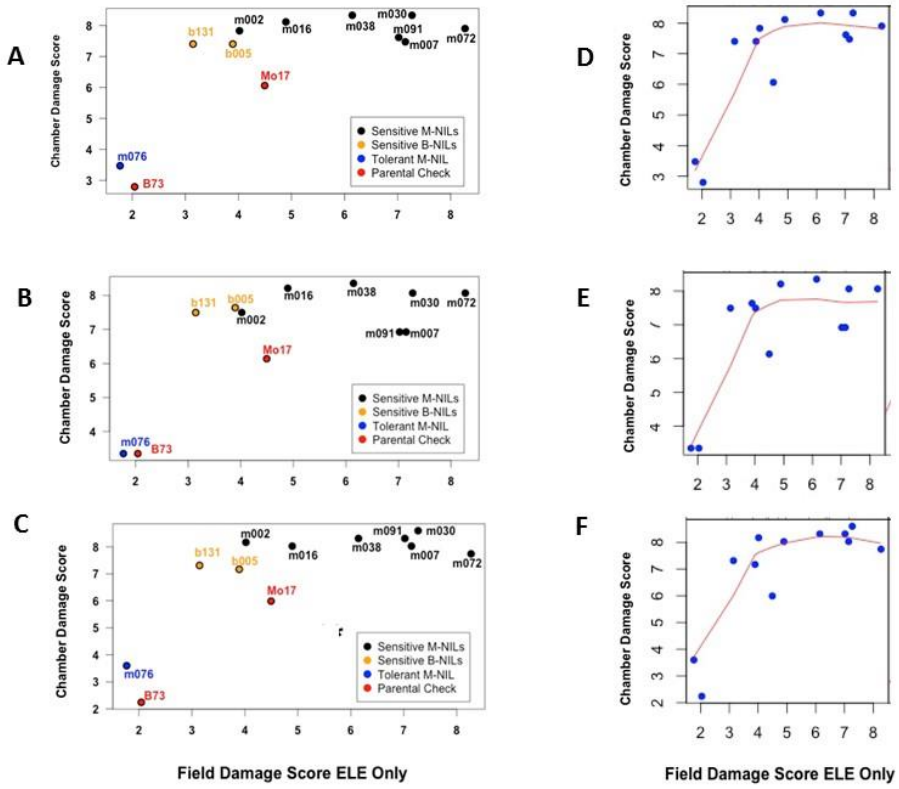

Figure 3.6 Estimation of Gene Action. Images from each leaf were taken and leaf damage score distributions plotted. Damage scores were calculated by combining 5th and 6th leaf measurements. (A & B) In a Mo17 background, the B73 QTL allele on chromosome 2 appears to confer O_3 sensitivity in a dominant fashion, (C) whereas the B73 allele(s) conferring resistance in m076 appear to act additively. (D & E) Sensitive B73 NILs, b131 and b005, appear to confer O_3 sensitivity in a dominant fashion.

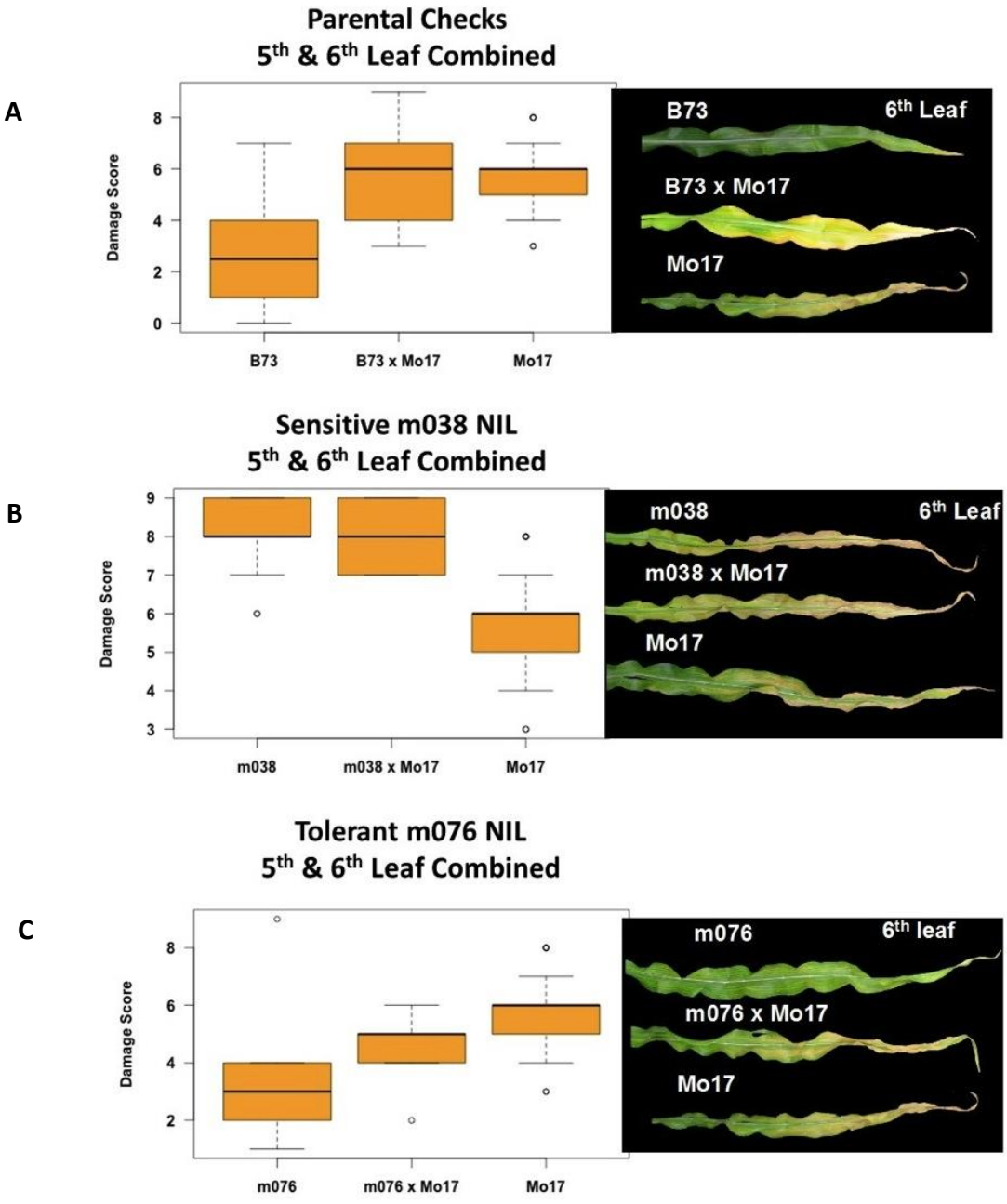

Figure 3.6 (cont.)

D

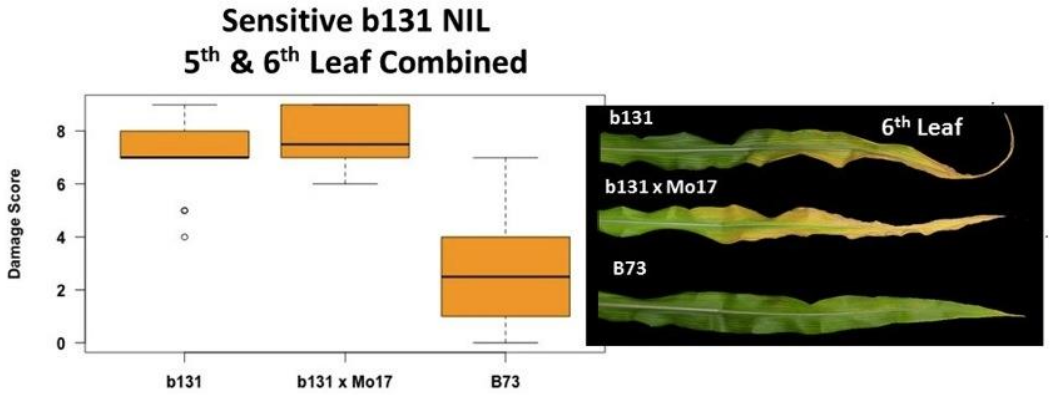

E

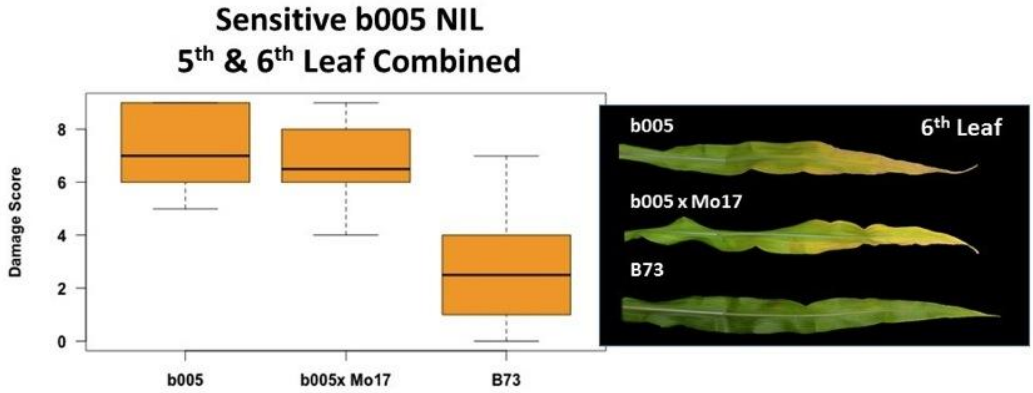

REFERENCES CITED

Ainsworth, E. A. (2017). Understanding and improving global crop response to ozone pollution. The Plant Journal, 90(5), 886-897.

Ainsworth, E. A., Rogers, A., & Leakey, A. D. (2008). Targets for crop biotechnology in a future high-CO_2 and high-O_3 world. Plant Physiology, 147(1), 13-19.

Bates, D., Maechler, M., Bolker, B., & Walker, S. (2015). Fitting linear mixed-effects models using lme4. Journal of Statistical Software, 67(1), 1-48.

Fasoula, D.A. & V.A. Fasoula. (2010). Gene action and plant breeding. In Plant Breeding Reviews, John Wiley & Sons, Inc., New York, N.Y., Chapter 9.

Frei, M. (2015). Breeding of ozone resistant rice: Relevance, approaches and challenges. Environmental Pollution, 197(1), 144–155.

R Core Team. (2015). R: A language and environment for statistical computing. R Foundation for Statistical Computing, Vienna, Austria.

Shalaby, T. A. (2013). Mode of gene action, heterosis and inbreeding depression for yield and its components in tomato (Solanum lycopersicum L.). Scientia Horticulturae, 164(1), 540-543.

Teixeira, E., Fischer, G., van Velthuizen, H., van Dingenen, R., Dentener, F., Mills, G., Walter, C. & Ewert, F., 2011. Limited potential of crop management for mitigating surface ozone impacts on global food supply. Atmospheric Environment, 45(15), 2569-2576.

CHAPTER 4

Yg3 (YELLOW-GREEN3), A NEW PARENTAL MARKER FOR DOUBLED HAPLOID INDUCERS

ABSTRACT

Yg3-N1582 (*Yellow-green*) is a dominant EMS-induced maize mutant isolated by Neuffer et al. (2011). It is non-lethal and homozygous-viable with no apparent deleterious effects, and the yellow-green color does not persist beyond the seedling stage. Dominant mutants from EMS mutagenesis are rare and *Yg3-N1582* has not previously been mapped. Results show that *Yg3-N1582* maps to 173-175Mb (AGPv3) on chromosome 5, and this interval does not coincide with any previously characterized *yg* mutant. Transcriptome profiling identified GRMZM2G165521 as a candidate gene that could underlie the mutant phenotype. GRMZM2G165521 is a predicted pentatricopeptide repeat (PPR) protein involved in RNA editing and is orthologous to a rice protein that produces *yg* phenotypes. Full gene sequencing of GRMZM2G165521 in the *Yg3-N1582/Yg3-N1582* background reveals a seven base pair insertion in the first intron relative to the wild-type reference line. This insertion results in an alternate transcription start site and open reading frame that eliminates the first exon of the PPR protein, which contains a predicted chloroplast transit peptide. Alignment of *Yg3-N1582*/+ RNAseq reads confirms transcription at the site of the insertion. Quantitative PCR of GRMZM2G165521 expression patterns revealed an upregulation during daytime indicating a potential for use in studies of photosynthesis. Additionally, crossing (*Yg3-N1582*/+) x B73 with diverse maize inbred lines confirms the marker color in different backgrounds. The *Yg3-N1582* mutation has potential as a haploid inducer marker in exotic germplasm and small breeding programs where the use of *R1-Navajo* and high oil inducers is not feasible.

INTRODUCTION

Maize genetic stock mutants are valuable because they are defined by a limited number of genomic variations or they can be utilized as genetic tools (Sachs 2009a). Examples of genetic stocks include: induced mutations, natural variants, unique phenotype combinations, linked mutant alleles, chromosomal abnormalities, RIL mapping populations, Robertson's Mutator lines, and the TILLing project lines (McGraw 2000, Lawrence 2004, Sachs 2009b). This diversity is sourced from geneticists and breeders from around the world (Sachs 2009a) and is considered an "international treasure" (McGraw 2000). The total core collection of the stock

center is over 7,500 stocks from approximately 100,000 individual pedigree samples (McGraw 2000, Sachs 2009a). A majority of mutants in the collection are utilized for basic research and provide critical information and understanding of biological pathways. Although most of the stock mutants are too extreme for commercial breeding a few have successfully affected the market and now carry agronomic importance. The most notable example of this is the sugary1 (*su1*) and shrunken2 (*sh2*) alleles now commonly found in sweet corn varieties (Hallauer 2000, Lertrat & Pulam 2007). White endosperm mutants (e.g., *y1*, *wx1* and *ae1*) have been used to breed special starch quality in commercial lines (Whitt et al. 2002, Wilson et al. 2004). Additionally, indeterminate gametophyte (*ig1*) mutant stock is utilized in breeding programs to increase the frequency of androgenetic haploids in progeny (Weber 2014). These examples show that documenting observed phenotypic diversity of stock mutants allows scientists to have a greater understanding of biological processes and can also lead to agronomic improvements (Neuffer et al. 1997, Hallauer 2000, Sachs 2005).

Yg3-N1582 (Figure 4.1) is a previously uncharacterized dominant yellow-green ethyl methanesulphonate (EMS) induced maize mutant (Neuffer et al. 1997, Neuffer et al. 2009, Weil & Monde 2009) isolated by Neuffer et al. (2011). The mutant was created by crossing mutagenized Mo17 pollen to A632. *Yg3-N1582* is non-lethal and homozygous-viable with no apparent deleterious effects. The yellow color expression begins at coleoptile emergence does not appear to persist beyond the seedling stage. Dominant mutants from EMS mutagenesis are rare and *Yg3-N1582* has not previously been mapped. Sachs & Stinard (2012) identified *Yg3-N1582* as a potential haploid inducer marker in exotic germplasm and small breeding programs where the use of *R1-Navajo* and high oil inducers is not feasible.

Doubled haploids (DH) are an alternative method for inbred line development (Figure 4.2) and provide many benefits to maize breeding programs (Sleper & Poehlman 2006). DH technologies provide fixed, pure lines from a donor parent in a single generation (Chang & Coe 2009). This quick return to homozygosity enables the development of the most homozygous genotypes possible for research purposes and cultivar release. Efficient use of DH in breeding requires i) a dependable method of producing haploids, ii) a method that produces haploids representing a random sample of gametes, iii) a reliable method of doubling chromosome number, and iv) adequate technical competence, facilities, time, and resources (Sleper & Poehlman 2006, Dwivedi et al. 2015). The key to effectively using DH in a commercial breeding

program is the availability and reliability of methods for their production. DH lines are available for over 250 crop species and over 300 DH-derived cultivars have been developed for many different species (Forester & Thomas 2005). With many species and techniques production of haploids is genotype specific (Chang & Coe 2009, Dwivedi et al. 2015). In maize, DH methods are advanced and have widespread application in breeding programs. However, DH resources for exotic germplasm are lagging behind (Kleiber et al. 2012, Couto et al. 2015, Dwivedi et al. 2015).

DH inducers are specialized genetic stocks (Prasanna et al. 2012). When an inducer is crossed to diploid maize plant the resulting progeny segregate for diploid (2N) and haploid (N) kernels because of anomalous fertilization. Currently the most widely used paternal marker in haploid inducers is *R1-Navajo (R1-nj),* which gives a pigmented kernel crown and embryo (Couto et al. 2015a & 2015b, Dwivedi et al. 2015). Additionally, *B1* + *Pl1* markers can give pigmented plant tissue. However, in germplasm with dominant *R1*, *B1*, and *Pl1* alleles these markers are not useful (Couto et al. 2015b).

Chromosome duplication is the most critical step in obtaining DH maize. DH production is time consuming and labor intensive, therefore the efficient detection and selection of DHs is desirable at an early seedling stage. However, the ability to select haploids produced by inducer lines is heavily based on anthocyanin color expression in the seed and/or other tissues at adult stages of plant growth (Sleper & Poehlman 2006). Couto et al. (2015b) evaluated the efficiency of DH selection using the *R1-Navajo* marker. The analysis found an error rate of 33.5% associated with the use of the *R1-Navajo* morphological marker, concluding that it is inefficient and that other markers need to be used in the selection of doubled haploids. Additionally, Chaikam et al. (2015) tested the accuracy of haploid identification based on *R1-Navajo* expression and found a higher probability of misclassification when the marker is used for classification of tropical germplasm. Alternative anthocyanin markers have been proposed (Chaikam et al. 2016) in which expression occurs in the seedling plant root system. Although this method shows a lower false positive rate than the *R1-Navajo* marker it still presents logistical challenges of being able to observe plant roots in an efficient manner without disturbing the plant development in a high throughput fashion. Alternatively the use of oil content markers has been utilized to detect doubled haploids. A drawback of oil markers is they require a full plant life cycle and specialized equipment is often needed (Couto et al. 2015b,

Chaikam et al. 2016). *Yg3-N1582* has been identified as a new potential paternal marker during haploid induction because it has color expression at coleoptile emergence and it is homozygous viable (Sachs & Stinard 2012).

Disruption of pentatricopeptide repeat (PPR) proteins causes seedling specific albino or yellow phenotypes in maize, Arabidopsis, and rice orthologs (Khrouchychova et al. 2012, Su et al. 2012, Asano et al. 2013). Functional analysis has relied heavily on utilizing mutants as genetic tools. Phenotypes are often diverse and have strong effect. With few exceptions, most PPR mutants affect core organelle functions and are lethal (Schmitz-Linneweber & Small 2008). One such exceptional viable PPR mutant from rice is *young seedling albino* (*ysa*; Su et al. 2012), where early seedling leaves are white, which then recover to green by the sixth leaf stage. The *ysa* phenotype displays no apparent negative effects and RNA profiling suggests a role in chloroplast biogenesis. *ysa* has been proposed as an early marker for efficient selection in rice for identification and elimination of false hybrids in commercial production (Su et al. 2012).

The PPR gene family represents one of the largest gene families in higher plants (Barkan & Small 2014), however few PPR proteins have been studied in detail (Manna 2015). PPR proteins are degenerate 35 amino acid motifs tandemly repeated (Small & Peeters 2000) and the number of motifs can range from two to greater than 26 (Lurin et al. 2004). PPR proteins are classified based on domain architecture into distinct classes and subclasses (Manna 2015). The functions and mechanisms of proteins in the PPR family are poorly understood (Bieck et al. 2008). Proteins containing PPR motifs have known roles involved in transcription, RNA processing, splicing, stability, editing, and translation (Delannoy et al. 2007, Schmitz-Linneweber & Small 2008). Current data suggest that PPR proteins play a central, and broad role, in modulating the expression of organellar genes in plants (Barkan & Small 2014, Manna 2015). PPR proteins are predicted to localize to plastids or mitochondria (Manna 2015). It is generally thought that the repeats of PPR proteins form a superhelical structure to bind a specific ligand, likely a single-stranded RNA molecule, and modulate its expression (Lurin et al. 2004, Manna 2015). Genetic and biochemical data shows that most PPR proteins mediate specific post-transcriptional steps in organellar gene expression via direct interaction with RNA (Barkan & Small 2014, Manna 2015). Despite their integral role in nuclear and organellar functions, very little is known about the functions, substrates, or biochemical mechanisms of PPR proteins.

The objective of this study was to characterize maize stock mutant *Yg3-N1582*. This analysis intends to i) map the locus and, ii) identify and validate a candidate gene(s) underlying the mutation.

MATERIALS AND METHODS

Bi-Parental Mapping

(*Yg3-N1582/*+) x B73 was obtained from Dr. Marty Sachs of the Maize Genetics Cooperation Stock Center. (*Yg3-N1582*/+) x B73 was again crossed to B73 resulting in a (*Yg3-N1582/*+ x B73) x B73 line. (*Yg3-N1582/*+ x B73) x B73 was grown in the greenhouse under sand bench conditions. Leaf tissue was harvested at seedling stage. DNA was extracted from leaf tissue by using a CTAB protocol in a 96 well plate format. GBS Illumina library prep workflow was modified from Poland & Rife (2012); 360 *(Yg3-N1582/*+ x B73) x B73 of 180 green and 180 yellow, eight B73, eight *Yg3-N1582/*+, and eight blank were used in genotyping. In total 384 DNAs at 20-50 ng/ul were processed in the analysis. Restriction and ligation was completed with *PstI-HF/BfaI* and 384 barcodes. Ampure XP bead cleaning was followed by 15 cycles of PCR and another round of Ampure XP bead cleaning. Estimated average size (basepair) and concentration (ng/ul) was determined with an Agilent DNA7500 chip. Samples were diluted to ten nmol for Illumina sequencing. SNP calling was completed using the TASSEL GBS pipeline (Glaubitz et al. 2014). Imputation was completed using FSFHAP (Swarts et al. 2008). Resulting in 4,375 SNPs across 345 (*Yg3-N1582/*+ x B73) x B73 with a 96% genotyping success rate (345/360). Mapping was coded in R. The phenotype (0=green; 1=yellow) was regressed upon genotype (0=B73; 1=heterozygous).

mRNA Extraction, Libraries, and Sequencing

(*Yg3-N1582/*+ x B73) x B73 was grown in greenhouse under sand bench conditions. Leaf tissue was harvested for three time points (8 DAP, 10 DAP, and 12 DAP) by yellow and green leaf tissue pools. mRNA was extracted using Sigma-Aldrich's Spectrum™ Plant Total RNA Kit according to manufactures protocol. The RNAseq libraries were prepared with Illumina's 'TruSeq Stranded mRNAseq Sample Prep kit' (Illumina). Sequencing was completed at the Roy J. Carver Biotechnology Center at the University of Illinois Urbana-Champaign. Sequence of adaptors used to make the libraries (used blue bold portion for adaptor trimming). Adaptor sequence in read1:

AGATCGGAAGAGCACACGTCTGAACTCCAGTCACNNNNNNATCTCGTATGCCGTCTT CTGCTTG (NNNNNN= 6 nt index).

Adaptor sequence in read2:

AGATCGGAAGAGCGTCGTGTAGGGAAAGAGTGTAGATCTCGGTGGTCGCCGTATCA T. The libraries were quantitated by qPCR and sequenced on one lane for 101 cycles from one end of the fragments on a HiSeq2500 using a HiSeq SBS sequencing kit version 4. Resulting in 147,347,874 100nt single-end reads. Fastq files were generated and demultiplexed with the bcl2fastq v2.17.1.14 Conversion Software (Illumina). The quality-scores line in fastq files used an ASCII offset of 33 known as Sanger scores.

Transcriptome Profiling

Expression analysis was completed on a transcript level using a HISAT (Kim et al. 2015), StringTie (Pertea et al. 2015), and Ballgown (Frazee et al. 2015) also known as the "new Tuxedo" package bioinformatics pipeline (Pertea at al. 2016). These programs are free and open-source software tools for comprehensive analysis in RNAseq experiments (Pertea at al. 2016) available at http://ccb.jhu.edu/software.shtml. In general, reads were aligned to the maize genome (AGPv3) using HISAT with annotated reference genes and transcripts. StringTie was then used to assemble and quantify the transcripts in each sample. After initial assembly the transcripts were merged together by StringTie creating a uniform set of transcripts from all samples. Genes and transcripts were then compared to the annotation using gffcompare producing comparison statistics. StringTie then processed the read alignments and either merged transcripts or the reference annotation. This input was used by StringTie to re-estimate abundance (if necessary) and create transcript tables for Ballgown. The Ballgown program compared all transcripts across experimental conditions and produced tables and plots of differentially expressed genes and transcripts. Analysis was completed using the linux (Linus Torvalds 2015) command line terminal, R (R Core Team 2015), and biocondutor (Gentleman et al. 2004).

mRNA Read Alignment and Variant Calling

GATK best practices (McKenna et al. 2010, Depristo et al. 2011, Van der Auwera et al. 2013) are broken down into two analysis phases, i) data preprocessing and, ii) variant discovery. Data clean up involves preprocessing the raw sequence data to produce analysis-ready BAM files. This involves alignment to a reference genome as well as cleanup operations to correct for

technical biases and make the data suitable for analysis. Reads were aligned using STAR 2Pass (Dobinet et al. 2013) and the GATK (McKenna et al. 2010, Depristo et al. 2011, Van der Auwera et al. 2013) clean up pipeline was implemented. The steps involved are; mapping and marking duplicates, followed by local realignment around indels and base quality score recalibration. Once the data was pre-processed it was put through the variant discovery process. This is where the pipeline identifies sites in which the data displays variation relative to the reference genome, and analyzes genotypes for each sample at that site. This involves identifying genomic variation in one or more individuals and applying filtering methods appropriate to the experimental design. The output is in VCF format and was visualized in VGI viewer (Robinson et al. 2011).

Full Gene Sequencing

Yg3-N1582/Yg3-N1582 seed homozygous for the dominant mutant *Yg3* allele was obtained from Dr. Marty Sachs at the Maize Genetics Cooperation Stock Center. Plants were grown in field conditions in Savoy, IL. Six individual plants were sampled for young leaf tissue and stored at -80°C. Plant leaf samples were kept separate (not pooled). Extracted DNA samples were quantified by nanodrop spectrophotometry and Qubit. Sequences for candidate gene GRMZM2G165521 were obtained from two online databases:

Phytozome v12.1, Phytomine

https://phytozome.jgi.doe.gov/phytomine/portal.do?externalid=PAC:30991057&class=gene

EnsemblPlants

http://plants.ensembl.org/Zea_mays/Transcript/Exons?db=otherfeatures;g=GRMZM2G165521;r=5:177557687-177561750;t=GRMZM2G165521_T01

Primers were designed using primer3 to flank and partition the 3,097bp GRMZM2G165521 transcript into smaller components. Primers were BLASTN against the maize genome using EnsemblPlants to ensure uniqueness. Expected amplicon size was calculated. DNA working stocks were made to 1ug. Go Taq/Green master mix PCR protocols were completed by manufactures protocol; each 25ul reaction contained 12.5ul Master Mix, 10ul H2O, 0.5ul forward primer, 0.5ul reverse primer, and 1.5ul DNA. PCR program was run at 95°C 3min, 95°C 30sec, 56°C 1:10 min, 72°C 1min, go to step2, 35x, 72°C 5min, 10°C hold and then optimized accordingly. PCR product was cleaned using QIAquick PCR Purification kit according to manufactures protocols (Qiagen Cat No./ID: 28106). Sanger sequencing was

completed at the Roy J. Carver Biotechnology Center at the University of Illinois Urbana-Champaign. The full gene sequence was assembled in Sequencher (Sequencher® version 5.4.6).

RTqPCR

(Yg3-N1582/+ x B73) x B73 plants were grown in the growth chamber and samples collected at 8 DAP, 10 DAP, 12 DAP at daytime (12PM "noon") and nighttime (12AM "midnight") for green and yellow phenotypes; six time points times two genotypes equals 12 total samples. Four biological replicates of leaf tissue were pooled for each genotype at each time point and stored at -80°C. RNA was extracted using Trizol phase separation RNA isolation procedure according to manufactures protocol (Ambion/ Life Technologies Cat No. 15596-018). RNA was quantified by Nanodrop spectrophotometry and Ribogreen assay run on a BioRad plate reader. Primers were designed in the exons of gene GRMZM2G165521. Positive control primers EIF4A, bTUB, EF1a, and CYP were selected based on Lin et al. (2014). Expected product size was calculated. First strand cDNA was synthesized from extracted RNA by a simple reverse transcriptase reaction using Superscript II manufactures protocol (Invitrogen/Life Technologies Cat No. 18064-022) with random primers. Primers and cDNA were used for PCR optimization. PCR was preformed using GoTaq Green master mix according to manufactures protocol (Promega Cat No. M7122). PCR optimal setting: 95°C at 3:00min, 95°C at 0:30sec, 54°C at 1:10min, 72°C at 1:00min, go to step2 35x, 72°C 5:00min, 10°C infinite hold. The resulting product and 100bp ladder was run on a 1% TAE agarose gel at 90V for 43min. RTqPCR master mixes were made using Power SYBR Green Master Mix (Applied Biosystems) according to manufactures protocols. Plates were run at the Roy J. Carver Biotechnology Center on an ABI 7900 real time PCR machine. QuantStudio Flex 7 software was used to complete quality control on the datasets.

Relative Quantification Using the Comparative CT Method ($\Delta\Delta C_T$)

Relative fold change calculated by elative quantification using the comparative C_T method $\Delta\Delta C_T$ (Livak, & Schmittgen 2001). The average of the raw C_T values for the housekeeping gene (EIF4a) and the gene being tested (GRMZM2G165521) in experimental (Yellow) and control (green) conditions were calculated. Resulting in four values: gene being tested experimental (TE), gene being tested control (TC), housekeeping gene experimental (HE), and housekeeping control (HC). The difference between TE and HE (TE-HC) and TC and HC (TC-HC) were calculated. These are the ΔC_T values for the experimental (Δ C_TE) and the control

($\Delta C_T C$). The difference between $\Delta C_T E$ and $\Delta C_T C$ (ΔCTE - ΔCTC) was calculated. This calculated difference ($\Delta C_T E$ - $\Delta C_T C$) is the double delta C_T value ($\Delta\Delta C_T$). All calculations were in log base two. Calculate the values of 2^-$\Delta\Delta$CT to get fold change expression. The fold change is shown as linear; below one is target down regulated relative to control, above one target upregulated relative to control, and one equals no change in expression.

Gene Feature Prediction

Open reading frames were identified using SMS (Stothard 2000), NCBI (Coordinaters 2016), and DNAstar (GeneQuest ®. Version 12.0). Peptide identification was completed using WoLFPSORT (Horton et al. 2007), TARGETP (Emanuelsson et al. 2000), and iPSORT (Banani et al. 2002).

UniformMu Insert Screens

UFMu-06653, which carries insert *Mu1053333*, was crossed to *(Yg3-N1582/+* x B73) x B73 segregating for yellow phenotype in the 2017 summer nursery. The resulting seed that displayed kernel colored patterning indicative of successful Mu insertion were planted in a seedling screen. Two individual ears from separate plants were screened in 96 well flats in a growth chamber. Plants were visually assessed for yellow or green phenotype. Tissue was harvested from 13 yellow individuals. DNA was extracted using a CTAB protocol and quantified by nanodrop. Common PCR conditions (0.5ul primers, 1.5ul DNA, 0.6 ul DMSO, 9.4ul H20, 12.5ul GO Taq master mix) were used. Thermocycling conditions were 95°C for 3 minutes, 95°C for 30 seconds, 54°C for 1:10 minutes, 72°C for 1 minute, go to step2 for 35x, 72°C for 5 minutes, 10°C infinite hold. Mu Specific primers TIR6_forward and 5R were visualized by electrophoresis on a 1% gel (1x TBA) stained with gel red at 90V for 45 min. Gene specific primers 1F (anchored in exon 1) and 2R (anchored in exon 2) were visualized by electrophoresis on a 1% gel (1x TBA) stained with gel red at 90V for 45 min. PCR based genotyping was completed according to McCarthy et al. (2013).

Color Expression in Different Backgrounds

(*Yg3-N1582/+*) x B73 was crossed with a subset of NAM founder accessions (CML103, CML247, CML333, IL14H, KY21, M37W, Mo18W, P39, TX303, B97, Mo17, MS71, NC358, and Oh43) in the field. The resulting *(Yg3-N1582* /+ x B73) x NAM were grown under growth chamber conditions and visually assessed for segregating yellow and green phenotypes.

RESULTS AND DISCUSSION

Maize stock mutant *Yg3-N1582* maps to 173-175 Mb on chromosome 5 (Figure 4.3 A). This interval does not coincide with a previously characterized *yg* mutant. Under this interval there are 57 unique genes and 137 unique transcript variants (AGPv3, Figure 4.3 B, Kersey et al. 2018). From this list it was found that the syntenic paralog of GRMZM2G165521 is GRMZM2G114653 and both are orthologs of rice LOC_Os05g38190 [MSU] = Os05g0455900 [Gramene]. Differential expression revealed no expression differences at the gene level under this interval. However, there were transcripts with differences in expression between the mutant and wild type. Differential expression analysis identified GRMZM2G165521 as a candidate gene that could underlie the mutant phenotype (Figure 4.4). GRMZM2G165521 is a predicted PPR, DYW subclass protein involved in RNA editing and is orthologous to a rice protein that produces *yg* phenotypes. Full gene sequencing of GRMZM2G165521 in *Yg3-N1582* / *Yg3-N1582* reveals 3 SNPs, one deletion, and a seven base pair insertion in the first intron relative to the wild-type reference line (Table 4.1 & Figure 4.5). This insertion results in an alternate transcription start site and open reading frame that eliminates the first exon of the PPR protein (Table 4.2). Sequencing of the highly repetitive coding region was completed using internal primers to ensure shorter, higher quality reads. Internal primers were spaced approximately 100-300bp apart. The alignment of *Yg3-N1582* /+ RNAseq reads confirm transcription at the site of the insertion (Figure 4.6). Additionally, variant calling confirms the SNP identified in exon 2 (*Yg3-N1582*/+) x B73 crossed with a NAM subset confirms the marker color expression in different backgrounds (Table 4.3). Quantitative PCR of GRMZM2G165521 expression patterns revealed an up regulation during daytime samples indicating a potential for use in studies of photosynthesis (Figure 4.7). Most dominant mutations are gain of function and GRMZM2G165521 has a Mu transposon in its 5' UTR region. To determine if GRMZM2G165521-Mu/ GRMZM2G165521-Mu has a phenotype individuals were identified (Figure 4.8) and grown in the greenhouse. The recovered Mu/Mu (-/-) plants had a slightly yellowish green phenotype and were selfed.

Disruption of PPR proteins causes seedling specific albino or yellow phenotypes in maize, Arabidopsis, and rice orthologs (Khrouchychova et al. 2012, Su et al. 2012, Asano et al. 2013). Several mutations of PPR proteins have been shown to disrupt the splicing of group II introns resulting in a yellow-green, pale yellow, or albino seedling stage leaf phenotype. THA8

(Khrouchtchove et al. 2012), PPR4 (Schmitz-Linneweber et al. 2006), PPR5 (Beick et al. 2008), OTP51 (Longevialle et al. 2008), OsPPR1 (Gothandam et al., 2005), OsPPR4 (Asano et al. 2014), and ALS3 (Lin et al. 2015) have been identified. All of these mutants described are seedling-lethal and do not grow out of the seedling stage color phenotype before death. However, viable PPR mutants have been identified in Arabidopsis and rice. OTP70 is an Arabidopsis mutant, which has a pigment-defective splicing mechanism that causes pale yellow seedling cotyledons (Chateigner-Boutin et al. 2011). In these mutants seedling growth was delayed compared with wild type and true leaves developed green. Rice albino leaf PPR mutant *young seedling albino* (*ysa*) is reported to have a white phenotype before leaf stage three and then recovers to green by the sixth leaf stage (Su et al. 2012). This rice ortholog's phenotype displays no apparent negative effects and its relative expression RNA profiling also suggests a role in chloroplast biogenesis. *YSA* has been proposed as an early marker for efficient selection in rice for identification and elimination of false hybrids in commercial production (Su et al. 2012).

Understanding why *Yg3* mutants, and rice *ysa* mutants, display a seedling stage specific leaf color phenotype is an interesting question. One explanation is that other related genes may compensate for the absence of the mutated gene during later developmental stages. If PPR proteins bind RNA by the mechanism that is currently hypothesized (Fujii et al. 2011, Prikryl et al. 2011, Rackham & Filipovska 2012), it seems unlikely that isolated PPR motifs can account for all stabilizing and specific editing tasks. Detecting interactions between variant PPRs and RNA or other splicing factors could account for transition to the green phenotype seen in later developmental stages of the viable mutants. Or it is also possible that the gene is not required for later developmental stages of chloroplast development. Later stage greening suggests the possibility that additional genes and proteins may be involved in recruiting to the chloroplast. In maize, the molecular mechanisms of leaf-color mutations and the loci responsible are not fully understood and further mutant analysis is an effective approach to explore the function of genes in chloroplast development (Belcher et al. 2015). These results suggest that the disruption of GRMZM2G165521, a PPR protein, causes a chlorophyll-deficient seedling stage leaf color phenotype and may play an important role in the early stages of chloroplast biogenesis.

CONCLUSIONS

GRMZM2G165521 is a candidate gene that could underlie the seedling stage dominant yellow-green leaf phenotype of *Yg3-N1582*. This research identifies a possible mutation, which

could be utilized as a marker to develop DH inducers for breeding programs using exotic germplasm, including the current CML collection (Wu et al. 2016). Furthermore, *Yg3-N1582* may also have value as a general research tool for the study of early stages of chloroplast biogenesis.

FIGURES AND TABLES

Figure 4.1 *Yg3-N1582* Color Expression. The mutant has (A & B) no color expression in the embryo or before emergence. Color expression is observed at (C) coleoptile emergence and extends through (D - F) seedling stages, eventually turning WT green. The phenotype is observed in the greenhouse and the (G & H) field.

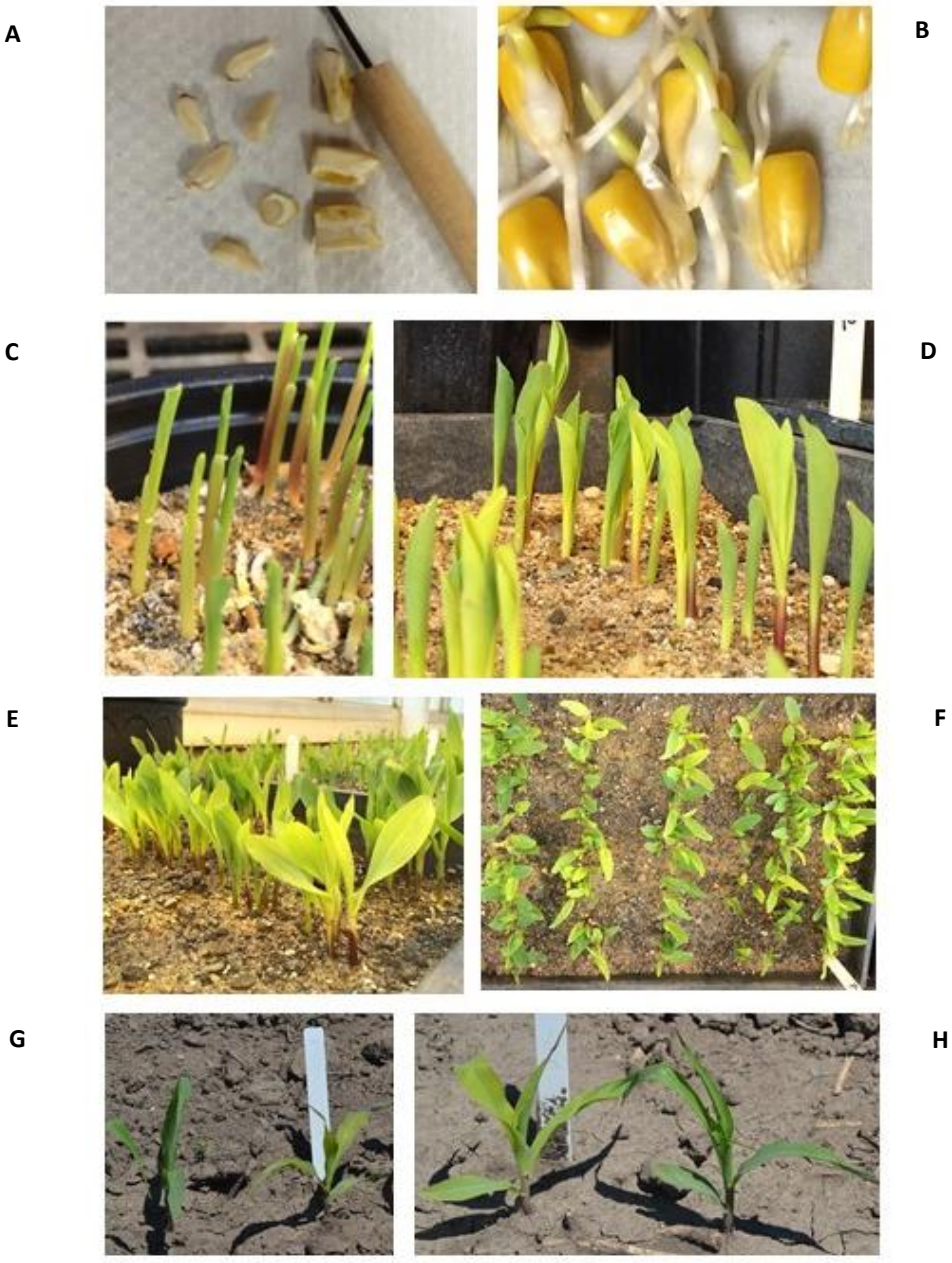

Figure 4.2 Doubled Haploid Breeding Schematic and Proposed Alternative Induction Markers. (Top) Currently the most widely used paternal marker in haploid inducers is *R1-Navajo* (*R1-nj*), which gives a pigmented kernel crown and embryo. (Bottom) Proposed alternative markers for DH induction detection red roots (Chaikam et al. 2016), oil content markers (Oregon State University 2017), and stock mutant *Yg3-N1582* (Sachs & Stinard 2012).

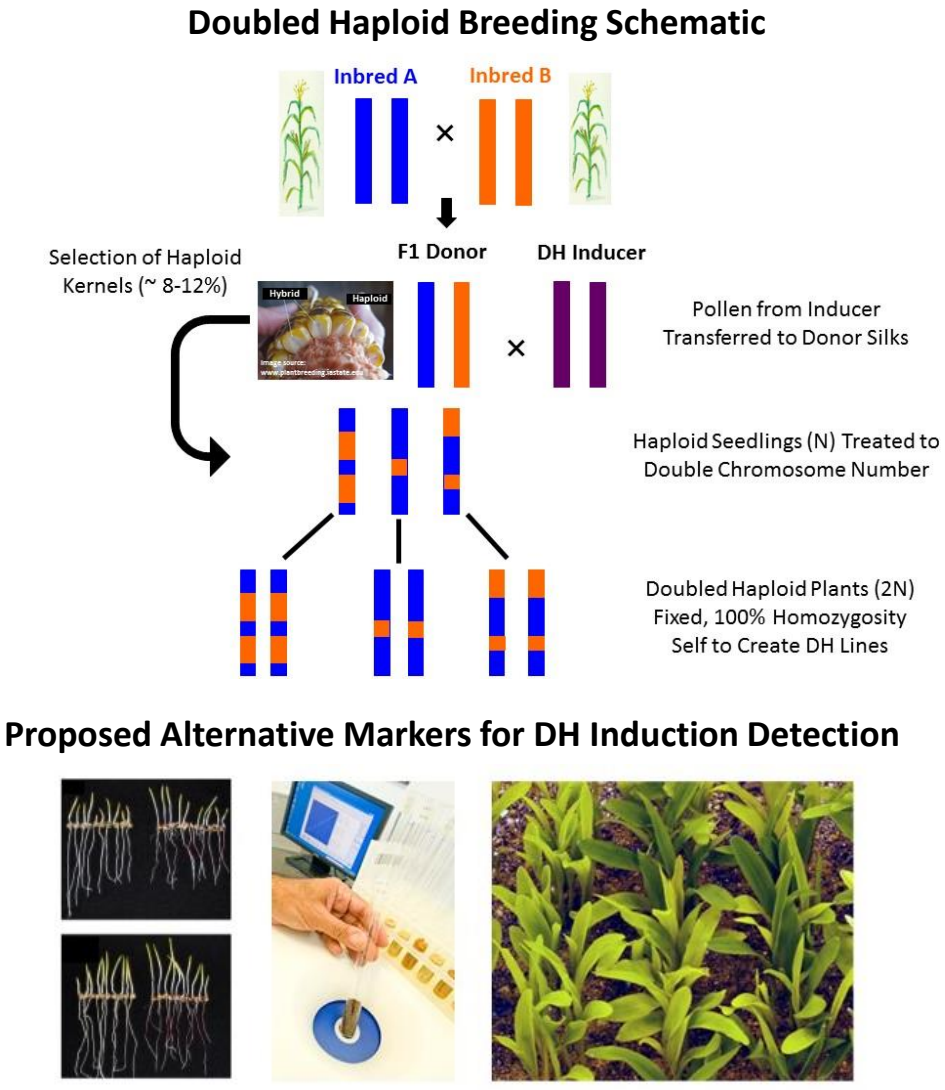

Figure 4.3 Mapping Results. Maize stock mutant *Yg3-N1582* maps to (A) 173-175 Mb on chromosome 5. This interval does not coincide with a previously characterized *yg* mutant. (B) Under this interval there are 57 unique genes and 137 unique transcript variants (AGPv3, Kersey et al. 2018). From this list it was found that the syntenic paralog of GRMZM2G165521 is GRMZM2G114653 and both are 'best hit' orthologs of rice LOC_Os05g38190 [MSU] and Os05g0455900 [Gramene].

A

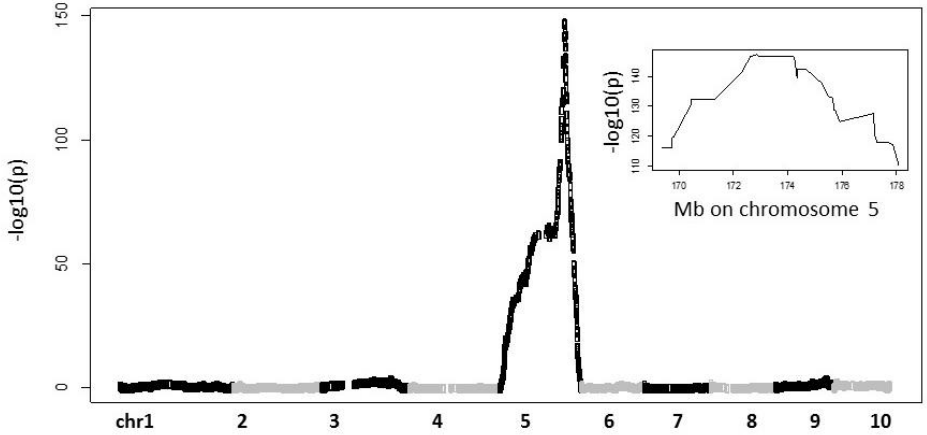

B

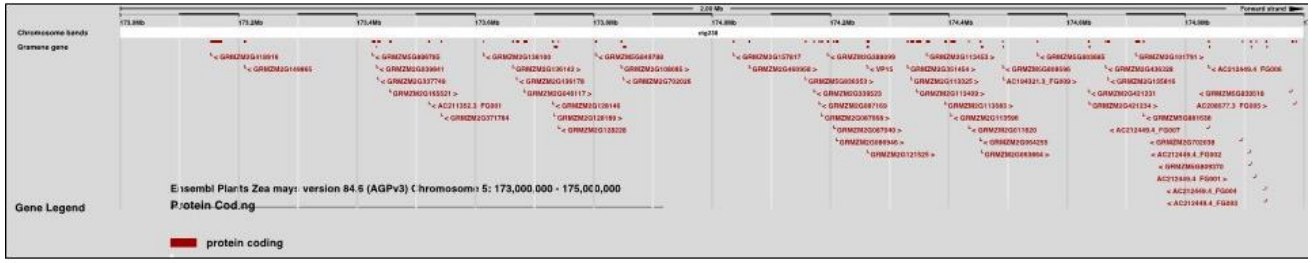

Figure 4.4 Transcriptome Profiling. Differential expression analysis identified GRMZM2G165521 as a candidate gene that could underlie the mutant phenotype. GRMZM2G165521 is a predicted PPR protein involved in RNA editing. The syntenic paralog of GRMZM2G165521 is GRMZM2G114653 and both are 'best hit' orthologs of rice LOC_Os05g38190 [MSU] and Os05g0455900 [Gramene]. GRMZM2G165521 gene model, Chr5: 173,454,046 - 173,460,109 AGPv3 (A) wild type green plants express the B73 AGPv3 annotated gene. The gene has no splice variants. (B) *Yg3-N1582/+* plants express a truncated version of the B73 AGPv3 annotated gene. Within the truncated exon one there is also a smaller repeat fragment aligning. At later seedling stages it then expresses the B73 AGPv3 annotated gene. (C & D) Transcript expression by FPKM.

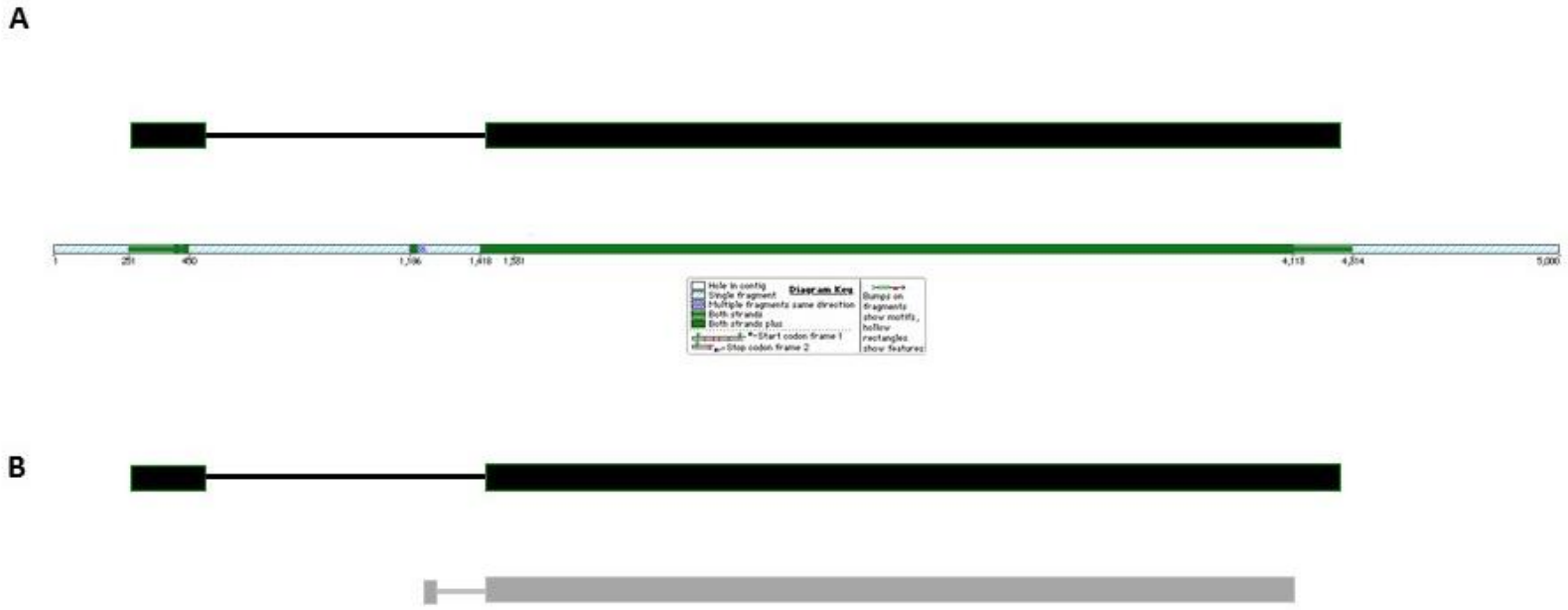

Figure 4.4 (cont.)

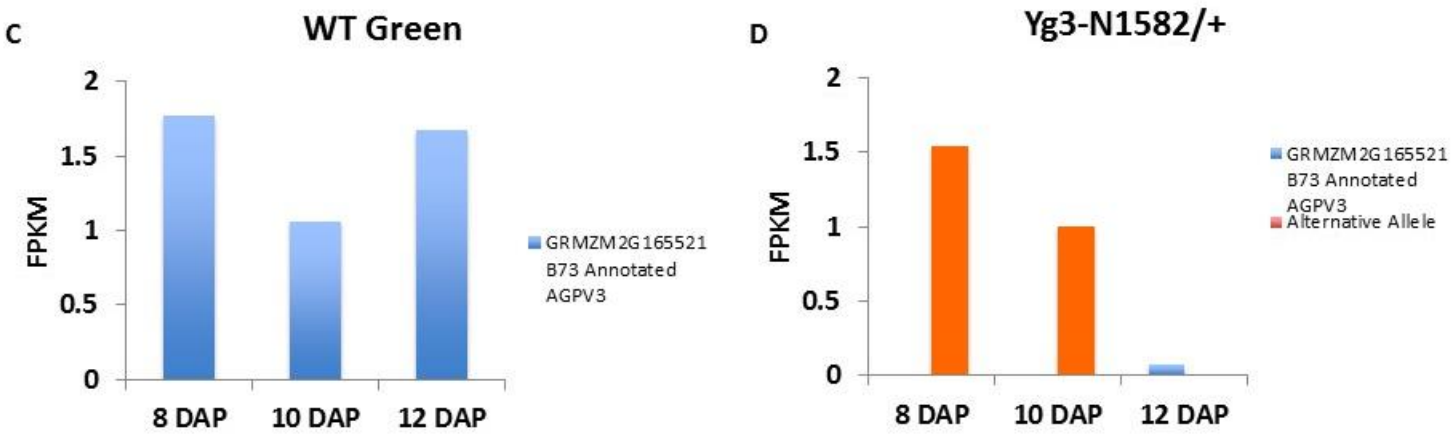

Table 4.1 *Yg3-N1582* / *Yg3-N1582* Full Gene Sequencing Results. Full gene sequencing of GRMZM2G165521 in the *Yg3-N1582* / *Yg3-N1582* background reveals a seven base pair insertion in the first intron relative to the wild-type reference line. This insertion results in an alternate transcription start site (TSS).

Zea_chr5 Reference Location (bp)	Gene Model Feature	Feature Identified	Resulting Change
568	Intron	SNP	T -> G
603	Intron	Deletion	remove T
700	intron/ open reading frame	Insertion (7bp)	TSS
913	Intron	SNP	T -> G
3471	exon2/coding region	SNP	G -> A

Figure 4.5 Insertion Feature Identified in *Yg3-N1582/Yg3-N1582* Full Gene Sequencing. *Yg3-N1582/Yg3-N1582* seed homozygous for the dominant mutant *Yg3* allele was Sanger sequenced at the Roy J. Carver Biotechnology Center at the University of Illinois Urbana-Champaign. The full gene sequence was assembled in Sequencher (Sequencher® version 5.4.6) and reveals a seven base pair insertion in the first intron relative to the wild-type reference line.

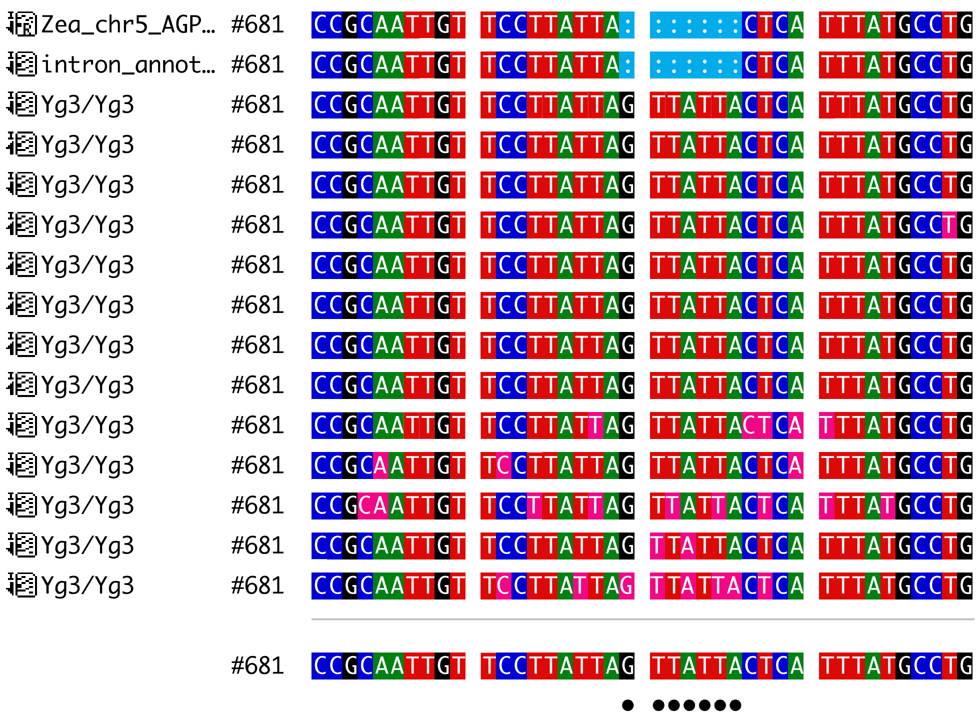

Table 4.2 GRMZM2G165521 Predicted Gene Features. Open reading frames were identified using SMS (Stothard 2000), NCBI (Coordinaters 2016), and DNAstar (GeneQuest ®. Version 12.0). Peptide identification was completed using WoLFPSORT (Horton et al. 2007), TARGETP (Emanuelsson et al. 2000), and iPSORT (Banani et al. 2002). The mutation results in the elimination of a chloroplast transit peptide (cTP). This insertion results in an alternate transcription start site and open reading frame that eliminates the first exon of the PPR protein.

Gene Model Feature	Transit Peptide Prediction			Open Reading Frame Prediction			Protein Prediction	
	TARGETP	iPSORT	WoLFPSORT	DNAstar	SMS	NCBI		
Annotated Exon1	cTP	cTP	cTP	-	-	-	-	-
Truncated Exon1	none	none	none	-	-	-	-	-
Nested Fragment	none	none	none	-	-	-	-	-
Annotated Intron	-	-	-	3' Open reading frame	3' Open reading frame	3' Open reading frame	-	-
Intron w/ Insertion	-	-	-	ATG in frame w/exon2	ATG in frame w/exon2	ATG in frame w/exon2	-	-
Annotated Exon2	-	-	-	-	-	-	PPR	PPR
Truncated Exon2	-	-	-	-	-	-	PPR	PPR

Figure 4.6 RNAseq Read Alignments to the Intron for *Yg3-N1582*/+. Reads were aligned using STAR 2Pass (Dobinet et al. 2013) and the GATK (McKenna et al. 2010, Depristo et al. 2011, Van der Auwera et al. 2013) clean up pipeline was implemented. The output VCF file was visualized in VGI viewer (Robinson et al. 2011). The alignment of *Yg3-N1582*/+ RNAseq reads confirm transcription at the site of the insertion. Variant calling identifies the same SNP in exon 2 as in full gene sequencing results**.**

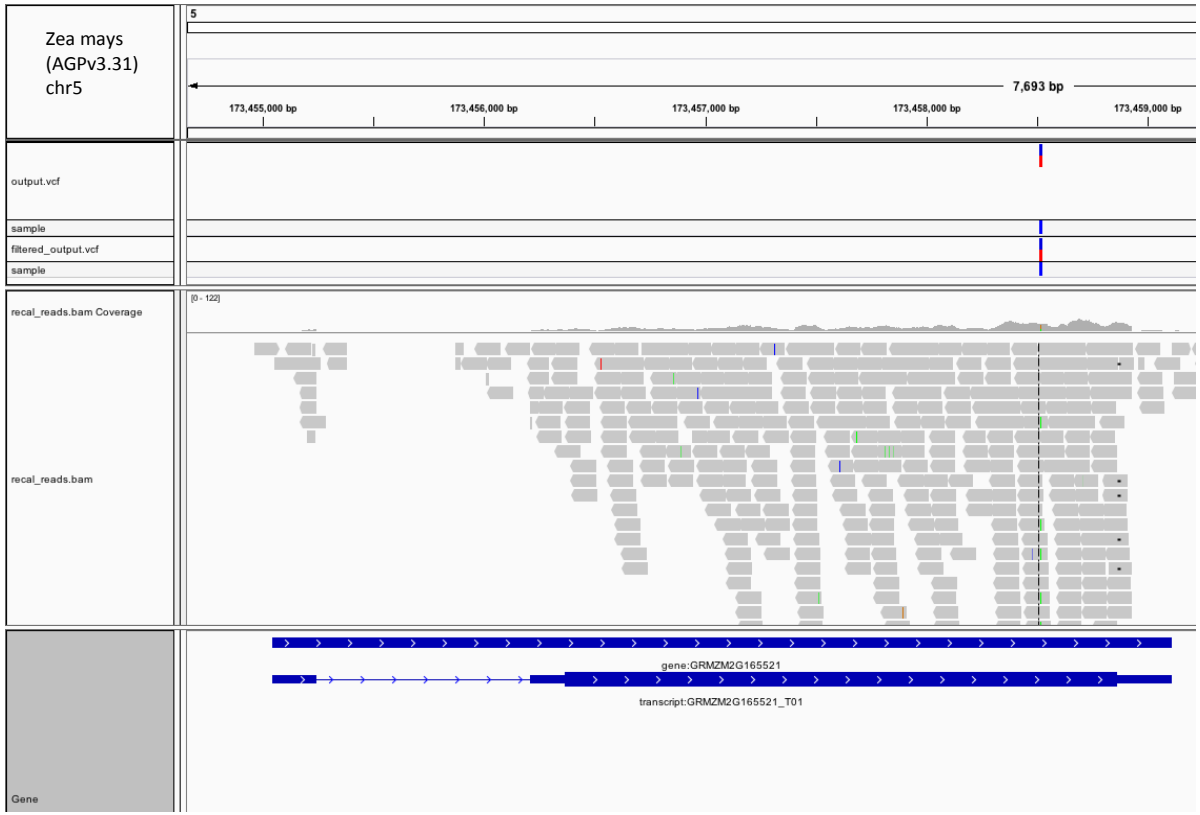

Table 4.3 Yellow-Green Segregation Ratios in Different Backgrounds. *(Yg3-N1582/+)* x B73 was crossed with a subset of NAM founder accessions (CML103, CML247, CML333, IL14H, KY21, M37W, Mo18W, P39, TX303, B97, Mo17, MS71, NC358, and Oh43) in the field. The resulting (*Yg3-N1582* /+ x B73) x NAM were grown under growth chamber conditions and visually assessed for segregating yellow and green phenotypes. 1 Yellow:1 Green color expression was expected when crossing *Yg3-N1582/+* x B73 with different background from a subset of NAM lines. Chi square values are within the expected distributions and no significant difference from the expected ratio was observed. This suggests that *Yg3* could be used as an induction marker in diverse backgrounds.

Cross Produced	Number Yellow	Number Green	Chi Square Value	Degrees of Freedom	P-Value
(Yg3-N1582/+ x B73) x CML103	21	25	0.348	1	0.5553
(Yg3-N1582/+ x B73) x CML247	18	27	1.800	1	0.1797
(Yg3-N1582/+ x B73) x CML333	11	18	1.690	1	0.1936
(Yg3-N1582/+ x B73) x IL14HH	20	26	0.783	1	0.3763
(Yg3-N1582/+ x B73) x KY21	19	25	0.818	1	0.3657
(Yg3-N1582/+ x B73) x M37W	13	18	0.806	1	0.3692
(Yg3-N1582/+ x B73) X Mo18W	10	12	0.182	1	0.6698
(Yg3-N1582/+ x B73) x P39	11	13	0.167	1	0.6831
(Yg3-N1582/+ x B73) x Tx303	11	12	0.043	1	0.8348
B97 x (Yg3-N1582/+ x B73)	17	19	0.111	1	0.7389
Mo17 x (Yg3-N1582/+ x B73)	13	21	1.882	1	0.1701
MS71 x (Yg3-N1582/+ x B73)	16	20	0.444	1	0.5050
NC358 x (Yg3-N1582/+ x B73)	21	27	0.750	1	0.3865
Oh43 x (Yg3-N1582/+ x B73)	19	27	1.391	1	0.2382

Figure 4.7 Diurnal Changes in *Yg3* Candidate Gene Expression During Early Seedling Development. Relative fold change calculated by the comparative C_T method $\Delta\Delta C_T$ (Livak, & Schmittgen 2001). The average of the raw C_T values for the housekeeping gene (EIF4a) and the gene being tested (GRMZM2G165521) in experimental (Yellow) and control (green) conditions were calculated. The difference between $\Delta C_T E$ and $\Delta C_T C$ (ΔCTE - ΔCTC) was calculated. This calculated difference ($\Delta C_T E$ - $\Delta C_T C$) is the double delta C_T value ($\Delta\Delta C_T$). All calculations were in log base two and the values of 2^-$\Delta\Delta$CT were calculated to get fold change expression. The fold change is shown as linear; below one is target down regulated relative to control, above one target upregulated relative to control, and one equals no change in expression. Quantitative PCR of GRMZM2G165521 expression patterns revealed an up regulation during daytime samples indicating a potential for use in studies of photosynthesis.

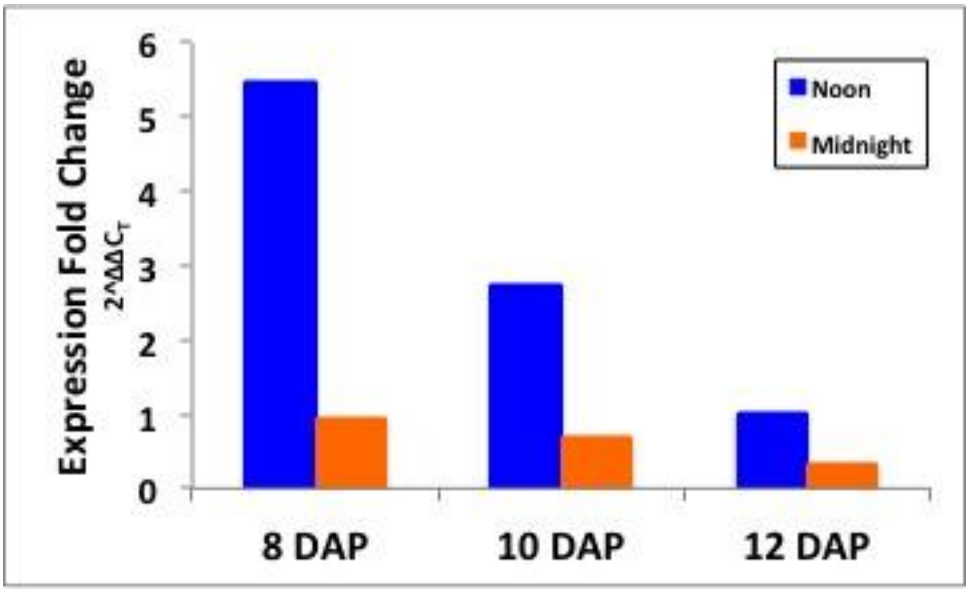

Figure 4.8 UniformMu Insert Screens. (A) UFMu-06653, which carries Mu1053333, was crossed to *(Yg3-N1582/+* x B73) x B73 segregating for yellow phenotype. The resulting seed that displayed kernel colored patterning indicative of successful Mu insertion were planted in a seedling screen. (B) PCR based genotyping was completed according to McCarthy et al. (2013). PCR genotyping results: wild type allele present (+), Mu insertion allele present (-), Lane1 100bp ladder, lanes 2-14 Individuals 1-13; in Mu Specific lane 15 is positive control (4_upstream5R). (C) -/- Individuals were retained and grown in the greenhouse. These plants display a slightly yellowish green phenotype, similar to the *Yg3-N1582/Yg3-N1582* phenotype observed in the field. -/- individuals appear viable and were selfed.

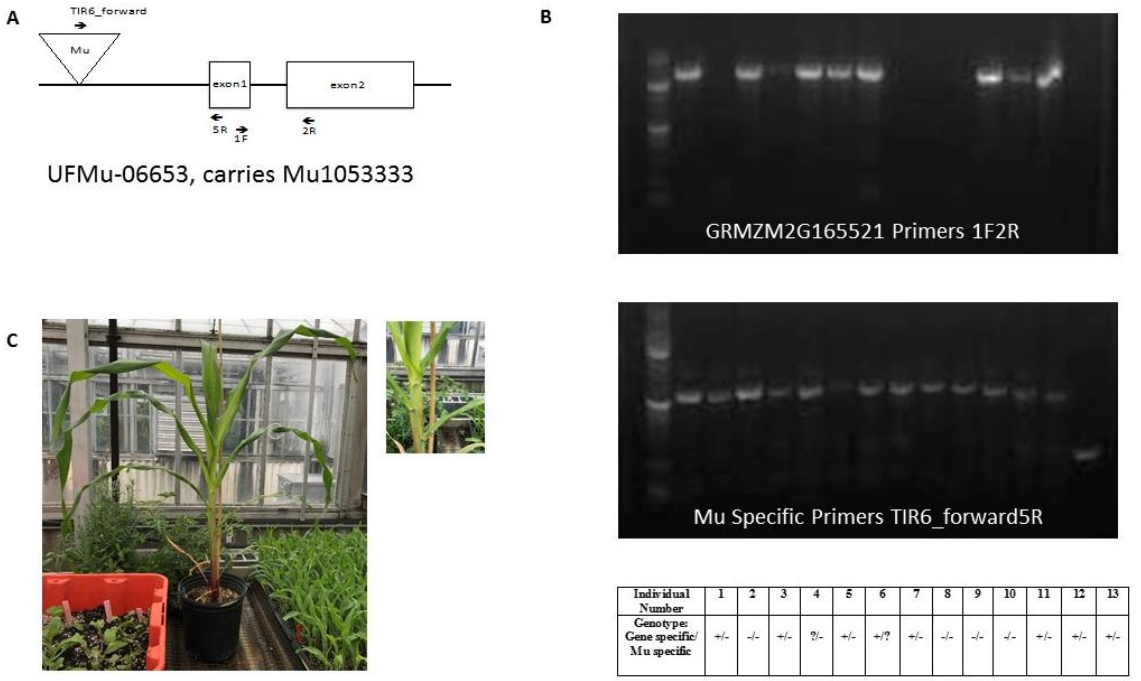

Individual Number	1	2	3	4	5	6	7	8	9	10	11	12	13
Genotype: Gene specific/ Mu specific	+/-	-/-	+/-	?/-	+/-	+/?	+/-	-/-	-/-	-/-	+/-	+/-	+/-

REFERENCES CITED

Asano, T., Miyao, A., Hirochika, H., Kikuchi, S., & Kadowaki, K. I. (2013). A pentatricopeptide repeat gene of rice is required for splicing of chloroplast transcripts and RNA editing of ndhA. Plant Biotechnology, 30(1), 57-64.

Bannai, H., Tamada, Y., Maruyama, O., Nakai, K., & Miyano, S. (2002). Extensive feature detection of N-terminal protein sorting signals. Bioinformatics, 18(2), 298-305.

Barkan, A., & Small, I. (2014). Pentatricopeptide repeat proteins in plants. Annual Review of Plant Biology, 65(1), 415-442.

Beick, S., Schmitz-Linneweber, C., Williams-Carrier, R., Jensen, B., & Barkan, A. (2008). The pentatricopeptide repeat protein PPR5 stabilizes a specific tRNA precursor in maize chloroplasts. Molecular and Cellular Biology, 28(17), 5337-5347.

Belcher, S., Williams-Carrier, R., Stiffler, N., & Barkan, A. (2015). Large-scale genetic analysis of chloroplast biogenesis in maize. Biochimica et Biophysica Acta Bioenergetics, 1847(9), 1004-1016.

Chaikam, V., Martinez, L., Melchinger, A.E., Schipprack, W., & Boddupalli, P.M. (2016). Development and validation of red root marker-based haploid inducers in maize. Crop Science, 56(4), 1678-1688.

Chaikam, V., Nair, S.K., Babu, R., Martinez, L., Tejomurtula, J., & Boddupalli, P.M. (2015). Analysis of effectiveness of R1-nj anthocyanin marker for in vivo haploid identification in maize and molecular markers for predicting the inhibition of R1-nj expression. Theoretical and Applied Genetics, 128(1), 159–171.

Chateigner-Boutin, A.L., des Francs-Small, C.C., Delannoy, E., Kahlau, S., Tanz, S.K., de Longevialle, A.F., Fujii, S., &Small, I. (2011). OTP70 is a pentatricopeptide repeat protein of the E subgroup involved in splicing of the plastid transcript rpoC1. The Plant Journal, 65(4), 532-542.

Coe, E.H. & Sarkar, K.R. (1964). The detection of haploids in maize. Journal of Heredity, 55(1), 231–233.

Coordinators, N. R. (2016). Database resources of the national center for biotechnology information. Nucleic Acids Research, 44(Database issue), D7.

Couto, E.G. de O., Pinho, É.V. de R.V., Pinho, R.G.V., Veiga, A.D., Bustamante, F. de O., & Dias, K.O. das G. (2015a). In vivo haploid induction and efficiency of two chromosome duplication protocols in tropical maize. Ciência E Agrotecnologia, 39(1), 435–442.

Couto, E.G. de O., Pinho, E.V. de R.V., Pinho, R.G. V., Veiga, A.D., Carvalho, M.R., Bustamante, F., & Nascimento, M.S. (2015b). Verification and characterization of chromosome duplication in haploid maize. Genetics and Molecular Research 14(1), 6999–7007.

Delannoy, E., Stanley, W. A., Bond, C. S., & Small, I. D. (2007). Pentatricopeptide repeat (PPR) proteins as sequence-specificity factors in post-transcriptional processes in organelles. Biochemical Society Transactions, 35(6), 1643-1647.

DePristo, M., Banks, E., Poplin, R., Garimella, K., Maguire, J., Hartl, C., Philippakis, A., del Angel, G., Rivas, M.A., Hanna, M., McKenna, A., Fennell, T., Kernytsky, A., Sivachenko, A., Cibulskis, K., Gabriel, S., Altshuler, D., & Daly, M. (2011). A framework for variation discovery and genotyping using next-generation DNA sequencing data. Nature Genetics, 43(1), 491-498.

Dobin, A., Davis, C.A., Schlesinger, F., Drenkow, J., Zaleski, C., Jha, S., Batut, P., Chaisson, M. & Gingeras, T.R. (2013). STAR: ultrafast universal RNA-seq aligner. Bioinformatics, 29(1), 15-21.

Dwivedi, S.L., Britt, A.B., Tripathi, L., Sharma, S., Upadhyaya, H.D., & Ortiz, R. (2015). Haploids: Constraints and opportunities in plant breeding. Biotechnology Advances, 33(6), 812–829.

Emanuelsson, O., Nielsen, H., Brunak, S., & Von Heijne, G. (2000). Predicting subcellular localization of proteins based on their N-terminal amino acid sequence. Journal of Molecular Biology, 300(4), 1005-1016.

Forster, B.P. and Thomas, W.T. (2010). Doubled haploids in genetics and plant breeding. Plant Breeding Reviews, 25(1), 57-88.

Frazee, A.C., Pertea, G., Jaffe, A.E., Langmead, B., Salzberg, S.L., & Leek, J.T. (2015). Ballgown bridges the gap between transcriptome assembly and expression analysis. Nature Biotechnology, 33(3), 243–246.

Fujii, S., & Small, I. (2011). The evolution of RNA editing and pentatricopeptide repeat genes. New Phytologist, 191(1), 37-47.

GeneQuest ®. Version 12.0. DNASTAR. Madison, WI.

Gentleman, R.C., Carey, V.J., Bates, D.M., Bolstad, B., Dettling, M., Dudoit, S., Ellis, B., Gautier, L., Ge, Y., Gentry, J., & Hornik, K. (2004). Bioconductor: open software development for computational biology and bioinformatics. Genome Biology, 5(10), 80-92.

Glaubitz, J.C., Casstevens, T.M., Lu, F., Harriman, J., Elshire, R.J., Sun, Q., & Buckler, E.S. (2014). TASSEL-GBS: a high capacity genotyping by sequencing analysis pipeline. PLOS One, 9(2), 90346-90352.

Gothandam, K. M., Kim, E. S., Cho, H., & Chung, Y. Y. (2005). OsPPR1, a pentatricopeptide repeat protein of rice is essential for the chloroplast biogenesis. Plant Molecular Biology, 58(3), 421-433.

Hallauer, A. R. (2000). Specialty corns. CRC press.

Horton, P., Park, K.J., Obayashi, T., Fujita, N., Harada, H., Adams-Collier, C.J., & Nakai, K. (2007). WoLF PSORT: protein localization predictor. Nucleic Acids Research, 35(supplemental 2), 585-587.

Kersey, P.J., Allen, J.E., Allot, A., Barba, M., Boddu, S., Bolt, B.J., Carvalho-Silva, D., Christensen, M., Davis, P., Grabmueller, C., & Kumar, N. (2017). Ensembl Genomes 2018: an integrated omics infrastructure for non-vertebrate species. Nucleic Acids Research, 46(D1), 802-808.

Khrouchtchova, A., Monde, R. A., & Barkan, A. (2012). A short PPR protein required for the splicing of specific group II introns in angiosperm chloroplasts. Rna, 18(6), 1197-1209.

Kim, D., Langmead, B., & Salzberg, S.L. (2015). HISAT: a fast spliced aligner with low memory requirements. Nature Methods, 12(4), 357–360.

Kleiber, D., Prigge, V., Melchinger, A.E., Burkard, F., San Vicente, F., Palomino, G., & Gordillo, G.A. (2012). Haploid Fertility in Temperate and Tropical Maize Germplasm. Crop Science, 52(5), 623–630.

Lawrence, C.J., Dong, Q., Polacco, M.L., Seigfried, T.E., & Brendel, V. (2004). MaizeGDB, the community database for maize genetics and genomics. Nucleic Acids Research, 32(supplemental 1), D393–D397.

Lertrat, K., & Pulam, T. (2007). Breeding for increased sweetness in sweet corn. International Journal of Plant Breeding, 1(1), 27–30.

Lin, D., Gong, X., Jiang, Q., Zheng, K., Zhou, H., Xu, J., Teng, S., & Dong, Y. (2015). The rice ALS3 encoding a novel pentatricopeptide repeat protein is required for chloroplast development and seedling growth. Rice, 8(1), 17-25.

Lin, Y., Zhang, C., Lan, H., Gao, S., Liu, H., Liu, J., Cao, M., Pan, G., Rong, T., & Zhang, S. (2014). Validation of potential reference genes for qPCR in maize across abiotic stresses, hormone treatments, and tissue types. PLOS One, 9(5), 95445-95458.

Linus Torvalds. (2015). Linux (4.1-rc8) [Operating System]. Retrieved from https//:github.com/Torvalds/linus/releases/tag/v4.1-rc8.

Livak, K.J. & Schmittgen, T.D. (2001). Analysis of relative gene expression data using real-time quantitative PCR and the $2^{-\Delta\Delta CT}$ method. Methods, 25(4), 402-408.

Longevialle, D., Falcon, A., Hendrickson, L., Taylor, N.L., Delannoy, E., Lurin, C., Badger, M., Millar, A.H., & Small, I. (2008). The pentatricopeptide repeat gene OTP51 with two LAGLIDADG motifs is required for the cis-splicing of plastid ycf3 intron 2 in Arabidopsis thaliana. The Plant Journal, 56(1), 157-168.

Lurin, C., Andrés, C., Aubourg, S., Bellaoui, M., Bitton, F., Bruyère, C., Caboche, M., Debast, C., Gualberto, J., Hoffmann, B., & Lecharny, A. (2004). Genome-wide analysis of Arabidopsis pentatricopeptide repeat proteins reveals their essential role in organelle biogenesis. The Plant Cell, 16(8), 2089-2103.

Manna, S. (2015). An overview of pentatricopeptide repeat proteins and their application. Biochimie, 133(1), 93-99.

McCarty, D.R., Suzuki, M., Hunter, C., Collins, J., Avigne, W.T., & Koch, K.E. (2013). Genetic and molecular analyses of UniformMu transposon insertion lines. In Plant Transposable Elements. Humana Press, Totowa, N.J.

McGraw, L. (2000). Corn: Talking genetic stock. USDA Agricultural Research Newsletter, 18–19.

McKenna, A., Hanna, M., Banks, E., Sivachenko, A., Cibulskis, K., Kernytsky, A., Garimella, K., Altshuler, D., Gabriel, S., Daly, M., & DePristo, M.A. (2010). The Genome Analysis Toolkit: a MapReduce framework for analyzing next-generation DNA sequencing data. Genome Research, 20(9), 1297-1303.

Neuffer, M.G., Chang, M., Sylvester, A.W., Lawrence, C.J., & Hake, S. (2011). New dominant mutants from EMS mutagenesis. Maize Genetics Conference Abstracts, 135.

Neuffer, M.G., Coe, E.H., Jr, & Wessler, S.R. (1997). Mutants of maize. Cold Spring Harbor Laboratory Press.

Neuffer, M.G., Johal, G., Chang, M.T., & Hake, S. (2009). Mutagenesis – the key to genetic analysis. In Handbook of Maize, J.L. Bennetzen, and S. Hake, eds., New York, NY, Springer, 63–84.

Pertea, M., Kim, D., Pertea, G.M., Leek, J.T., & Salzberg, S.L. (2016). Transcript-level expression analysis of RNA-seq experiments with HISAT, StringTie and Ballgown. Nature Protocols 11(9), 1650–1667.

Pertea, M., Pertea, G.M., Antonescu, C.M., Chang, T.-C., Mendell, J.T., & Salzberg, S.L. (2015). StringTie enables improved reconstruction of a transcriptome from RNA-seq reads. Nature Biotechnology, 33(3), 290–295.

Poland, J.A., & Rife, T.W. (2012). Genotyping-by-Sequencing for plant breeding and genetics. The Plant Genome, 5(3), 92–102.

Prasanna, B.M., Pixley, K., Warburton, M.L., & Xie, C. X. (2010). Molecular marker-assisted breeding options for maize improvement in Asia. Molecular Breeding, 26(2), 339–356.

Prikryl, J., Rojas, M., Schuster, G., & Barkan, A. (2011). Mechanism of RNA stabilization and translational activation by a pentatricopeptide repeat protein. Proceedings of the National Academy of Sciences, 108(1), 415-420.

R Core Team. (2015). R: A language and environment for statistical computing. R Foundation for Statistical Computing, Vienna, Austria.

Rackham, O., & Filipovska, A. (2012). The role of mammalian PPR domain proteins in the regulation of mitochondrial gene expression. Biochimica et Biophysica Acta (BBA)-Gene Regulatory Mechanisms, 1819(9), 1008-1016.

Robinson, J. T., Thorvaldsdóttir, H., Winckler, W., Guttman, M., Lander, E. S., Getz, G., & Mesirov, J. P. (2011). Integrative genomics viewer. Nature Biotechnology, 29(1), 24.

Sachs, M.M. (2005). Maize mutants: resources for research. Maydica, 50(1), 305.

Sachs, M.M. (2009a). Cereal germplasm resources. Plant Physiology, 149(1), 148–151.

Sachs, M.M. (2009b). Maize genetic resources. In Molecular Genetic Approaches to Maize Improvement, P.D.A.L. Kriz, and P.D.B.A. Larkins, eds., Springer, Berlin, Heidelberg, 197–209.

Sachs, M.M., & Stinard, P. (2012). Yg*-N1582 is homozygous viable and has potential for use as a marker in haploid induction. Maize Genetics Cooperation Newsletter 86.

Schmitz-Linneweber, C., & Small, I. (2008). Pentatricopeptide repeat proteins: a socket set for organelle gene expression.Trends in Plant Science, 13(12), 663-670.

Schmitz-Linneweber, C., Williams-Carrier, R. E., Williams-Voelker, P. M., Kroeger, T. S., Vichas, A., & Barkan, A. (2006). A pentatricopeptide repeat protein facilitates the trans-splicing of the maize chloroplast rps12 pre-mRNA. The Plant Cell, 18(10), 2650-2663.

Sequencher® version 5.4.6 DNA sequence analysis software, Gene Codes Corporation, Ann Arbor, MI USA http://www.genecodes.com

Sleper, D.A., & Poehlman, J.M. (2006). Breeding field crops. Wiley Publishers, New York, N.Y.

Small, I. D., & Peeters, N. (2000). The PPR motif–a TPR-related motif prevalent in plant organellar proteins. Trends in Biochemical Sciences, 25(2), 45-47.

Stothard, P. (2000). The sequence manipulation suite: JavaScript programs for analyzing and formatting protein and DNA sequences.

Su, N., Hu, M.L., Wu, D.X., Wu, F.Q., Fei, G.L., Lan, Y., Chen, X.L., Shu, X.L., Zhang, X., Guo, X.P., & Cheng, Z.J. (2012). Disruption of a rice pentatricopeptide repeat protein causes a seedling-specific albino phenotype and its utilization to enhance seed purity in hybrid rice production. Plant Physiology, 159(1), 227-238.

Swarts, K., Li, H., Romero Navarro, J.A., An, D., Romay, M.C., Hearne, S., Acharya, C., Glaubitz, J.C., Mitchell, S., Elshire, R.J. & Buckler, E.S. (2014). Novel methods to optimize genotypic imputation for low-coverage, next-generation sequence data in crop plants. The Plant Genome, 7(3), 274-293.

Van der Auwera, G.A., Carneiro, M.O., Hartl, C., Poplin, R., Del Angel, G., Levy-Moonshine, A., Jordan, T., Shakir, K., Roazen, D., Thibault, J., & Banks, E. (2013). From FastQ data to high-confidence variant calls: the genome analysis toolkit best practices pipeline. Current Protocols in Bioinformatics, 15(11), 11-10.

Weber, D.F. (2014). Today's use of haploids in corn plant breeding. Advances in Agronomy, 123(1), 123-144.

Weil, C.F., & Monde, R.A. (2009). EMS mutagenesis and point mutation discovery. In Molecular Genetic Approaches to Maize Improvement, P.D.A.L. Kriz, and P.D.B.A. Larkins, eds., Springer, Berlin, Heidelberg, 161–171.

Whitt, S.R., Wilson, L.M., Tenaillon, M.I., Gaut, B.S., & Buckler, E.S. (2002). Genetic diversity and selection in the maize starch pathway. Proceedings of the National Academy of Sciences, 99(20), 12959–12962.

Wilson, L.M., Whitt, S.R., Ibáñez, A.M., Rocheford, T.R., Goodman, M.M., & Buckler, E.S. (2004). Dissection of maize kernel composition and starch production by candidate gene association. Plant Cell, 16(10), 2719–2733.

Wu, Y., San Vicente, F., Huang, K., Dhliwayo, T., Costich, D.E., Semagn, K., Sudha, N., Olsen, M., Prasanna, B.M., Zhang, X., & Babu, R. (2016). Molecular characterization of CIMMYT maize inbred lines with genotyping-by-sequencing SNPs. Theoretical and Applied Genetics, 129(4), 753-765.

APPENDIX

GENETIC RESOURCE DEVELOPMENT

This research supplies the resources for future growth chamber fine mapping experiments to determine the gene(s) underlying this QTL for O_3 tolerance and sensitivity (Tables A.1 & A.2). Populations were developed to fine map in the B73-Mo17 NILs. Mo17 NILs were crossed with Mo17 resulting in an F_1. This F_1 was then selfed to create Mo17 NILs x Mo17 F_2s. Selected B73 NILs were crossed with B73 resulting in an F_1. These F_1s were then selfed to create F_2s. Additionally, all B73 NILs were crossed with B73 to create the full F_1 population.

This research also supplies the resources for future research of heritability studies by creating a half diallel population (Table A.3).

TABLES

Table A.1 Mo17 NIL Mapping Population

Genotype	Population Status	Last Date Advanced	Cold Storage Bin #	Seed Origin
m002xMo17	Mo17 NIL F2	Summer 2017	Mo17_NILs_1-4	Eichten et al. 2011
m007xMo17	Mo17 NIL F2	Summer 2017	Mo17_NILs_1-4	Eichten et al. 2011
m008xMo17	Mo17 NIL F2	Summer 2017	Mo17_NILs_1-4	Eichten et al. 2011
m011xMo17	Mo17 NIL F2	Summer 2017	Mo17_NILs_1-4	Eichten et al. 2011
m012xMo17	Mo17 NIL F2	Summer 2017	Mo17_NILs_1-4	Eichten et al. 2011
m014xMo17	Mo17 NIL F2	Summer 2017	Mo17_NILs_1-4	Eichten et al. 2011
m016xMo17	Mo17 NIL F2	Summer 2017	Mo17_NILs_1-4	Eichten et al. 2011
m017xMo17	Mo17 NIL F2	Summer 2017	Mo17_NILs_1-4	Eichten et al. 2011
m022xMo17	Mo17 NIL F2	Summer 2017	Mo17_NILs_1-4	Eichten et al. 2011
m024xMo17	Mo17 NIL F2	Summer 2017	Mo17_NILs_1-4	Eichten et al. 2011
m030xMo17	Mo17 NIL F2	Summer 2017	Mo17_NILs_1-4	Eichten et al. 2011
m031xMo17	Mo17 NIL F2	Summer 2017	Mo17_NILs_1-4	Eichten et al. 2011
m032xMo17	Mo17 NIL F2	Summer 2017	Mo17_NILs_1-4	Eichten et al. 2011
m037xMo17	Mo17 NIL F2	Summer 2017	Mo17_NILs_1-4	Eichten et al. 2011
m038xMo17	Mo17 NIL F2	Summer 2017	Mo17_NILs_1-4	Eichten et al. 2011
m040xMo17	Mo17 NIL F2	Summer 2017	Mo17_NILs_1-4	Eichten et al. 2011
m043xMo17	Mo17 NIL F2	Summer 2017	Mo17_NILs_1-4	Eichten et al. 2011
m046xMo17	Mo17 NIL F2	Summer 2017	Mo17_NILs_1-4	Eichten et al. 2011
m047xMo17	Mo17 NIL F2	Summer 2017	Mo17_NILs_1-4	Eichten et al. 2011
m048xMo17	Mo17 NIL F2	Summer 2017	Mo17_NILs_1-4	Eichten et al. 2011
m049xMo17	Mo17 NIL F2	Summer 2017	Mo17_NILs_1-4	Eichten et al. 2011
m051xMo17	Mo17 NIL F2	Summer 2017	Mo17_NILs_1-4	Eichten et al. 2011
m052xMo17	Mo17 NIL F2	Summer 2017	Mo17_NILs_1-4	Eichten et al. 2011
m054xMo17	Mo17 NIL F2	Summer 2017	Mo17_NILs_1-4	Eichten et al. 2011

Table A.1 (cont.)

Genotype	Population Status	Last Date Advanced	Cold Storage Bin #	Seed Origin
m060xMo17	Mo17 NIL F2	Summer 2017	Mo17_NILs_1-4	Eichten et al. 2011
m062xMo17	Mo17 NIL F2	Summer 2017	Mo17_NILs_1-4	Eichten et al. 2011
m065xMo17	Mo17 NIL F2	Summer 2017	Mo17_NILs_1-4	Eichten et al. 2011
m072xMo17	Mo17 NIL F2	Summer 2017	Mo17_NILs_1-4	Eichten et al. 2011
m073xMo17	Mo17 NIL F2	Summer 2017	Mo17_NILs_1-4	Eichten et al. 2011
m075xMo17	Mo17 NIL F2	Summer 2017	Mo17_NILs_1-4	Eichten et al. 2011
m076xMo17	Mo17 NIL F2	Summer 2017	Mo17_NILs_1-4	Eichten et al. 2011
m078xMo17	Mo17 NIL F2	Summer 2017	Mo17_NILs_1-4	Eichten et al. 2011
m079xMo17	Mo17 NIL F2	Summer 2017	Mo17_NILs_1-4	Eichten et al. 2011
m081xMo17	Mo17 NIL F2	Summer 2017	Mo17_NILs_1-4	Eichten et al. 2011
m082xMo17	Mo17 NIL F2	Summer 2017	Mo17_NILs_1-4	Eichten et al. 2011
m083xMo17	Mo17 NIL F2	Summer 2017	Mo17_NILs_1-4	Eichten et al. 2011
m091xMo17	Mo17 NIL F2	Summer 2017	Mo17_NILs_1-4	Eichten et al. 2011
m092xMo17	Mo17 NIL F2	Summer 2017	Mo17_NILs_1-4	Eichten et al. 2011
m093xMo17	Mo17 NIL F2	Summer 2017	Mo17_NILs_1-4	Eichten et al. 2011
m097xMo17	Mo17 NIL F2	Summer 2017	Mo17_NILs_1-4	Eichten et al. 2011
m098xMo17	Mo17 NIL F2	Summer 2017	Mo17_NILs_1-4	Eichten et al. 2011
m099xMo17	Mo17 NIL F2	Summer 2017	Mo17_NILs_1-4	Eichten et al. 2011
m100xMo17	Mo17 NIL F2	Summer 2017	Mo17_NILs_1-4	Eichten et al. 2011

Table A.2 B73 NIL Mapping Population

Genotype	Population Status	Last Date Advanced	Cold Storage Bin #	Seed Origin
b004xB73	B73 NIL F1	Summer 2017	B73_NILs_1-4	Eichten et al. 2011
b005xB73	B73 NIL F2	Summer 2017	B73_NILs_1-4	Eichten et al. 2011
b017xB73	B73 NIL F1	Summer 2017	B73_NILs_1-4	Eichten et al. 2011
b019xB73	B73 NIL F1	Summer 2017	B73_NILs_1-4	Eichten et al. 2011
b020xB73	B73 NIL F1	Summer 2017	B73_NILs_1-4	Eichten et al. 2011
b022xB73	B73 NIL F1	Summer 2017	B73_NILs_1-4	Eichten et al. 2011
b025xB73	B73 NIL F1	Summer 2017	B73_NILs_1-4	Eichten et al. 2011
b030xB73	B73 NIL F1	Summer 2017	B73_NILs_1-4	Eichten et al. 2011
b031xB73	B73 NIL F1	Summer 2017	B73_NILs_1-4	Eichten et al. 2011
b035xB73	B73 NIL F1	Summer 2017	B73_NILs_1-4	Eichten et al. 2011
b036xB73	B73 NIL F1	Summer 2017	B73_NILs_1-4	Eichten et al. 2011
b037xB73	B73 NIL F1	Summer 2017	B73_NILs_1-4	Eichten et al. 2011
b041xB73	B73 NIL F1	Summer 2017	B73_NILs_1-4	Eichten et al. 2011
b043xB73	B73 NIL F1	Summer 2017	B73_NILs_1-4	Eichten et al. 2011
b044xB73	B73 NIL F1	Summer 2017	B73_NILs_1-4	Eichten et al. 2011
b046xB73	B73 NIL F1	Summer 2017	B73_NILs_1-4	Eichten et al. 2011
b047xB73	B73 NIL F1	Summer 2017	B73_NILs_1-4	Eichten et al. 2011
b049xB73	B73 NIL F1	Summer 2017	B73_NILs_1-4	Eichten et al. 2011
b050xB73	B73 NIL F1	Summer 2017	B73_NILs_1-4	Eichten et al. 2011
b054xB73	B73 NIL F1	Summer 2017	B73_NILs_1-4	Eichten et al. 2011
b055xB73	B73 NIL F1	Summer 2017	B73_NILs_1-4	Eichten et al. 2011
b068xB73	B73 NIL F1	Summer 2017	B73_NILs_1-4	Eichten et al. 2011
b069xB73	B73 NIL F1	Summer 2017	B73_NILs_1-4	Eichten et al. 2011
b070xB73	B73 NIL F1	Summer 2017	B73_NILs_1-4	Eichten et al. 2011
b071xB73	B73 NIL F1	Summer 2017	B73_NILs_1-4	Eichten et al. 2011
b076xB73	B73 NIL F1	Summer 2017	B73_NILs_1-4	Eichten et al. 2011

Table A.2 (cont.)

Genotype	Population Status	Last Date Advanced	Cold Storage Bin #	Seed Origin
b086xB73	B73 NIL F1	Summer 2017	B73_NILs_1-4	Eichten et al. 2011
b087xB73	B73 NIL F1	Summer 2017	B73_NILs_1-4	Eichten et al. 2011
b089xB73	B73 NIL F1	Summer 2017	B73_NILs_1-4	Eichten et al. 2011
b094xB73	B73 NIL F1	Summer 2017	B73_NILs_1-4	Eichten et al. 2011
b099xB73	B73 NIL F1	Summer 2017	B73_NILs_1-4	Eichten et al. 2011
b102xB73	B73 NIL F1	Summer 2017	B73_NILs_1-4	Eichten et al. 2011
b118xB73	B73 NIL F1	Summer 2017	B73_NILs_1-4	Eichten et al. 2011
b123xB73	B73 NIL F1	Summer 2017	B73_NILs_1-4	Eichten et al. 2011
b125xB73	B73 NIL F1	Summer 2017	B73_NILs_1-4	Eichten et al. 2011
b126xB73	B73 NIL F1	Summer 2017	B73_NILs_1-4	Eichten et al. 2011
b131xB73	B73 NIL F2	Summer 2017	B73_NILs_1-4	Eichten et al. 2011
b132xB73	B73 NIL F1	Summer 2017	B73_NILs_1-4	Eichten et al. 2011
b135xB73	B73 NIL F1	Summer 2017	B73_NILs_1-4	Eichten et al. 2011
b139xB73	B73 NIL F1	Summer 2017	B73_NILs_1-4	Eichten et al. 2011
b148xB73	B73 NIL F1	Summer 2017	B73_NILs_1-4	Eichten et al. 2011
b149xB73	B73 NIL F1	Summer 2017	B73_NILs_1-4	Eichten et al. 2011
b152xB73	B73 NIL F1	Summer 2017	B73_NILs_1-4	Eichten et al. 2011
b154xB73	B73 NIL F1	Summer 2017	B73_NILs_1-4	Eichten et al. 2011
b164xB73	B73 NIL F1	Summer 2017	B73_NILs_1-4	Eichten et al. 2011
b165xB73	B73 NIL F1	Summer 2017	B73_NILs_1-4	Eichten et al. 2011
b172xB73	B73 NIL F1	Summer 2017	B73_NILs_1-4	Eichten et al. 2011
b177xB73	B73 NIL F1	Summer 2017	B73_NILs_1-4	Eichten et al. 2011
b182xB73	B73 NIL F1	Summer 2017	B73_NILs_1-4	Eichten et al. 2011

Table A.3 Half Diallel Population

Genotype	Population	Population ID	Last Date Advanced	Cold Storage Bin #	Seed Origin
B73 x Oh43	Half Diallel	D_011	Winter 2016	Half_Diallel_1-3	GRIN USDA
B73 x Ms71	Half Diallel	D_012	Winter 2016	Half_Diallel_1-3	GRIN USDA
B73 x Mo71	Half Diallel	D_013	Winter 2016	Half_Diallel_1-3	GRIN USDA
B73 x IL14H	Half Diallel	D_014	Winter 2016	Half_Diallel_1-3	GRIN USDA
B73x C123	Half Diallel	D_015	Winter 2016	Half_Diallel_1-3	GRIN USDA
B73x NC338	Half Diallel	D_016	Winter 2016	Half_Diallel_1-3	GRIN USDA
B73x CML333	Half Diallel	D_017	Winter 2016	Half_Diallel_1-3	GRIN USDA
B73 x M37W	Half Diallel	D_018	Winter 2016	Half_Diallel_1-3	GRIN USDA
B73 x Hp301	Half Diallel	D_019	Winter 2016	Half_Diallel_1-3	GRIN USDA
Oh43 x Ms71	Half Diallel	D_020	Winter 2016	Half_Diallel_1-3	GRIN USDA
Oh43 x Mo71	Half Diallel	D_021	Winter 2016	Half_Diallel_1-3	GRIN USDA
Oh43 x IL14H	Half Diallel	D_022	Winter 2016	Half_Diallel_1-3	GRIN USDA
Oh43 x C123	Half Diallel	D_023	Winter 2016	Half_Diallel_1-3	GRIN USDA
Oh43 x NC338	Half Diallel	D_024	Winter 2016	Half_Diallel_1-3	GRIN USDA
Oh43 x CML333	Half Diallel	D_025	Winter 2016	Half_Diallel_1-3	GRIN USDA
Oh43 x M37W	Half Diallel	D_026	Winter 2016	Half_Diallel_1-3	GRIN USDA
Oh43 x Hp301	Half Diallel	D_027	Winter 2016	Half_Diallel_1-3	GRIN USDA
Ms71 x Mo71	Half Diallel	D_028	Winter 2016	Half_Diallel_1-3	GRIN USDA
Ms71 x IL14H	Half Diallel	D_029	Winter 2016	Half_Diallel_1-3	GRIN USDA
Ms71 x C123	Half Diallel	D_030	Winter 2016	Half_Diallel_1-3	GRIN USDA
Ms71 x NC338	Half Diallel	D_031	Winter 2016	Half_Diallel_1-3	GRIN USDA
Ms71 x CML333	Half Diallel	D_032	Winter 2016	Half_Diallel_1-3	GRIN USDA
Ms71 x M37W	Half Diallel	D_033	Winter 2016	Half_Diallel_1-3	GRIN USDA
Ms71 x Hp301	Half Diallel	D_034	Winter 2016	Half_Diallel_1-3	GRIN USDA
Mo71 x IL14H	Half Diallel	D_035	Winter 2016	Half_Diallel_1-3	GRIN USDA
Mo71 x C123	Half Diallel	D_036	Winter 2016	Half_Diallel_1-3	GRIN USDA

Table A.3 (cont.)

Genotype	Population	Population ID	Last Date Advanced	Cold Storage Bin #	Seed Origin
Mo71 x CML333	Half Diallel	D_038	Winter 2016	Half_Diallel_1-3	GRIN USDA
Mo71 x M37W	Half Diallel	D_039	Winter 2016	Half_Diallel_1-3	GRIN USDA
Mo71 x Hp301	Half Diallel	D_040	Winter 2016	Half_Diallel_1-3	GRIN USDA
IL14H x C123	Half Diallel	D_041	Winter 2016	Half_Diallel_1-3	GRIN USDA
IL14H x NC338	Half Diallel	D_042	Winter 2016	Half_Diallel_1-3	GRIN USDA
IL14H x CML333	Half Diallel	D_043	Winter 2016	Half_Diallel_1-3	GRIN USDA
IL14H x M37W	Half Diallel	D_044	Winter 2016	Half_Diallel_1-3	GRIN USDA
IL14H x Hp301	Half Diallel	D_045	Winter 2016	Half_Diallel_1-3	GRIN USDA
C123 x NC338	Half Diallel	D_046	Winter 2016	Half_Diallel_1-3	GRIN USDA
C123 x CML333	Half Diallel	D_047	Winter 2016	Half_Diallel_1-3	GRIN USDA
C123 x M37W	Half Diallel	D_048	Winter 2016	Half_Diallel_1-3	GRIN USDA
C123 x Hp301	Half Diallel	D_049	Winter 2016	Half_Diallel_1-3	GRIN USDA
NC338 x CML333	Half Diallel	D_050	Winter 2016	Half_Diallel_1-3	GRIN USDA
NC338 x M37W	Half Diallel	D_051	Winter 2016	Half_Diallel_1-3	GRIN USDA
NC338 x Hp301	Half Diallel	D_052	Winter 2016	Half_Diallel_1-3	GRIN USDA
CML333 x M37W	Half Diallel	D_053	Winter 2016	Half_Diallel_1-3	GRIN USDA
CML333 x Hp301	Half Diallel	D_054	Winter 2016	Half_Diallel_1-3	GRIN USDA
M37W x Hp301	Half Diallel	D_055	Winter 2016	Half_Diallel_1-3	GRIN USDA
B73	Half Diallel Parent	D_001	Winter 2016	Half_Diallel_1-3	GRIN USDA
Oh43	Half Diallel Parent	D_002	Winter 2016	Half_Diallel_1-3	GRIN USDA
Ms71	Half Diallel Parent	D_003	Winter 2016	Half_Diallel_1-3	GRIN USDA
Mo17	Half Diallel Parent	D_004	Winter 2016	Half_Diallel_1-3	GRIN USDA
Il14H	Half Diallel Parent	D_005	Winter 2016	Half_Diallel_1-3	GRIN USDA
C123	Half Diallel Parent	D_006	Winter 2016	Half_Diallel_1-3	GRIN USDA
NC338	Half Diallel Parent	D_007	Winter 2016	Half_Diallel_1-3	GRIN USDA
CML333	Half Diallel Parent	D_008	Winter 2016	Half_Diallel_1-3	GRIN USDA

Table A.3 (cont.)

Genotype	Population	Population ID	Last Date Advanced	Cold Storage Bin #	Seed Origin
M37W	Half Diallel Parent	D_009	Winter 2016	Half_Diallel_1-3	GRIN USDA
Hp301	Half Diallel Parent	D_010	Winter 2016	Half_Diallel_1-3	GRIN USDA